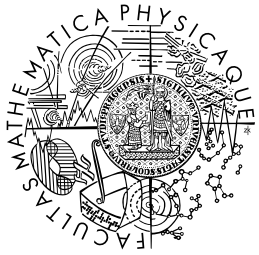

FACULTY
OF MATHEMATICS
AND PHYSICS
Charles University

MASTER THESIS

Štěpán Šubík

Study of Thermal Comfort in the Urban Environment

Department of Atmospheric Physics

Supervisor of the master thesis:	RNDr. Eva Holtanová, Ph.D.
Advisor of the master thesis:	Mgr. Michal Žák, Ph.D.
Study programme:	Physics
Study branch:	Meteorology and Climatology

Prague 2020

I declare that I elaborated this master thesis independently and only with the cited sources, literature and other professional sources.

I understand that my work relates to the rights and obligations under the Act No. 121/2000 Sb., the Copyright Act, as amended, in particular the fact that the Charles University has the right to conclude a license agreement on the use of this work as a school work pursuant to Section 60 subsection 1 of the Copyright Act.

In Prague date ..... signature of the author

Title: Study of Thermal Comfort in the Urban Environment

Author: Štěpán Šubík

Department: Department of Atmospheric Physics

Supervisor: RNDr. Eva Holtanová, Ph.D., Department of Atmospheric Physics

Advisor: Mgr. Michal Žák, Ph.D., Department of Atmospheric Physics

Abstract: This thesis is written to compare indices, which describe the perceived temperature of human body in thermal environment and apply them to study the thermal comfort of city inhabitants. The thesis is divided into five parts.

In the first part, many thermal indices are presented and classified into empirical, commercially used or analytical indices by their definition. The practical usage of thermal indices is mentioned in the next chapter.

In the third chapter, the most suitable thermal indices for describing the urban thermal comfort are found. Those are UTCI, PET, PT, SET* and mPET. Thermal index mPET .has been chosen to be used further in this study.

The fourth chapter includes the application of mPET on meteorological data from Prague, Berlin, Hamburg, Nürnberg, Köln and Frankfurt. The frequencies and long-term behaviour are studied as well as the effect of the street canyon for Prague's streets Dělnická, Rohanské nábřeží, Legerova and Vinohradská.

The last part discusses the results. The thermal comfort in Prague and Berlin, together with the effects of the street canyon in Prague are studied more closely. It was found that in Prague, Berlin, Hamburg, Nürnberg and Frankfurt, the frequencies of evening thermal discomfort, in terms of heat stress, are higher in the cities than in surrounding areas which is a consequence of UHI. Furthermore, the frequency of days with heat stress increases and the number of days with cold stress decreases in Prague, Berlin, Nürnberg, Köln and Frankfurt. Besides, the simulation of the street canyon model showed the importance of tree planting in Prague streets Legerova and Vinohradská and the importance of using high albedo materials for building in Dělnická and Rohanské nábřeží street in order to achieve more comfortable thermal environment.

Keywords: Thermal comfort, Urban heat island, Thermal index, mPET, Central Europe, Rayman

Název práce: Studium tepelného komfortu městského prostředí

Autor: Štěpán Šubík

Katedra: Katedra fyziky atmosféry

Vedoucí diplomové práce: RNDr. Eva Holtanová, Ph.D., Katedra fyziky atmosféry

Konzultant: Mgr. Michal Žák, Ph.D., Katedra fyziky atmosféry

Abstrakt: Práce pojednává o popisu tepelného komfortu na základě tepelných indexů, které popisují teplotu, kterou vnímá lidské tělo z okolního prostředí. Indexy jsou poté použity ke studiu tepelného komfortu obyvatel měst. Studie se dělí do pěti částí.

V první kapitole jsou prezentovány různé tepelné indexy, které jsou rozděleny do tří skupin - experimentální, komerční a analytické - dle jejich definice. V následující kapitole jsou uvedena různá praktická využití tepelných indexů.

Vhodné tepelné indexy jsou vybrány ve třetí kapitole tak, aby co nejlépe popisovaly městský tepelný komfort. Jako vhodné indexy byly vybrány UTCI, PET, PT, SET* a mPET. Pro účely této studie byl vybrán tepelný index mPET.

Čtvrtá kapitola obsahuje samotnou aplikaci mPET na meteorologická data z Prahy, Berlína, Hamburku, Norimberku, Kolína a Frankfurtu. Pro všechna města je provedena studie výskytu nepříznivých tepelných podmínek ve městě a okolí a jejich dlouhodobého chování. Chování mPET v závislosti na výskytu a charakteru uličního kaňonu bylo simulováno pro pražské ulice Dělnická, Rohanské nábřeží, Legerova a Vinohradská.

V poslední kapitole jsou výsledky diskutovány. Tepelný komfort v Praze a Berlíně je studován detailněji než v ostatních městech. V Praze, Berlíně, Hamburku, Norimberku a Frankfurtu byly frekvence dní s tepelným stresem vyšší než na referenčních stanicích, které reprezentují mimoměstské oblasti. Frekvence těchto dní se navíc zvyšuje a frekvence dní se stresem způsobeným chladem se snižuje, což platí pro Prahu, Berlín, Norimberk, Kolín a Frankfurt. Simulace uličního kaňonu ukázaly, že pro zvýšení městského tepelného komfortu je důležitá výsadba stromů v ulicích Legerova a Vinohradská a také používání materiálů s vysokým albedem na budovách v ulicích Dělnická a Rohanské nábřeží pro zvýšení městského tepelného komfortu.

Klíčová slova: Tepelný komfort, Městský tepelný ostrov, Tepelné indexy, mPET, Střední Evropa, Rayman

I would like to thank my supervisor RNDr. Eva Holtanová, Ph.D. and my consultant Mgr. Michal Žák, Ph.D. for very smooth communication, helpful advice, quick reactions to my questions even during non-working hours and unlimited patience. I am grateful for all knowledge that the Department of Atmospheric Physics provided to me and I thank all of my lecturers for their guidance and patience. Special thanks go to Jan Václavík, who did the language correction and helped me to improve my English skills. My thanks also go to my girlfriend Klára, who advised me with the graphics and I thank her also for the help and kind words. Big thanks go to my parents for their support throughout the whole study. Last but not least, I thank my family and all my friends for support and help in times of need.

Contents

Introduction

Thermal comfort is one of the fundamental indicators of suitability for the environment to host life. The organisms living in cold Antarctic climate adapted to the coldness during the whole year as well as the organisms living in a subtropical climate did in a warmer climate. The other organisms attempt to move to another place with every change where they can find their former comfort—the same stands for humans.

Humans live in different climates, and in each of them, they are used to the temperatures that change throughout the year, to the precipitation with its yearly course, wind direction and velocity that differs from mountains through lowlands to seashores and more. All of those variables are measurable, and they can be used to describe thermal comfort.

According to Goodfellow and Tähti [2001], thermal comfort is defined as the condition of mind that expresses satisfaction with the thermal environment. It is an entirely subjective term, but in general, the difference among people's choices are small enough to consider a mean for many nations or smaller groups. The thermal environment includes the body's physiological response usually denoted as strain and the atmospheric heat exchanges with the body usually denoted as stress, as described in Jendritzky and de Dear [2009].

The thermal comfort is connected to the weather conditions which defines climates. The close relationship between humans and the thermal component of the atmospheric environment is evident and daily experienced by everyone. Thus, issues related to the thermal comfort, discomfort, and health impacts are the reason that the assessment, useful and practical forecast of the thermal environment is one of the fundamental topics of human biometeorology.

Biometeorology is a study of the relationship between atmospheric conditions, i. e. temperature, humidity and air movement, and living organisms. In our case, the thermal comfort of humans is considered; therefore, the balancing human heat budget will be studied. The equilibration of the organism represents the problem to the various environmental and metabolic heat load. The heat load is controlled by an autonomous thermoregulatory system that is additionally supported by behavioural adaptation. It consists of eating, drinking, clothing, activity, exposure and migration, which are driven by human sensations of thermal discomfort. These capabilities help a human being to live in different climate zones, though the climates would cause different degrees of discomfort, according to Jendritzky and de Dear [2009].

Rapid urbanization has led to massive migrations of all people to urban regions. Recently, the proportion of the world population living in urban regions is over 50%, according to Liu et al. [2019]. However, due to global climate change and enhanced urban heat island effects, the human thermal comfort has become more important and the warming environment more harmful to citizens' health not only psychologically, i.e. in terms of thermal sensation, mood, and concentration, but also physiologically by way of sunburn, heatstroke, and sweating.

The research of the human body's responses, both psychological and physiological, is expected to provide an insight into the thermal comfort and health of humans in urban areas. The main aim is to receive sustainability and comfort

for the inhabitants in different microclimates to eliminate thermal discomfort in the cities. There are still many responses and equations to be found for the description of the human body and the thermal environment system. As for the known relationships, some models connect the weather to the thermal comfort via thermal indices, indicators of thermal comfort.

The meteorological variables, in our consideration of the thermal environment, are affected by the physical environment, e.g. wind can be enhanced by a plain grassland or weakened by a forest or city buildings, and humidity can be influenced by a river or a nearby sea. According to the surface, other variables can be similarly changed. The most significant changes are found in the urban area where the urban heat island (UHI) takes place.

The UHI phenomenon is an effect which increases the temperature in the urban areas compared to the surrounding areas. As a result, the UHI leads to increased energy needs due to the energy consumed by air-conditioners in terms of cooling of the environment, environmental issues. It implies a more frequent formation of smog and enhanced air pollutants and health consequences which are connected to the human thermal comfort. According to (Rodríguez et al. [2020]), the heatwave that took place in Europe in July 2019 set all-time high-temperature records in several countries such as Belgium, Germany, France, the Netherlands or the United Kingdom. The combination of UHI and climate change only increases the effect of the UHI and leads to a higher airconditioning demand on electricity. It forces the innovations in electricity generation, transmission and distribution infrastructures.

According to Rodríguez et al. [2020], heat islands are mainly classified as either atmospheric (Canopy Layer UHI or Boundary Layer UHI) or surface UHI. Surface UHI refers to the increased warmth of urban surfaces, measured on a large scale by using thermal infrared data from remote sensors in satellites or aircraft. On the other hand, the Canopy Layer UHI is the one directly related to human exposure where both air and surface temperatures influence outdoor thermal comfort. We will aim at the Canopy Layer UHI to study the effect on humans.

Many factors can influence the heat island, such as the climate characteristics (solar radiation, wind and clouds, for instance). In general, the strong wind and cloudy sky can reduce the UHI because the wind would cause mixing of the air in the urban area and the air in the outer area and clouds will reduce the solar energy reaching the city. Calm winds will make the air in the city more isolated and clear sky would give higher solar energy to the surface, causing an enhancement of the UHI.

The season and time of day also affect the UHI intensity, as well as the characteristics of the city (ratios of buildings, pavement and vegetation) and the anthropogenic heat release (metabolic heat from humans, traffic, and heat released from buildings). For example, according to as Rodríguez et al. [2020], who studied UHI intensity in Seville (Spain), the intensity may vary between 0.4 °C and 11 °C, with an average of 4.1 °C.

This study aims at the thermal comfort of humans in six cities: Prague, Berlin, Hamburg, Frankfurt am Main, Nürnberg and Köln. In the first chapter, there is an introduction of the thermal indices as the indicators of thermal comfort in outdoor areas. The next chapter offers the practical usage of the thermal

indices presenting their non-scientific importance in architecture and tourism. Furthermore, different thermal indices are compared to select the most suitable one for this study in chapter three. After the selection, the chosen index is used to compare thermal comfort in the chosen cities and the surrounding rural areas in chapter four. In Prague, a few areas are modelled in order to study the effect of the street canyon with different scenarios of the thermal environment. In chapter five, there is an interpretation of the results with discussion. Ultimately, the results are discussed, including the effect of urban planning consisting of tree planting and building design.

1. Thermal indices

When the news media integrated the weather forecast in its program, there was a pressure to produce data more applicable and useful for everyday life. The temperature forecast can determine the appropriate clothing and precipitation will tell us whether to take an umbrella or not. However, it has been recorded that for example in 15 °C and low wind with no precipitation one can have only light jacket whereas in 15 °C and stronger wind with at least little rain one would need a sweater and a jacket not to feel cold.

In 1938, Büttner recognised the fact and postulated: "If one wants to assess the influence of climate on the human organism in the widest sense, it is necessary to evaluate the effects not only of a single parameter but of all thermal components. This leads us to the necessity of modelling the human heat balance" as Höppe [1999] reads. The fact arranges a way to measure human thermal comfort as the function of weather. From the definition, the weather is a state of the atmosphere in a given time at a given place described by meteorological variables, i.e. wind, temperature, cloudiness, moisture, pressure and more. Therefore, thermal indices as the indicators of human thermal comfort have been developed to summarise the information of the weather conditions. Currently, there are more than 165 indices, as Staiger et al. [2019] claims, which has been simply categorised into three groups, referring to the complexity of their definition and the common usage.

1.1 Empirical indices

Since there was a need for a straightforward number to determine the thermal comfort, there were many meteorologists that wanted to find the index. The first indices were simply determined by formulae and used different complexity of using the meteorological parameters. As a base variable air temperature was used in most of them joined by relative humidity or wind velocity. Many of them are not used daily, although they can occur in specialised studies. Below are described two of the indices, Discomfort Index and Wind-chill index. More examples can be found in Auliciems and Szokolay [2007], Section Empirical indices.

1.1.1 Discomfort Index

Discomfort Index (DI) was first introduced by THOM [1959] to describe the human comfort using two parameters: air temperature and relative humidity. The formula for DI is as follows:

$$\mathrm{DI} = T - \left[(0.55 - 0.0055RH)(T - 14.5)\right], \tag{1.1}$$

where T stands for air temperature in °C and RH is the relative humidity of air in %. In the definition, the critical temperature is 14.5 °C, which is not affected by the humidity change. When the temperature is higher, an increasing DI with a higher RH may be observed whereas below the critical temperature the DI is decreasing with higher relative humidity. The subjective comfort is given by Table 1.1.

Table 1.1: Discomfort conditions according to Discomfort Index according to Yousif and Tahir [2013]

Condition	DI
No discomfort	<21
Under 50% of population feels discomfort	21-24
Over 50% of population feels discomfort	25-27
Most of population suffers discomfort	28 - 29
Everyone feels stress	30-32
State of medical emergency	> 32

1.1.2 Wind-Chill Index

Wind-Chill Index (WCI) is described in Steadman [1959]. Its main aim is to determine the cooling effect of wind when the temperatures are low. It is defined by two equations:

$$\mathrm{WCI} = h(33 - T_a), \tag{1.2}$$
$$h = 9.0 + 10.9\sqrt{v} - v, \tag{1.3}$$

where T_a is ambient temperature in °C and v is the wind speed in ms^{-1}. The definition is parabolic in v, so the maximum effect is at 25 ms^{-1}. It has no table of comfort defined, more likely it is seen as a cooling factor.

1.2 Commercially used indices

Many forecasting centres and commercial companies have been developing their indices since the 1990s to forecast the "real feel temperature". Those indices usually have simple definition using a formula or more complex definition using computations and algorithms. The idea of a thermal index used in the public media to describe and forecast thermal comfort has been the engine of the whole research of the thermal indices. Many companies and institutes have developed their "thermal sensation" temperature in the means of temperature modified by other variables. The most common and still valid commercial indices are Heat Index, Humindex and Apparent temperature.

1.2.1 Heat Index

The National Weather Service in the USA uses Heat Index (HI). As described in National Weather Service [2018], it uses air temperature and relative humidity to forecast the heat index. The definition is based on a quite complex equation

described in National Weather Service [2016]:

$$\begin{aligned} \mathrm{HI} = &-42.379 + (2.04901523 \times T) + (10.14333127 \times RH) \\ &- (0.22475541 \times T \times RH) - (6.83783 \times 10^{-3} \times T^2) \\ &- (5.481717 \times 10^{-2} \times RH^2) + (1.22874 \times 10^{-3} \times T^2 \times RH) \\ &+ (8.5282 \times 10^{-4} \times T \times RH^2) - (1.99 \times 10^{-6} \times T^2 \times RH^2), \end{aligned} \tag{1.4}$$

where T is the air temperature in °F and RH is the relative humidity in %. The discomfort is then given by Figure 1.1.

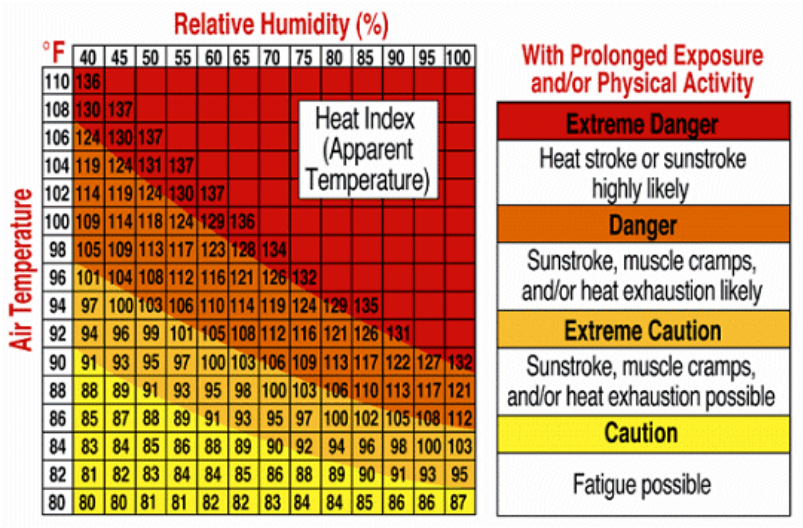

Figure 1.1: Thermal comfort conditions according to Heat Index, taken from Ambient Weather [2017]

1.2.2 Humindex

Canadian meteorologists use Humindex (Hum) to describe how hot the weather feels to the average person. It is done by combining the effect of heat and humidity. The formulas

$$\mathrm{Hum} = T + h \tag{1.5}$$

$$h = 0.5555(e - 10.0) \tag{1.6}$$

$$e = 6.11 \exp\left(5417.7530 \left(\frac{1}{273.16} - \frac{1}{T_d}\right)\right) \tag{1.7}$$

were developed by J. M. Masterton and F. A. Richardson of Canada's Atmospheric Environment Service in 1979, as describes PlanetCalc [2016]. The T stands for air temperature in °C and T_d is the dewpoint temperature in °C, PhysLink [1995]. The comfort is described in Table 1.2

1.2.3 Apparent temperature

The Apparent temperature, also called Australian Apparent temperature (AT), is index developed by Robert Steadman to forecast a thermal comfort for people in

Table 1.2: Discomfort degrees described according to Humindex, cited from PlanetCalc [2016]

Condition	Humindex	Recommendation
No discomfort	<25	None
	25-29	Supply water to workers on an "as needed" basis.
Some discomfort	30-33	Post Heat Stress Alert notice. Encourage workers to drink extra water. Start recording hourly temperature and relative humidity.
	34-37	Post Heat Stress Warning notice. Notify workers that they need to drink extra water. Ensure workers are trained to recognize symptoms.
	38-39	Work with 15 minutes relief per hour can continue. Provide adequate cool (10-15°C) water. At least 1 cup (240 mL) of water every 20 minutes. Workers with symptoms should seek medical attention.
Great discomfort; avoid exertion	40-41	Work with 30 minutes relief per hour can continue. Provide adequate cool (10-15°C) water. At least 1 cup (240 mL) of water every 20 minutes. Workers with symptoms should seek medical attention.
	42-44	If feasible, work with 45 minutes relief per hour can continue. Provide adequate cool (10-15 °C) water. At least 1 cup (240 mL) of water every 20 minutes. Workers with symptoms should seek medical attention.
Dangerous; possible heat stroke	> 44	Only medically supervised work can continue.

Australia. The original formula described in PlanetCalc [2012] took into account the dry bulb temperature, humidity, wind speed, humidity and radiation from the sun as follows:

$$\mathrm{AT} = T_a + 0.348e - 0.70v + 0.70\frac{Q}{v+10} - 4.25, \tag{1.8}$$

where T_a is the dry bulb temperature in °C, v is the wind speed in ms^{-1}, Q is the net radiation absorbed per unit area of body surface in Wm^2 and e is the water vapour pressure in hPa that can be calculated using relative humidity RH in % as

$$e = \frac{RH}{100}6.105\exp\left(\frac{17.27T_a}{237.7+T_a}\right). \tag{1.9}$$

The formula was updated and simplified by the author himself into a current form:

$$\mathrm{AT} = T_a + 0.33e - 0.70v - 4.00, \tag{1.10}$$

where the net radiation absorbed per unit area of body surface does not take place, and other variables refer to those in the former formulae ((1.8) and (1.9)). Thus, in vCalc [2019] it is called non-radiation version of the Australian Apparent Temperature.

1.3 Analytical indices

All of the former indices are simple and experimentally determined by one or more researches as Auliciems and Szokolay [2007] reads. They are defined by fitting various meteorological variables to reach the optimal formulae to get a function which can be then connected with a thermal sensation scale given mostly by questionnaires. Therefore, many scientists were wondering if there is any analytical index derived from physical equations. As a result, they built models that provide an insight into the processes of heat exchange between the human body and the environment and metabolic reactions on the heat stress.

In Thompson and Perry [1997], there is considered a full view of the energy balances of the environment and a human body. As for the human body, the homeothermy has a precondition of maintaining a constant core temperature near 37 °C. Hand in hand, there are seven interlaced groups of adaptation strategies to atmospheric, especially thermal, stimuli which Thompson and Perry [1997] defined as:

1. "Physiological adjustment, ranging from minor vasomotor to major sweating and metabolic responses"
2. "Acclimatisation (including habituation) of both physiological and psychological mechanisms by periodic exposure to a thermal stimulus"
3. "Food energy intake and dietary alterations"
4. "Metabolic alterations in the scheduling of activities, selection and curtailment of particular tasks or their sequencing."

5. "Migration, either temporary or permanent avoidance of particular stress conditions."

6. "Clothing and building fabric interposition between the source of stress and the organism."

7. "External energy generation for space heating and cooling."

The most desired adaptation strategy in urban areas is number 6 for its strategy of shading the environment to avoid heat stress. As an example, we can use the study Lin et al. [2010] where the shading effect in Taiwan university is being examined, and the results bring numerous positive findings of the modelling of the urban thermal environment and the shading effect on outdoor thermal comfort.

The best approach for the thermoregulatory responses is to use the human energy balance as shown in the following equation:

$$(M + W) + Q + R + C + E + S = 0, \tag{1.11}$$

where Thompson and Perry [1997] consider M metabolic heat, W is the energy used in work, Q stands for short-wave solar radiation income R, C, E represent the long-wave radiation, convection and evaporation, respectively and S is storage within body and must equal zero over time.

The equation 1.11 as an energy balance equation can be quantified by two personal and four atmospheric parameters, because the thermal condition is a function of the clothing insulation variable, as follows:

- Metabolic rate (M)
- Clothing insulation (I_{cl})
- Air temperature(T)
- Radiant temperature of surroundings(T_{MRT})
- Rate of air movement(v)
- Atmospheric humidity(RH)

The metabolic rate is the amount of energy used by a human per unit of time. The basal metabolic rate is defined as a metabolic rate at rest, so in every other state, the metabolic rate is higher than the basal metabolic rate, as shown in Figures 1.2 and 1.3.

Clothing insulation represents the amount and property of all clothing layers that human wear. Its units are Clo, where 1 Clo corresponds to a normal business suit with usual undergarments and footwear. Other examples are given by Figure 1.4 and 1.5.

Air temperature is the dry-bulb temperature measured in the area by either mechanical or digital thermometer. It is the most important input for the thermal comfort evaluation.

The radiant temperature of the surroundings is calculated by small-scale modelling (see Matzarakis et al. [2010b]), where the Stefan-Boltzmann law is used.

TABLE 2.1 **Metabolic Rates for Typical Tasks**

Activity	Metabolic Rate[a] met units[b]	Btu/h ft²	W/m²
Resting			
Sleeping	0.7	13	40
Reclining	0.8	15	45
Seated, quiet	1.0	18	60
Standing, relaxed	1.2	22	70
Walking (on the level)			
2 mph (0.9 m/s)	2.0	37	115
3 mph (1.2 m/s)	2.6	48	150
4 mph (1.8 m/s)	3.8	70	220
Office activities			
Reading, seated	1.0	18	60
Writing	1.0	18	60
Typing	1.1	20	65
Filing, seated	1.2	22	70
Filing, standing	1.4	26	80
Walking about	1.7	31	100
Lifting, packing	2.1	39	120
Driving/flying			
Car	1.0–2.0	18–37	60–115
Aircraft, routine	1.2	22	70
Aircraft, instrument landing	1.8	33	105
Aircraft, combat	2.4	44	140
Heavy vehicle	3.2	59	185
Miscellaneous occupational activities			
Cooking	1.6–2.0	29–37	95–115
House cleaning	2.0–3.4	37–63	115–200
Seated, heavy limb movement	2.2	41	130
Handling 110-lb (50-k) bags	4.0	74	235
Pick and shovel work	4.0–4.8	74–88	235–280
Machine work			
Sawing (table saw)	1.8	33	105
Light (electrical industry)	2.0–2.4	37–44	115–140
Heavy	4.0	74	235
Miscellaneous leisure activities			
Dancing, social	2.4–4.4	44–81	140–255
Calisthenics/exercise	3.0–4.0	55–74	175–235
Tennis, singles	3.6–4.0	66–74	210–270
Basketball	5.0–7.6	90–140	290–440
Wrestling, competitive	7.0–8.7	130–160	410–505

Source: Reprinted with permission of the American Society of Heating, Refrigerating, and Air-Conditioning Engineers, Inc. From 1997 *ASHRAE Handbook of Fundamentals.*

[a]For average adult with body surface area of 19.6 ft² (1.8 m²). For whole-body average heat production, see also Table 5.21.

[b]One met = 18.4 Btu/h ft² = 58.2 W/m².

Figure 1.2: Metabolic rate for different normal day activities suggested by Oliveira and Andrade [2007]

Activity	Metabolic rate (W m^{-2})
Resting (sitting)	60
Standing	90
Reading/ writing	100
Talking	100
Walking slowly	120
Walking fast	160
Other	Variable

Figure 1.3: Metabolic rate table for different normal day activities suggested by University of Oregon [2020]

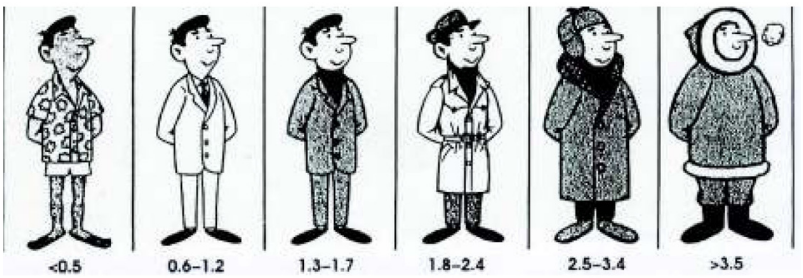

Figure 1.4: An overview on the Clo unit representation, Auliciems and Szokolay [2007]

TABLE 3 Insulating value of clothing elements

Man		clo	Women		clo
underwear	singlets	0.06	underwear	bra + panties	0.05
	T-shirt	0.09		half slip	0.13
	briefs	0.05		full slip	0.19
	long, upper	0.35		long, upper	0.35
	long, lower	0.35		long, lower	0.35
shirt	light, short sleeve	0.14	blouse	light	0.20
	light, long sleeve	0.22		heavy	0.29
	heavy, short sleeve	0.25	dress	light	0.22
	heavy, long sleeve	0.29		heavy	0.70
	+5% for tie or turtle-neck)				
vest:	light	0.15	skirt	light	0.10
	heavy	0.29		heavy	0.22
trousers	light	0.26	slacks	light	0.26
	heavy	0.32		heavy	0.44
pullover	light	0.20	pullover	light	0.17
	heavy	0.37		heavy	0.37
jacket	light	0.22	jacket	light	0.17
	heavy	0.49		heavy	0.37
socks	ankle length	0.04	stockings	any length	0.01
	knee length	0.10		panty-hose	0.01
footwear	sandals	0.02	footwear	sandals	0.02
	shoes	0.04		shoes	0.04
	boots	0.08		boots	0.08

based on ASHRAE 1985

Figure 1.5: A detailed Clo unit description, Auliciems and Szokolay [2007]

The model uses air temperature and cloud cover or global solar radiation as inputs.

Rate of air movement is usually described by the wind velocity where the direction is not needed in many models. Therefore the simple wind speed is being used.

Atmospheric humidity is one of the earliest variable used to calculate the "real feel temperature". It is often referred to as relative humidity (RH) and it is interchangeable with water vapour pressure (p_{WV}) using the saturation water vapour pressure (p_{SWV}):

$$RH = \frac{p_{WV}}{p_{SWV}}. \tag{1.12}$$

All of those variables are used in numerical calculations of the models for thermal comfort. For its nature, the atmospheric components are measured in time series at meteorological stations, whereas metabolic rate and clothing insulation are usually set constant on reasonable values.

Below are mentioned mainly those indices used in this study. For more thermal comfort indices, see Auliciems and Szokolay [2007], Section Analytical indices.

1.3.1 Klima Michel model

As the most simple indices using models we consider the Predicted Mean Vote (PMV) and Predicted Percentage of Dissatisfied (PPD) mentioned in Höppe [1999] and mainly thought to help air-conditioning engineers to create a thermally comfortable indoor climate. Later on, it was adjusted to outdoor conditions, and now it is also known as the Klima Michel model. PMV is based on an equation in Figure 1.6 where all variables are labelled. The large bracket in Figure 1.6 is the thermal load defined as the difference between the internal heat production and the heat loss to the actual environment.

American Society of Heating, Refrigerating and Air-Conditioning Engineers (ASHRAE) then extended the calculated PMV with a comfort scale (Table 1.3) where the values of PMV have a connection to the thermal sensation of persons as Mayer and Höppe [1987] states. Rosenfelder et al. [2016] extended the table to Table 1.4, where each of the classified value refers to the physical stress caused by the thermal environment.

PPD is derived from PMV as

$$\mathrm{PPD} = 100 - 95\exp(-0.03353\mathrm{PMV}^4 - 0.2179\mathrm{PMV}^2). \tag{1.13}$$

Therefore, the PPD establishes a quantitative prediction of the percentage of thermally dissatisfied people determined from PMV. For example, when the PMV is between -0.5 and 0.5, the corresponding PPD drops below 10%.

The model was made for calculating an integral index for the thermal component of climate. It was not established to give a realistic description of the thermal conditions of the human body. Therefore, it could be accepted without considering the body response on the change in thermal conditions. For instance, in Fanger's approach (Fanger [1972]) sweat rate and the mean skin temperature are quantified as comfort values. They are considered to be dependent only on activity and not on climatic conditions at all, as Höppe [1999] states.

$$PMV = (0.303e^{-0.036M} + 0.028) \times [(M - W') - 3.05 \times 10^{-3} \cdot \{5733 - 6.99(M - W') - Pa\} - 0.42\{(M - W') - 58.15\} - 1.7 \times 10^{-5} \cdot M \cdot (5867 - Pa) - 0.0014 \cdot M \cdot (34 - Ta) - 3.96 \cdot 10^{-8} \cdot fcl \cdot \{(Tcl + 273)^4 - (Tr + 273)^4\} - fcl \cdot hc \cdot (Tcl - Ta)]$$

$$Tcl = Tsk - 0.155 \cdot Icl \cdot [3.96 \times 10^{-8} \cdot fcl \cdot \{(Tcl + 273)^4 - (Tr + 273)^4\} + fcl \cdot hc \cdot (Tcl - Ta)]$$

$$hc = \begin{cases} 2.38(Tcl - Ta)^{0.25} \\ \quad for\ 2.38(Tcl - Ta)^{0.25} > 12.1\sqrt{Vair} \\ 12.1\sqrt{Vair} \\ \quad for\ 2.38(Tcl - Ta)^{0.25} \leq 12.1\sqrt{Vair} \end{cases}$$

Tcl = clothing surface temperature
Tsk = skin temperature

Figure 1.6: The definition of PMV Kon [1992]

Table 1.3: ASHRAE Psycho-Physical Voting Scale, taken from Mayer and Höppe [1987]

PMV	Sensation
-3	cold
-2	cool
-1	slightly cool
0	neutral
+1	slightly warm
+2	warm
+3	hot

Table 1.4: Classification of PMV values into thermal stress classes, according to Rosenfelder et al. [2016]

PMV	Thermal perception	Grade of physical stress
< -3.5	Very cold	Extreme cold stress
-3.5 to -2.5	Cold	Strong cold stress
-2.5 to -1.5	Cool	Moderate cold stress
-1.5 to -0.5	Slightly cool	Slight cold stress
-0.5 to 0.5	Comfortable	No thermal stress
+0.5 to +1.5	Slightly warm	Slight heat stress
+1.5 to +2.5	Warm	Moderate heat stress
+2.5 to +3.5	Hot	Strong heat stress
> +3.5	Very hot	Extreme heat stress

PT

Another thermal comfort index based on the Klima Michel model is the perceived temperature (PT). As the Jendritzky et al. [2000] states, PT is used in the routine procedure of the Deutscher Wetterdienst (German Weather Service). Although it can be considered as a commercial index, it is viewed for its complexity to be more suitable among the analytical and modelled indices.

As Jendritzky et al. [2000] defines, PT refers to a reference environment, in which the perception of cold and heat would be the same as under the actual conditions. The wind velocity is reduced to a slight draught, and the mean radiant temperature is equal to the air temperature in the reference environment. The water vapour pressure is identical to the actual environment. It is only reduced by condensation. Perceived heat and cold is computed using the comfort equation by Fanger [1972], which is based on a complete heat budget model of the human body.

Compared to the PMV and PPD, the PT is more difficult to compute for its need for iterations in the algorithm used to achieve the values. Utilising complexity, PMV is similar to the indices defined by the MEMI model such as PET and SET*.

1.3.2 MEMI Model

The Munich energy-balance model for individuals (MEMI) is a more advanced thermo-physiological heat-balance model using the human energy balance (1.11). Two other equations used to establish the mean surface temperature of the clothing (T_{cl}), the mean skin temperature (T_{sk}) and the core temperature (T_c). These equations describe the heat flows from body core to skin surface (F_{CS}), (1.14) and from skin surface through the clothing layers to the clothing surface, (F_{SC})

(1.15).

$$F_{CS} = v_b \rho_b c_b (T_c - T_{sk}) \tag{1.14}$$

$$F_{SC} = \frac{1}{I_{cl}} (T_{sk} - T_{cl}) \tag{1.15}$$

In (1.14), v_b stands for the blood flow from body core to skin ($\mathrm{ls^{-1}m^{-2}}$, depending on the level of skin and core temperature), ρ_b for blood density ($\mathrm{kgl^{-1}}$) and c_b for the specific heat ($\mathrm{WsK^{-1}kg^{-1}}$). In (1.15) I_{cl} is the heat resistance of the clothing ($\mathrm{Km^2W^{-1}}$). For these equation is MEMI model considered as a two-node model.

SET*

According to Ye et al. [2003], "SET* Index is defined as the equivalent temperature of an isothermal environment at 50% RH in which a subject while wearing clothing standardised for the activity concerned, would have the same heat stress (skin temperature, T_{sk}) and thermoregulatory strain (skin wettedness w) as in the actual test environment. Isothermal environment means the environment at sea level, in which the air temperature equals the mean radiant temperature, and the air velocity is zero." H_{sk} is defined as the heat loss from the skin, i.e. the thermal load of skin, and it can be expressed as:

$$H_{sk} = h_s(T_{sk} - \mathrm{SET^*}) + w h_{s,e}(p_{wv,s} - 0.5 p_{SET*}), \tag{1.16}$$

where h_s stands for standard heat transfer coefficient in $\mathrm{Wm^{-2}\ ^\circ C}$, $h_{s,e}$ is the standard evaporative heat coefficient in $\mathrm{Wm^{-2}kPa^{-1}}$, w the fraction of the wetted skin surface, $p_{wv,s}$ the water vapour pressure at skin, normally assumed to be that of saturated water vapour at T_{sk} in kPa and p_{SET*} refers to the saturated water vapour pressure at SET* in kPa, as Ye et al. [2003] continues. It is not necessarily defined on a MEMI model. Also, another two-node model can be used for it is not specified.

PET

As one of the most used indices, physiological equivalent temperature (PET) was introduced in 1987, as Höppe [1999] reads. Physiological equivalent temperature (PET) has definition valid outdoors and indoors. Let us assume a typical indoor setting, where the heat balance of the human body is based on work metabolism of 80 W (light activity), basic metabolism and a heat resistance of clothing 0.9 Clo. PET is the equivalent to the air temperature which, in such environment, is maintained with core and skin temperatures equal to those under the conditions being studied, Höppe [1999] continues.

For indoor PET, there are a few simplifications of the model, such as:

- Mean radiant temperature equals air temperature
- Air velocity is set to 0.1 $\mathrm{ms^{-1}}$

- Water vapour pressure is set to 12 hPa (approximately equivalent to a relative humidity of 50% at air temperature 20 °C))

Calculation of the thermal conditions of the body with MEMI for a given meteorological parameters, iteration of the firstly guessed values for mean skin temperature and core temperature is then put into the model MEMI and the equation system ((1.11), (1.14) and (1.15)) for air temperature T (with v = 0.1ms^{-1}, p_{WV}= 12hPa and $T_{MRT} = T$) is being solved. The resulting air temperature is equivalent to PET.

1.3.3 FPC advanced Model

Since 2005, the COST Action 730 (Cooperation in Science and Technology, supported by the EU RTD Framework Programme) joined a Commission "On the development of a Universal Thermal Climate Index (UTCI)" that has provided the basis for European scientists from 19 countries and more to collaborate on the development of a corresponding index (COST UTCI 2004). As Jendritzky et al. [2012] state, "the aim was an international standard based on the latest scientific progress in human-response-related thermo-physiological modelling over the last four decades. The term universal must be understood in terms of being appropriate for all assessments of the outdoor thermal conditions in the major human biometeorological applications such as daily forecasts and warnings of extreme weather, to bioclimatic mapping, urban and regional planning, environmental epidemiology and climate impact research. This covers the fields of public weather service, the public health system, careful planning, and climate impact research in the health sector." Jendritzky et al. [2012] continues, the UTCI must meet the following requirements:

1. "Thermo-physiologically responsive to all modes of heat exchange between body and environment"
2. "Applicable for whole-body calculations but also for local skin cooling (frostbite)"
3. "Valid in all climates, seasons, and time and spatial scales"
4. "Appropriate for key applications in human biometeorology (listed below)"

The passive system of the Fiala's multi-node human physiology and thermal comfort (FPC) model includes a multi-segmental and multi-layered representation of the human body using spatial subdivisions, as Jendritzky and de Dear [2009] reads. Appropriate thermo-physical and thermophysiological properties give all tissue nodes. An average person is replicated by the data with consideration of body weight, body fat content, and Dubois surface area. The overall data creates a basal heat output and basal cardiac output which are appropriate for a nude adult body in a thermo-neutral environment of 30°C. In these conditions, the thermoregulatory activity is minimal.

FPC was adopted in terms of thermo-physiology and heat exchange theory. The next logical step is a state-of-the-art adaptive clothing model, which was developed and integrated to upgrade the FPC model. According to Jendritzky et al. [2012], the model considers:

1. "The behavioural adaptation of clothing insulation observed for the general urban population concerning the actual environmental temperature."

2. "The distribution of the clothing over different body parts providing local insulation values for the different anatomical segments."

3. "The reduction of thermal and evaporative clothing resistances caused by wind and limb movements of the wearer, who is assumed to be walking at a speed of 4 kmh^{-1} on level ground (2.3 met = Wm^{-2})."

UTCI

Universal Thermal Climate Index (UTCI) was then developed identically as an equivalent temperature (ET*), see Auliciems and Szokolay [2007]. It is one of the youngest indices, and its necessity has been discussed in Jendritzky et al. [2012]. The discovery involved a definition of a reference environment with 50% relative humidity (but vapour pressure not exceeding 20 hPa), with calm air and radiant temperature equalling air temperature, to which all other climatic conditions are compared, as Jendritzky et al. [2012] reads. Identical physiological conditions are ensured by the equivalence of the dynamic physiological response predicted by the model for the reference and the actual environment. The dynamic response is multidimensional (body core temperature, sweat rate, and skin wettedness, and more, at different exposure times). Also, by principal component analysis as a single-dimensional representation of the model response, a strain index was calculated, as Bröde et al. [2010] states.

For a given combination of air temperature, wind speed, radiation and humidity, the UTCI is defined as the air temperature of the reference environment that produces the same strain index value, as Jendritzky et al. [2012] states. The calculation of the UTCI equivalent temperatures by repeatedly running the thermoregulation model could take too much time. Therefore, a new quick calculation procedure has been developed and made available, as Bröde et al. [2010] claims.

The UTCI is calculated on a multi-node advanced FPT model, to be precise 343-node multi-segment model using more than 1000 simulations cases, according to Chen and Matzarakis [2014].

1.3.4 YCC-thermoregulation model

The core of the YCC-thermoregulation model is 16- to 26- nodes that used the passive body model based on Pennes' bio-heat equation (Ennes [1998]). The YCC model was created when those equations were applied in Fiala's model and convective and radiant principles in MEMI model, as Chen and Matzarakis [2014] reads. It is the combination of the two former models that adapt the complexity of the FTP model and the universality of the MEMI model. A blood pool element and a bio-heat transfer principle has been used as well as a multi-layer clothing model with clothing insulation and vapour resistance. Due to this modifications, we can develop a new thermal comfort index, similar to PET.

mPET

The modified physiologically equivalent temperature (mPET) is defined identically to the PET, but instead of the two-node MEMI model, it uses YCC-thermoregulation model developed by Chen and Matzarakis [2014]. It was developed for universal application in different climate zones. The weaknesses of the original physiologically equivalent temperature (PET) has been overcome by enhancing evaluation of the humidity and clothing variability as well as using the more complex model, according to Chen and Matzarakis [2018].

2. The practical use of thermal indices

Thermal comfort in urban areas is affecting human lives from the quality of sleeping (Li et al. [2020]) up to daily activities (Brandenburg et al. [2007]). Apparently, in comfortable weather, there are more activities taking part outside. Weather affects our behaviour and is related to recreational activities, i.e. sports, cycling, walking, gardening, and more, as well as everyday activities. i.e. commuting to work or school, shopping, working, and more. Cycling includes both commuting and recreational aims. Brandenburg et al. [2007] explains the relationship of recreational cyclists and commuting cyclists to temperature, precipitation and thermal comfort. The study explains the importance of the thermal comfort model for the daily weather forecast in the meaning of additional information for the general public.

There were more appeals to the weather forecast media to include one of the thermal indices in the session. Meteorological centres in different countries have developed their thermal comfort index, and some of them are including the index in the forecast. There are even papers about the implementation of the indices in the forecast, i. e. the one mentioned in Giannaros et al. [2018]. However, the appearance of any thermal index is rather poor or none at all in public media. The usage reaches from architecture through tourism to everyday situations.

Other useful applications of the thermal indices are urban planning, including tree planting and using high albedo materials, tourism in the sense of climatological data and thermal discomfort followed by mortality.

2.1 Urban planning

With the ongoing urbanization, the effect of UHI is being enhanced as the cities grow, and the population is higher each decade. Thus, there were many studies trying to improve the thermal comfort in the cities by urban planning, see Wonorahardjo et al. [2020], Ouali et al. [2020], Feng et al. [2020], Gatto et al. [2020], Abdi et al. [2020] and Aram et al. [2019]. Such studies concentrate on the thermal comfort of humans outdoors considering different patterns, mainly of buildings and green areas. The results are similar for having high temperatures in summer, where green areas grant more comfortable sensations than other urban landscapes. Different approaches for enlargement of parks and pedestrian green areas are suggested in most cities.

Other studies go more into the combination of buildings and tree planting utilizing both into green roofs or green walls, as Netam et al. [2019] and Mutani and Todeschi [2020] states. They found the green roofs and green walls are increasing the thermal comfort outdoors and appeal to urban planners for using those new elements in building development.

Another point of view is the passive cooling of the buildings. Considering the indoor comfort, the size of windows has a small effect on the cooling effect as well as in some situations green roofs and green walls, as Netam et al. [2019] reads. However, the outdoor comfort is improved by green roofs and green walls as is

written above. The thermal comfort for buildings is being studied in terms of used material on the building. As an example, the study Wonorahardjo et al. [2020] is worth mentioning. For the energy heat balance, a net radiation equation has been used to study new possibilities of passive cooling, which lead to a study of high albedo materials. It is based on reducing the net radiation on the building and therefore passively cooling the indoor space. Falasca et al. [2019] and Taha et al. [1992] suggest using high albedo materials to not only reduce the indoor net heat and provide comfort. It is also meant to lower the energy needs of the building caused by cooling during summer, to increase pedestrian thermal comfort. It can also mitigate the consequences of heatwaves in cities.

2.2 Thermal indices in tourism

Thermal indices can also be used for tourism purposes. Some studies did extrapolations of the thermal index values for a large area as Matzarakis et al. [2010a] did and some went further to generally describe indices in different climate zones. For each climate, a new comfortable sensation range was defined when a study was published. The comfort zone was always defined, as shown in Lin and Matzarakis [2008]. The Table 2.1 shows the calculated comfortable sensation ranges for different Köppen-Geiger climatic zones according to the mentioned locations. Yang and Matzarakis [2016] compares different climatic zones in China to highlight the difficulty in the transition of the connection between thermal sensation and PET in different zones. It is suggested to calibrate the scale for every zone or study the differences via surveys for travellers. These findings can serve as an estimate thermal sensation for people from one climatic zone travelling to a different zone.

Matzarakis [2007b] has developed a simple graph for the general public called climate–tourism–information–scheme (CTIS) where important climate information for tourist about a destination can be found. The CTIS is meant to be used as a detailed leaflet to anticipate thermal comfort, as well as aesthetic and physical conditions for planning trips and holiday. In the graph, there are variables presented using frequencies, for each month in a year. The months are further divided into thirds (10-day interval). The factors and criteria shown in CTIS are originally stated in Matzarakis [2007b].

The CTIS has been developed based on Matzarakis [2006] in need of short and rich information for the public to educate about climate specifics in the destination. Since than it was used mainly for PET as can be seen in Zaninović and Matzarakis [2009], Matzarakis et al. [2013], Matzarakis [2007a] and Lin and Matzarakis [2008] where climatic information for tourists about different cities are summed in CTIS. An example of CTIS based on the data form this thesis is in Figure 2.2.

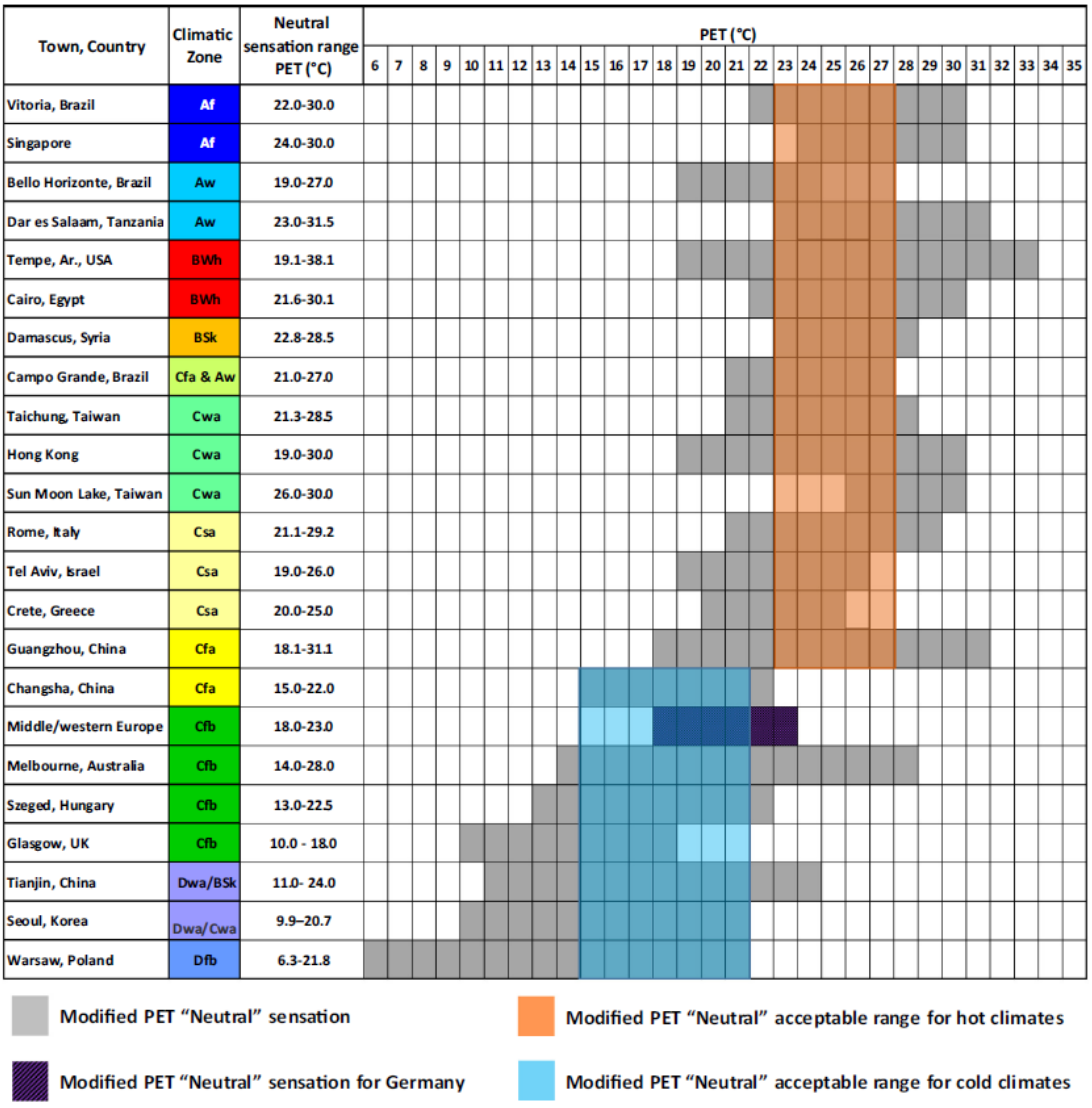

Figure 2.1: PET thermal index has in different climates specific comfortable zone as published in Potchter et al. [2018].

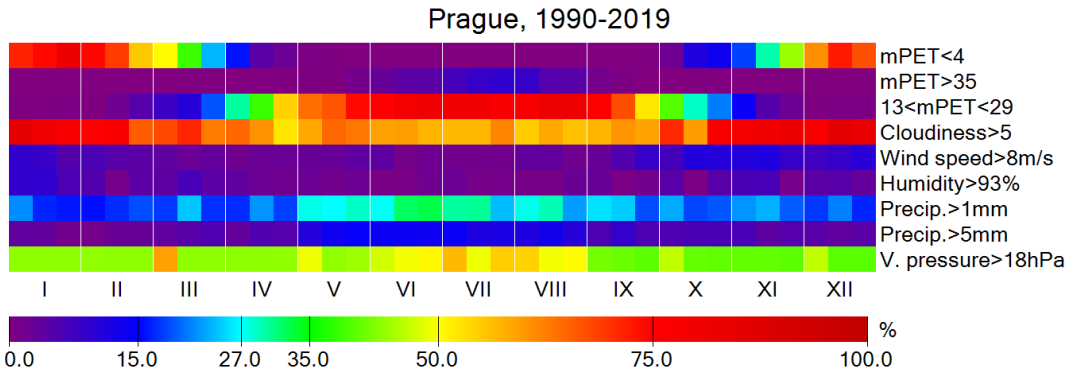

Figure 2.2: CTIS providing basic information about Prague serving also as tourist information. Variables are displayed based of their frequency of occurrence.

A similar approach has been described in De Freitas et al. [2008] where the probability CTIS scale is expressed in seven climate classes from very poor through marginal to ideal scale evaluating the variables in CTIS. For some variables, higher probability means less favourable conditions. It offers even more simplified information for even more general public. The cost of the simplification is losing the information of frequencies for further consideration of a trip or holiday. An example of the simplified CTIS based on the data form this thesis is in Figure 2.3.

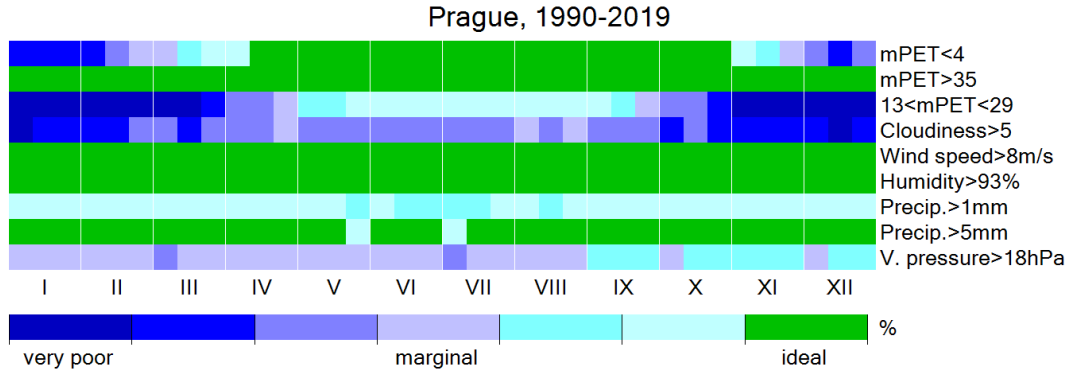

Figure 2.3: CTIS providing simplified information about Prague serving also as tourist information. Variables are rated according to suitability for visiting from very poor to ideal.

2.3 Effects on mortality

Thermal discomfort can be expressed by two extremes - cold, and heat discomfort connected to cold and heat stress. Humans have inhabited different areas on the Earth with a variety of specific climates and, in most of the areas, they have adapted to the thermal conditions. However, cold and heat extremes exist in many places in different seasons, e.g. cold spells or heat waves, causing discomfort to human beings.

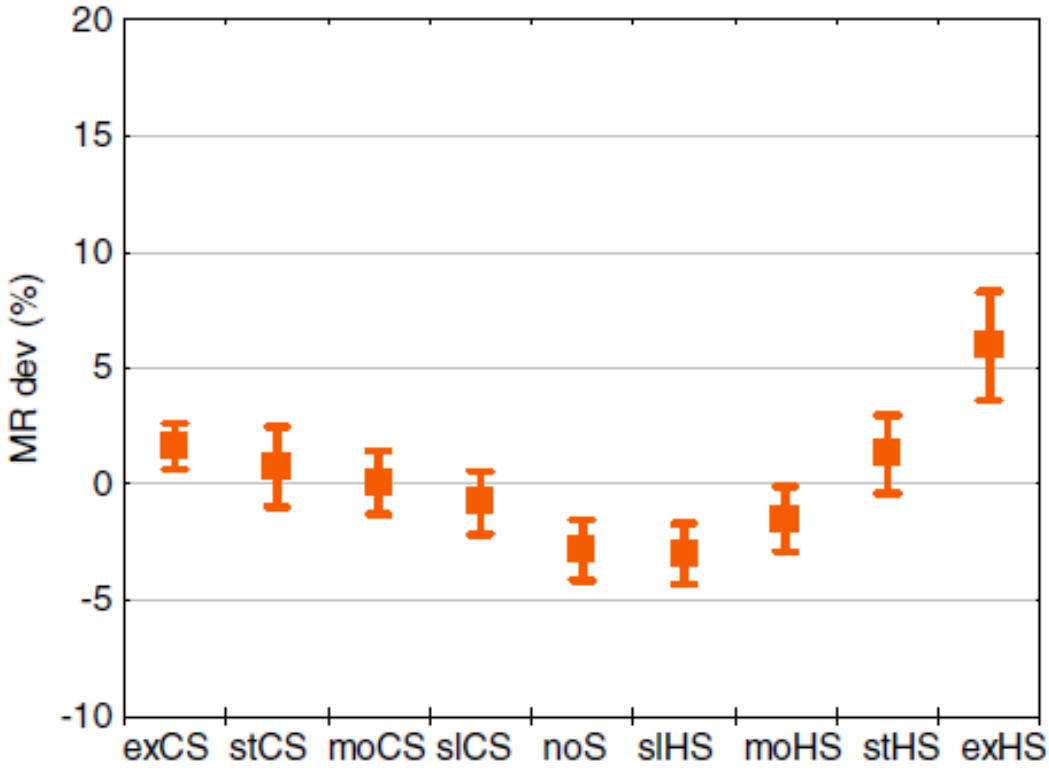

Figure 2.4: Mortality rate deviation in Croatian Zagreb by Zaninović and Matzarakis [2014], error bars show standard deviation. Graph shows mortality rate for different levels of thermal stress for PET at 14:00 with the inclusion of short-term adaptation. *ex* Extreme, *st* strong, *mo* moderate, *sl* slight, *HS* heat stress, *CS* cold stress, *noS* no thermal stress.

During the extreme conditions, women seem to be more vulnerable than men, probably due to a higher number of older women and their different thermophysiology, as Zaninović and Matzarakis [2014] states. Also, other people affected the most by the discomfort are socially sensitive people due to a reduced possibility of migration and those exposed to high or low temperature while at work. There are also proves of the thermal discomfort effect on mortality in various areas.

The mortality rate has been studied in different cities and climates. However, the general relationship with thermal comfort is similar. In Gabriel and Endlicher [2011], Urban and Kyselý [2014], Zaninović and Matzarakis [2014], Nastos and Matzarakis [2012], Matzarakis et al. [2011] and Ruuhela et al. [2017], the mortality rate in Germany, Czech Republic, Zagreb (Croatia), Vienna (Austria), Athens (Greece) and Finland respectively has been studied. The relationship between the thermal comfort and mortality rate, taken from Zaninović and Matzarakis [2014], is described in Figure 2.4. The overall result is summarized for mortality rate deviation which is at its lowest (negative) in no thermal stress and slight heat stress situations, and it increases (to positive) towards more cold stress as well as towards more heat stress. It is notable that with the increasing heat stress, the mortality rate deviation increases more quickly than with the increasing cold stress.

3. The most suitable indicators to describe the thermal comfort

3.1 The selection of appropriate thermal indices

As was described in the previous chapter, the number of all thermal comfort indices is more than 165. However, not all of them are relevant, some of them are dependent, and many are inappropriate or even inaccurate as Staiger et al. [2019] claims. In this chapter, the best thermal indices are to be found to use for the research based on data from meteorological stations.

The methodical framework for the selection of thermal indices for application in the research has met an agreement with the methodology of Staiger et al. [2019], i. e. only indices meeting the below-mentioned criteria are suitable:

1. "The index must be defined in a model providing a rational representation of the human body involving heat transfer between the body and the environment, the anthropometry and thermal properties of the body and a dynamic (transient) representation of the human thermoregulatory. It includes every complete model of the human energy balance, including passive and active thermoregulation which are integrated into a steady state." Cited also from Parsons [2014] and Yokota et al. [2014].

2. "The index needs to take a form of an equivalent temperature, i. e. there must be a comparison between an actual environment and a reference environment, where mean radiant temperature (T_{MRT}) equals the dry-bulb temperature, and the wind velocity is minor so that a reference subject will show identical (selected) thermo-physiological values in actual and in a reference environment."

3. "The index cannot be defined only for certain environments, it must be worldwide applicable."

Applying those criteria to all of the affordable indices, Staiger et al. [2019] has chosen seven indices appropriate to describe the thermo-physiologically consistent assessment of the human thermal environment. They all have been categorized as Energy balance stress index and refer to two- or multi-node models. The selected indices are the Universal Thermal Climate Index (UTCI), Physiologically Equivalent Temperature (PET), Perceived Temperature (PT), Standard Effective Temperature (SET*), Standard Effective Temperature Outdoors (OUT_SET*), Effective Temperature (ET*) and Humid Operative Temperature (HToh). Although PMV is still used as a simple thermal index with a simple scale for the explanation of thermal comfort for the general public as shown in Kumar [2019], it has not been selected for this study as an optimal index for its limited values.

In the closer look at the indices, three of them were excluded for different reasons. OUT_SET* was removed for its identical definition to SET*. The only difference was the calculation of the T_{MRT} outdoors, which has a significant problem resulting in unrealistic high values of absorbed radiant energy. ET* was not

selected also for its similarity with SET*. In contrast to ET*, the value of SET* and other selected indices vary with the clothing insulation and metabolic rate of interest of the subject concerned. Therefore, ET* is not universal. Finally, HToh is not considered for its similar definition to ET* and SET*, where the two are defined for RH = 50%, whereas HToh is set with RH = 100%. It is viewed as a non-realistic when it should be used worldwide.

Among the examined indices the new modified Physiologically Equivalent Temperature (mPET) was missing in Staiger et al. [2019]. It has been developed as an improvement of PET using the multi-node model defining UTCI. Therefore, it is considered as more advanced an at least as appropriate as the other four chosen indices.

In the end, the only indices that passed through the elimination system in Staiger et al. [2019] are UTCI, PET, PT and SET*. In this thesis, the four indices are joined by mPET as this was not considered in the cited study. All of them will be applied to the data, and according to the studied behaviours, one will be used primarily to describe the data in the present thesis.

3.2 The application of the human heat balance model

For the actual computation of the five chosen indices, the establishment of the human body and environment model is required. For the purpose of their calculation, the models RayMan (Matzarakis et al. [2007] and Matzarakis et al. [2010c]) and SkyHelios (Matzarakis and Matuschek [2011]) were considered for their capability and numerous usage in human thermal comfort research. For the numerical calculations of the above-chosen indices, RayMan model was used for its suitability and simplicity and the emerging fast integration to the whole process. The program SkyHelios was also tested, but it was not chosen for its unstable behaviour, not functioning methods and no solution for fixing the bugs. It can be caused by using a newer operating system or other technical issue and lack of support. More comparison is given by Matzarakis [2014].

3.2.1 RayMan model

RayMan stands for "radiation on the human body". It is a model of the human heat balance with the environment capable of evaluation of thermal indices PMV, PET, SET*, UTCI, PT and mPET. Thus, this ability is suitable for this thesis of thermal comfort in urban areas. It has been developed and updated mainly by Prof. Andreas Matzarakis. The program is free to use for scientific purposes (see https://www.urbanclimate.net/rayman/).

As inputs to the model, it is needed to provide at least four meteorological variables, geographical data, date and time data, personal data, clothing and activity. From the meteorological quantities, it is necessary to use the air temperature T, wind velocity v, relative humidity RH or water vapour pressure p_{WV} and global radiation G or cloud cover CC. As the geographical data, longitude, latitude and altitude are required as well as the timezone offset from the UTC. Date and time are inserted separately. Personal data consists of height, weight,

age and sex. Clothing is described in Clo units, activity is in watts according to the activity one is doing. Lastly, there is a switch between standing and sitting position. The main output is thermal indices.

The process is simplified by reading data from a datafile and inserting computed values straight to the text file. Using this approach leads to a faster evaluation of the thermal comfort indices as the given data from the meteorological stations are usually already in the appropriate input format.

The RayMan model requires the data of air temperature in °C, wind speed in ms^{-1}, relative humidity in % and cloud cover in octas (eights). As the output, the chosen five thermal indices were received.

Model Rayman also offers an option for basic modelling of the street canyon including buildings and trees with given emission coefficient and albedo. The model requires the point of calculation and the meteorological input to compute the resulting thermal environment. By this approach, the specific thermal comfort of a place in a city can be calculated.

3.3 Description of data

The five chosen indices have been calculated for the data provided by Deutscher Wetterdienst (DWD), German weather service, via Climate Data Center (CDC) and ČHMÚ, Czech weather service. The data consists of air temperature, wind speed, relative humidity, cloud cover, mean sea level pressure, dew-point temperature, wind direction and precipitation. The map in Figure 3.1 presents the locations of the meteorological stations in Germany and the map in Figure 3.2 shows the stations in the Czech republic which were considered in the study.

The choice was made to select big cities with more stations nearby. Therefore, Prague, Berlin, Hamburg, Nürnberg, Köln and Frankfurt were chosen with near stations around. The period of the data is from 1990 to 2019, i. e. 30 years of data, with measurements at 7, 14 and 21 hours each day, although not every station has been measuring through the whole thirty years. The selected stations are mentioned in Table 3.1. There are four city stations for Berlin, two city stations for Prague and one station for each of the other chosen cities. It also includes the rural stations. All stations are aligned using the city it was compared with and then alphabetically. The selection of the stations and the city it was compared with is based on a maximum 120 km distance. Another choice parameter for the stations was its altitude, where the difference of the altitudes of the station and the city cannot be larger than 150 m. Also, only stations with similarly long data series as the city stations are considered. The rural reference stations were also selected only from villages and cities with less than 25 000 citizens (except Potsdam, but the station is in a park far from the city centre).

As Table 3.1 shows, the comparisons will be made for Berlin 1990-2019, considering even stations Tegel and Tempelhof that were measured in years 1995-2019 and 1990-2008 and 2009-2019 separately for Dahlem. For Nürnberg are data in years 2002-2020 and for Köln, Prague and Frankfurt 1990-2019. The data from the whole 30-year period are not available in every station, especially in the rural stations, where the measurements began later.

After the selection, for every mentioned city, corresponding values for rural areas are calculated. The rural stations' set requires all stations with the same

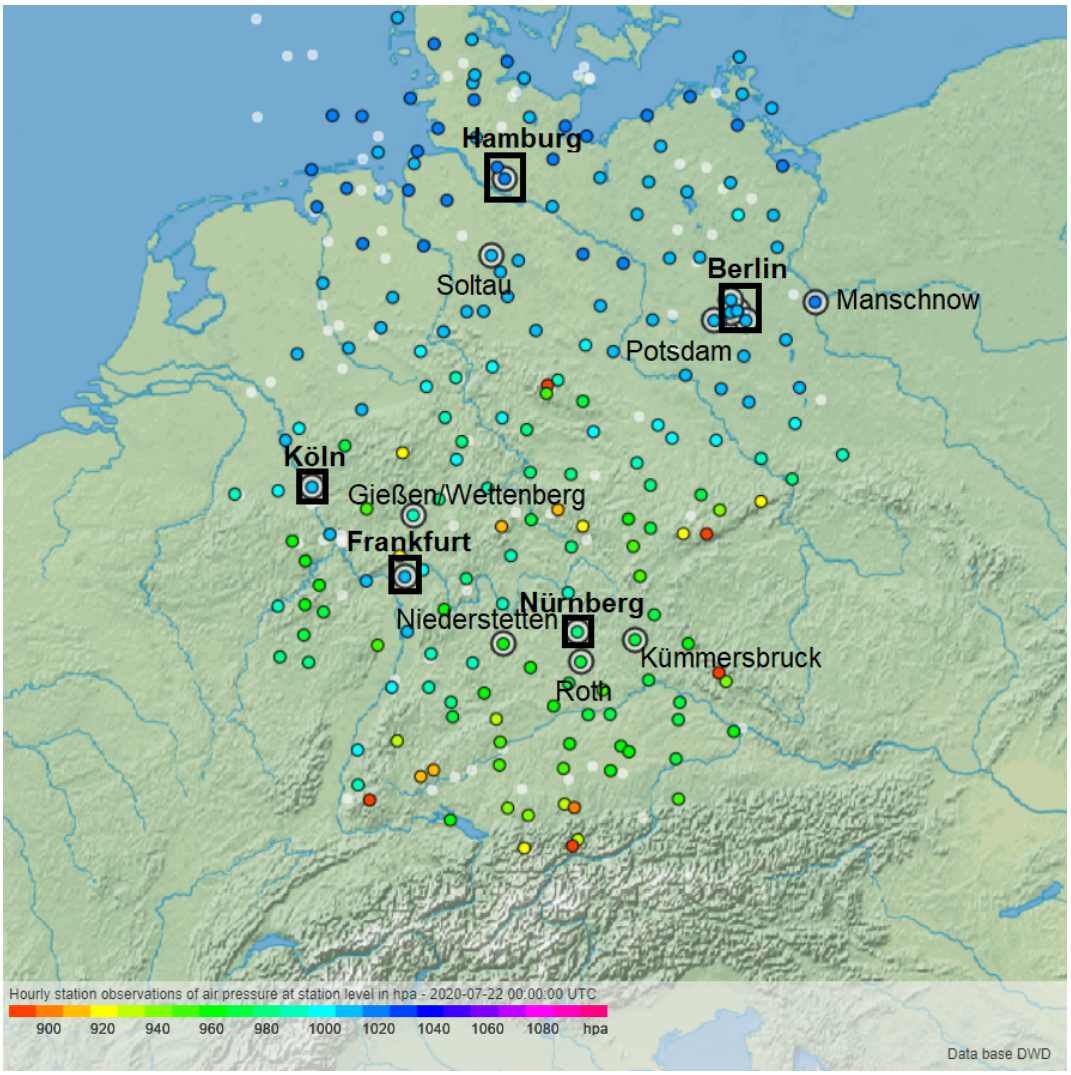

Figure 3.1: Map of meteorological stations in Germany. Colourful points represent all meteorological stations with the desired measured variables and encircled points are stations used in the study.

Table 3.1: The list of Meteorological stations used in the study with the names and locations. The city is the studied city the station is compared with - (B)erlin, (H)amburg, (N)ürnberg, (K)öln, (F)rankfurt, (P)rague - and Years are chosen according to availability of the temperature, humidity, wind speed and cloud cover data. The letter of city in brackets marks the city stations.

City	Name of the station	Longitude [°E]	Latitude [°N]	Altitude [m]	Years
P	Čáslav	15.393388	49.901637	251	1990-2019
P	Doksany	14.170976	50.458773	158	1990-2019
(P)	Praha-Karlov	14.427743	50.069181	260	1990-2019
(P)	Praha-Libuš	14.446957	50.007343	305	1990-2019
(B)	Berlin-Dahlem (FU)	13.3017	52.4537	51	2009-2019
(B)	Berlin-Schönefeld	13.5306	52.3807	46	1990-2019
(B)	Berlin-Tegel	13.3088	52.5644	36	1995-2019
(B)	Berlin-Tempelhof	13.4021	52.4675	48	1990-2008
B	Manschnow	14.5452	52.5468	12	1991-2019
B	Potsdam	13.0622	52.3813	81	1990-2019
(H)	Hamburg-Fuhlsbüttel	9.9881	53.6332	11	1990-2019
H	Soltau	9.793	52.9604	75	1990-2019
N	Kümmersbruck	11.9016	49.4283	417	2002-2019
N	Niederstetten	9.9666	49.3895	459	2002-2019
(N)	Nürnberg	11.0549	49.503	314	2002-2019
N	Roth	11.1036	49.2164	386	2002-2019
(K)	Köln-Bonn	7.1575	50.8646	92	1990-2019
(F)	Frankfurt am Main	8.5213	50.0259	100	1991-2019
F, K	Gießen/Wettenberg	8.6439	50.6017	203	1990-2019

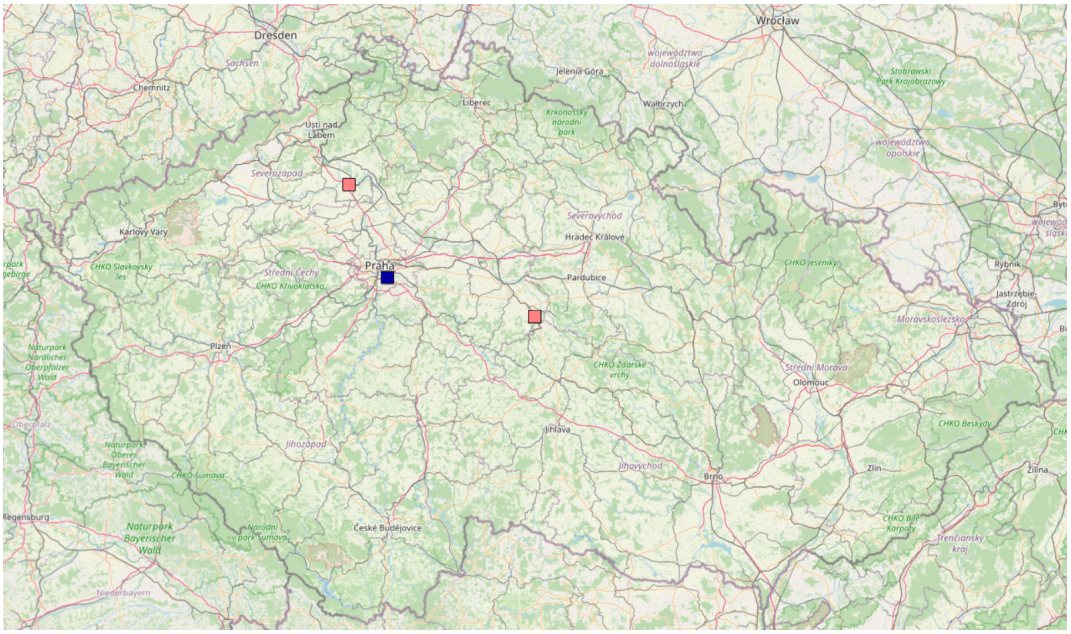

Figure 3.2: Map of meteorological stations in the Czech Republic. The blue square in Prague are the two city meteorological stations in Prague, and red squares represent the reference stations.

city omitting the actual city stations. The set is a weighted mean, where the mean is calculated using a reciprocal distance between the station and the city as a weight. The set was calculated using the original measured variables, and then the respective thermal indices were computed.

3.4 The variance of the thermal indices

Next step is to examine the variance of the thermal indices in dependency on the given meteorological inputs. In the Figures 3.3, 3.4, 3.5, 3.6, 3.7, 3.8, 3.9 and 3.10, there are shown the dependencies of the five chosen thermal indices on the air temperature, wind speed, relative humidity, cloud cover, mean sea level pressure, dew-point temperature, wind direction and hourly precipitation amount respectively. It includes all data form all stations mentioned in Table 3.1.

An overall comparison between the calculated indices is shown in Figures 3.3 - 3.10 at the bottom right corner. The most considerable spread has UTCI with a maximum without any outlying points, many outlying points decreasing the minimum and the lowest mean value. The lowest spread has mPET, which is also showing the highest mean of all indices.

From Figure 3.3 is evident that the UTCI has the most prominent spread for the temperatures in the situation with air temperature below 20°C. As for the higher values, all indices except UTCI show a comparable spread. PET is also the one showing the highest values. Not the highest nor the lowest values in the graph has the PT as it stands between UTCI and the rest of the indices. PET shows in the warm temperatures the highest values, whereas in cold temperatures mPET has the highest values.

In Figure 3.4, the cooling effect of the wind is significant for UTCI more than

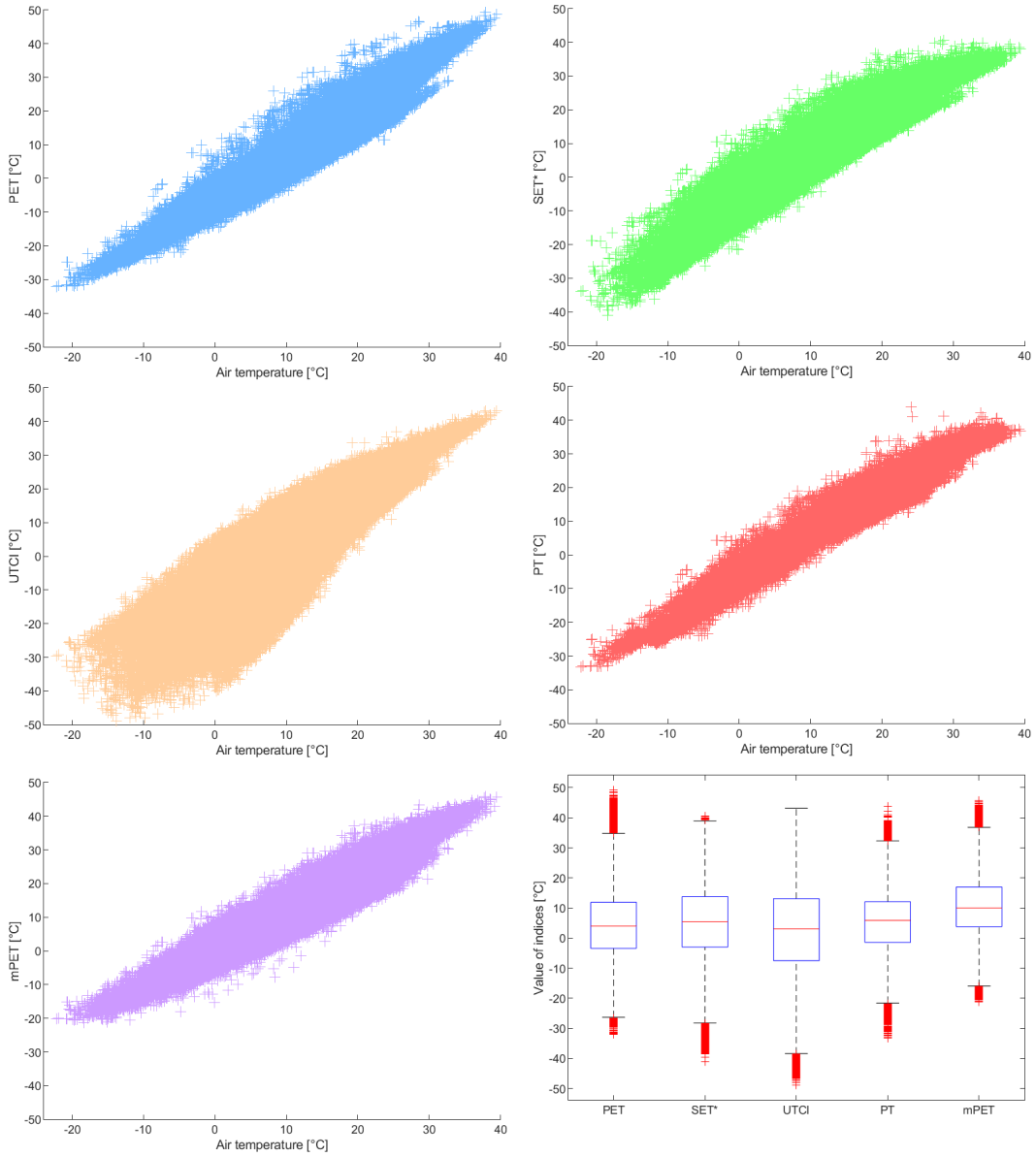

Figure 3.3: Five thermal indices dependencies on air temperature using all available data (1990-2019). The sixth graph (at bottom right) shows boxplot of the thermal indices with mean at the red line.

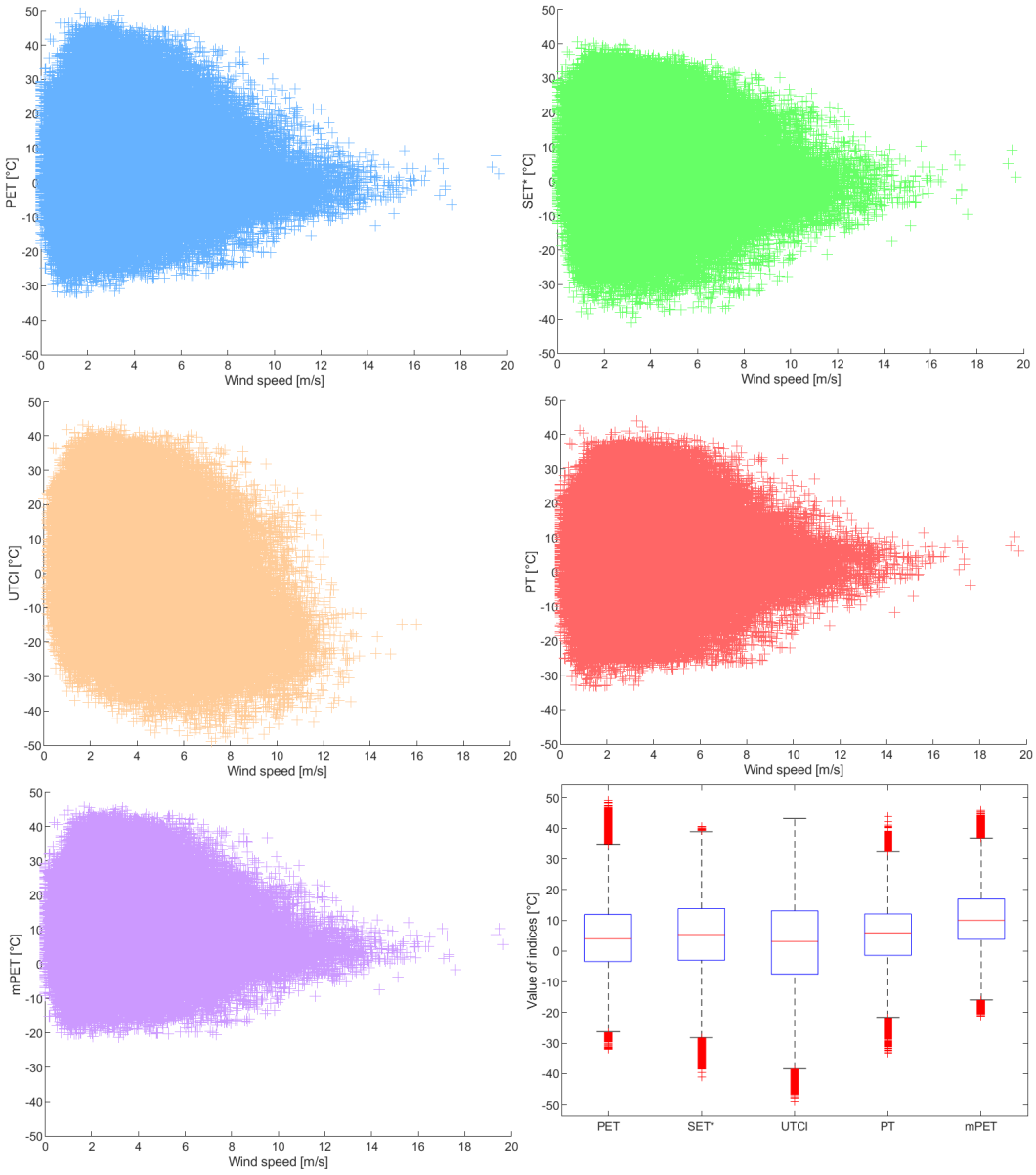

Figure 3.4: Same as Figure 3.3, but showing dependency on wind speed.

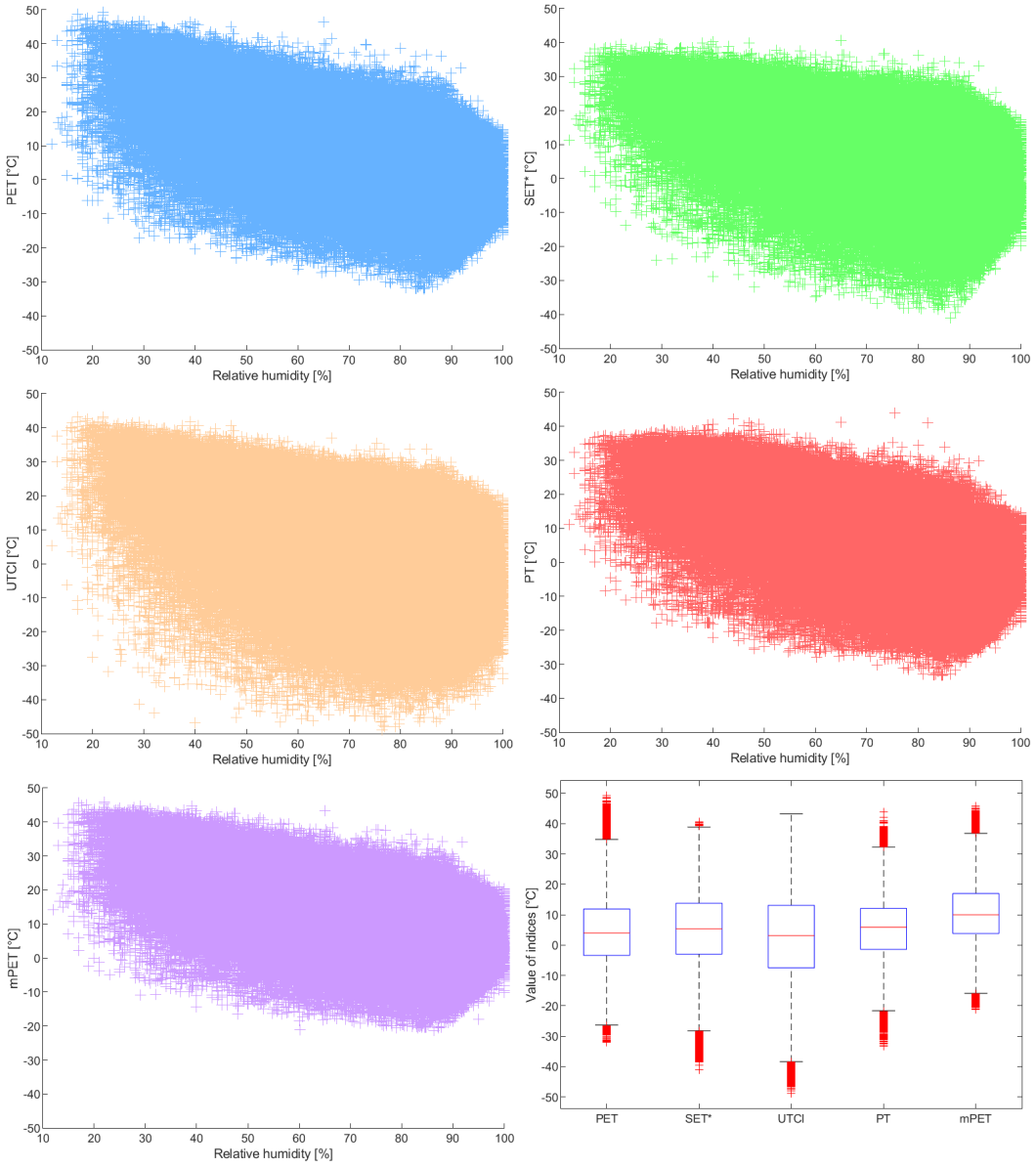

Figure 3.5: Same as Figure 3.3, but showing dependency on relative humidity.

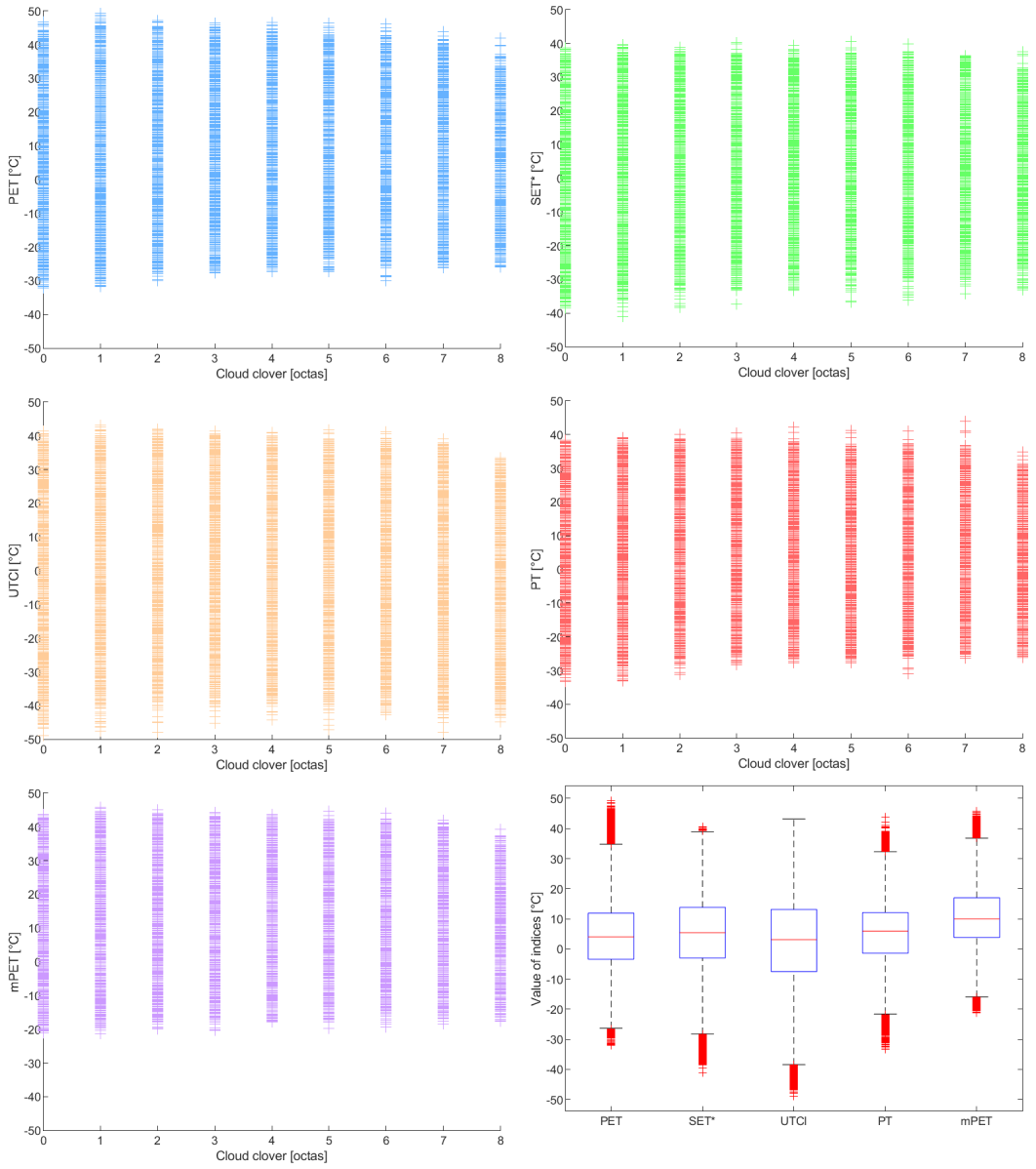

Figure 3.6: Same as Figure 3.3, but showing dependency on cloud cover.

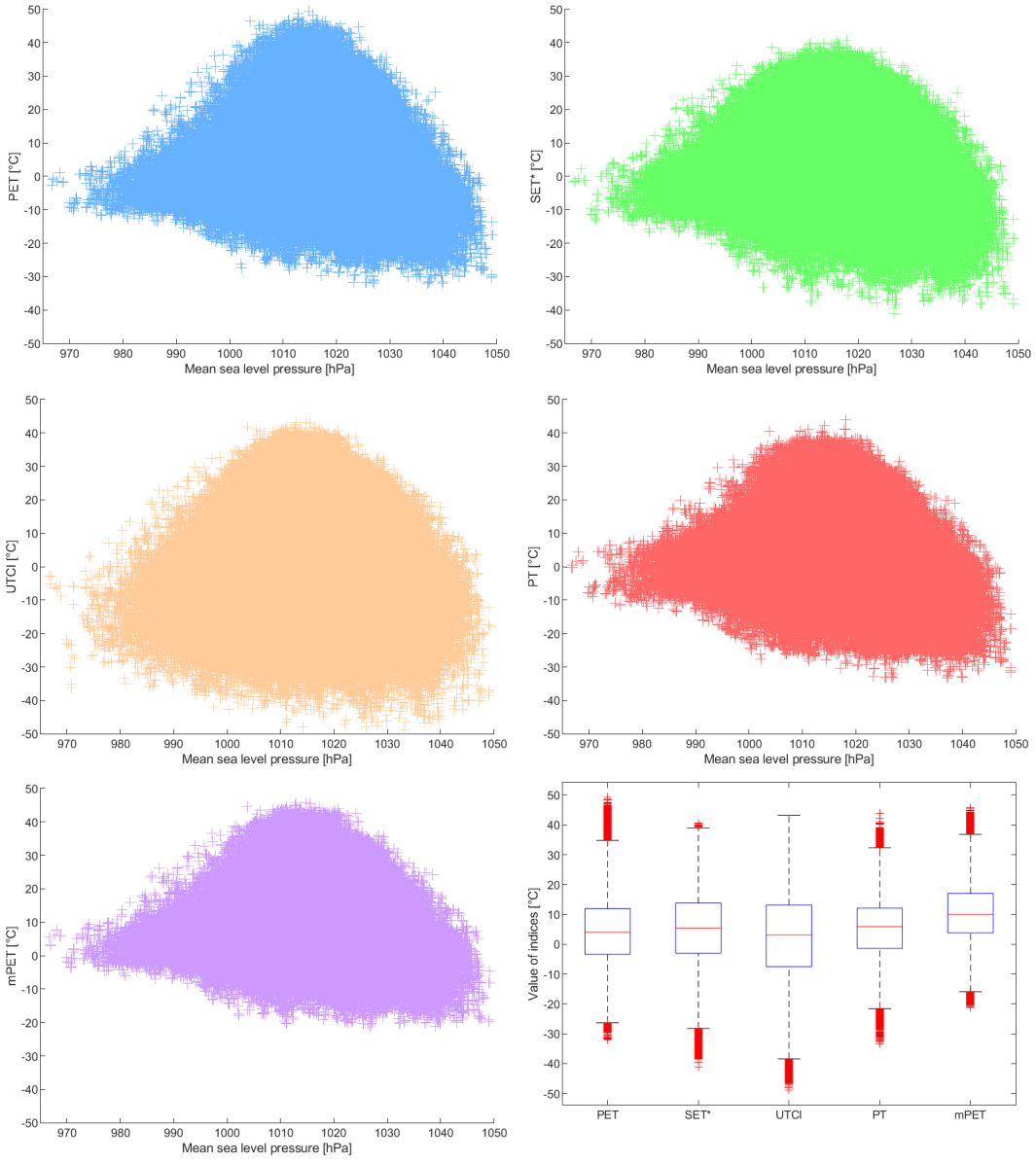

Figure 3.7: Same as Figure 3.3, but showing dependency on mean sea level pressure.

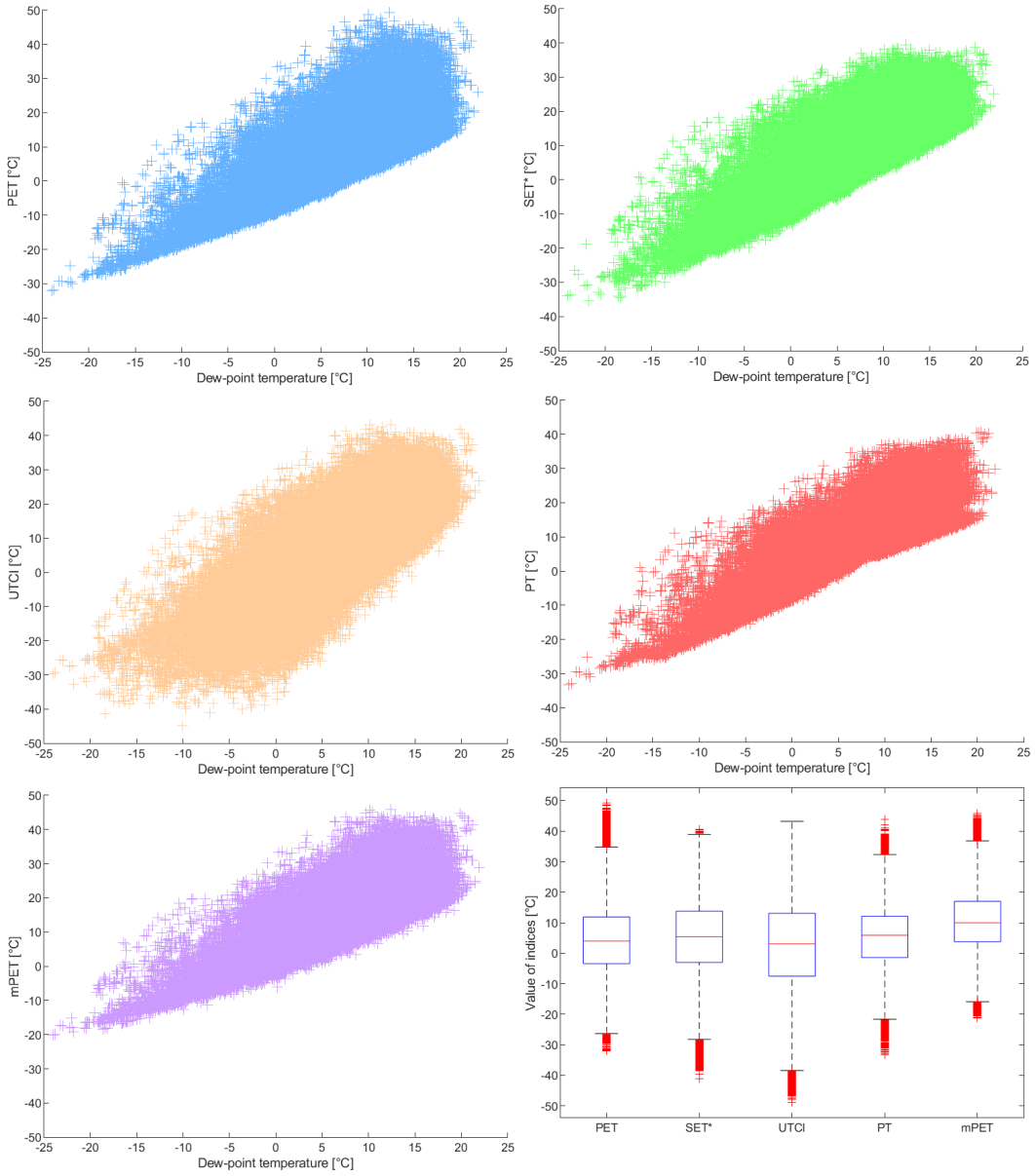

Figure 3.8: Same as Figure 3.3, but showing dependency on dew-point temperature.

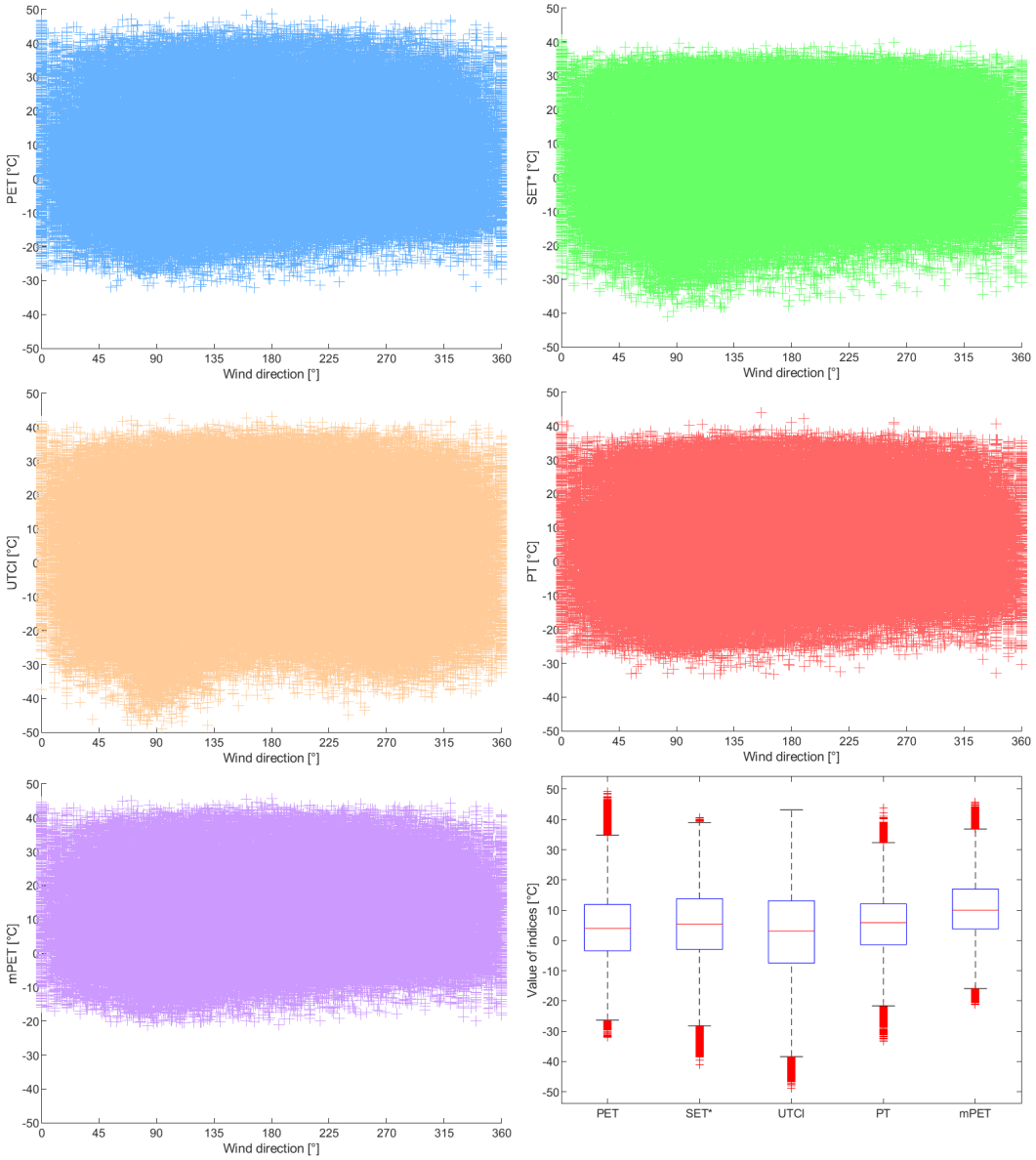

Figure 3.9: Same as Figure 3.3, but showing dependency on wind direction.

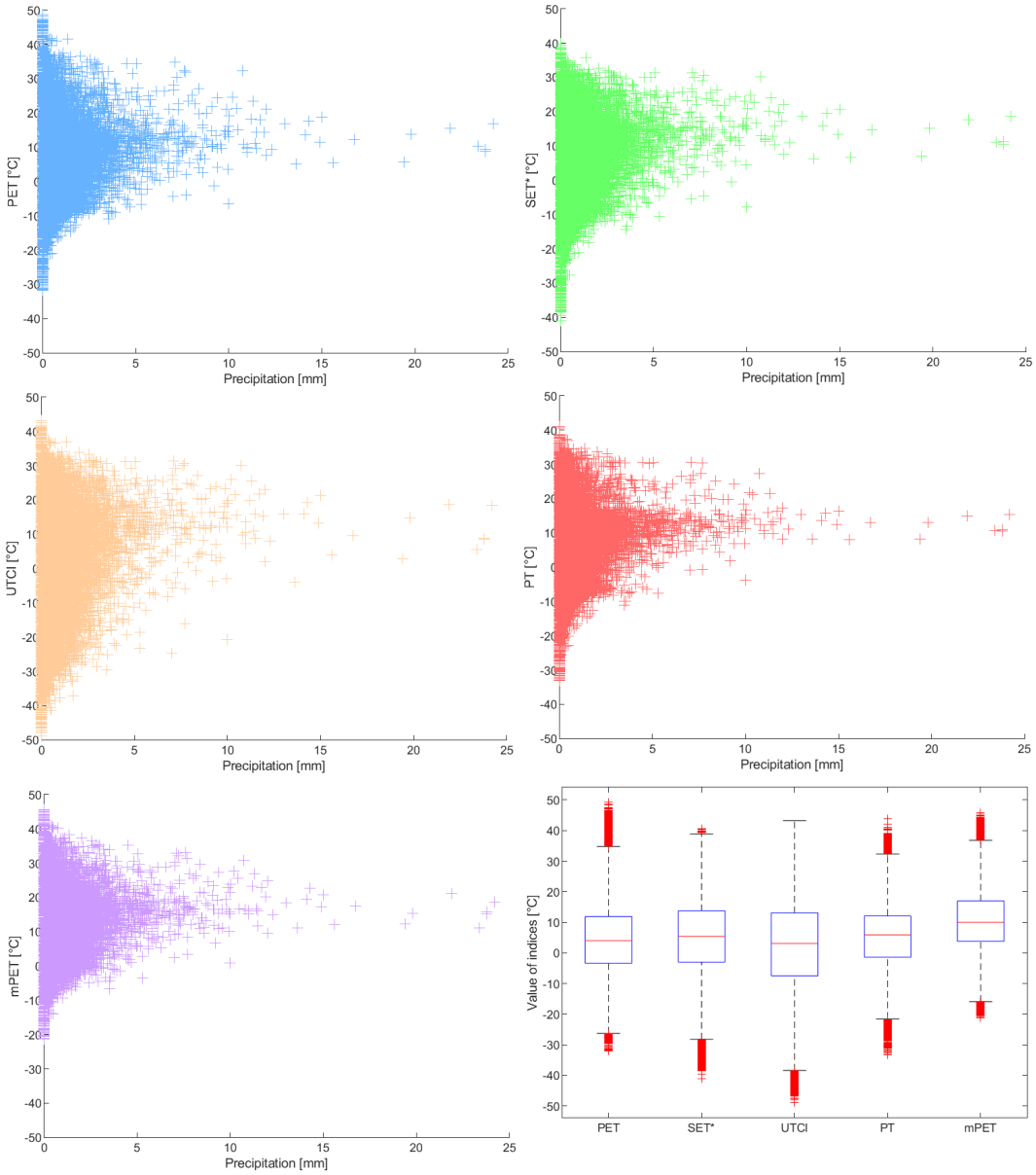

Figure 3.10: Same as Figure 3.3, but showing dependency on precipitation.

for the other indices. With higher wind speed, UTCI tends to have lower values than other indices. It is also important to mention that the UTCI model is less stable, especially in extreme weather conditions. Therefore, the calculation fails and some data are missing, which can be seen mainly in higher speeds of wind. They have a similar behaviour leading to a minor cooling effect of the wind, especially PT has the least dependency on the wind speed.

The dependency on humidity (Figure 3.5) underlines the large spread for UTCI and the higher values of all other indices. The mPET has the lowest spread for low humidity, and it increases towards the higher humidity up to 85%, and then it decreases. There is also shown the behaviour of the thermal indices with different relative humidity. The graph projects lower values of thermal indices towards higher humidity which can be caused by having higher temperatures in a dryer environment.

Figure 3.6 gives a view on the difference between a clear sky and overcast days. The dependence of the spread of the thermal indices on cloud cover is very low.

Figure 3.7 shows the behaviour of the indices depending on the mean sea level pressure. It shows the highest spread around 1012 hPa, where it is also expected to be the most situations. Towards lower and higher pressure, the spread is decreasing. The spreads of the indices differ mainly in conditions with pressure lower than 995 hPa. UTCI show the most significant spread for all measured pressure values.

Figures 3.9 and 3.10 confirm no specific direct dependencies of the thermal indices on precipitation and the direction of the wind. Therefore, the selection of the suitable thermal index should be made based on the spread of the indices. The most significant spread has UTCI, whereas other indices have a similar spread. Therefore, the four indices showing similar behaviour are preferred to use in this study.

The model has also made a few unrealistic values. The study considers only values of all thermal indices in the interval -100 and 100 °C. The amount of unrealistic values for UTCI is 0.03%, whereas for all of the other indices it is 0.005% which means that the model for UTCI has less realistic results than the other models.

The thermal sensation and thermal perception for UTCI, PET, SET* and PT shown in Table 3.2 are given in Zare et al. [2018], Ye et al. [2003] and Chen and Matzarakis [2018]. For the mPET index, the scale for PET was chosen for the similarity and comparability of those two indices, as Chen and Matzarakis [2014] states. SET* has a different scale of thermal sensation than the other chosen indices having only five different thermal perception and grades of physical stress instead of nine as the other indices. There are possibilities to define the missing four grades but in this thesis, only the five categories will be used. Therefore, the study will use the Table 3.2 with no extension of the SET* to all nine categories.

The indices cannot be compared to each other just by their values as there is no reason to behave similarly. Therefore, a comparison based on the thermal sensation has been made. Based on the data, the barplot (Figure 3.11) has been drawn. The graph considers the percentage of every category defined in Table 3.2 for the chosen indices. The similarity between PET and mPET is visible, although mPET has higher values of temperature and therefore more

Table 3.2: The classification of thermal perception and the grade of physical stress for UTCI, PET, PT, SET* and mPET

Thermal perception	Grade of physical stress	UTCI	PET	PT	SET*	mPET
Very hot	Extreme heat stress	>46	>41	>38	>37	>41
Hot	Strong heat stress	38 to 46	35 to 41	32 to 38	34 to 37	35 to 41
Warm	Moderate heat stress	32 to 38	29 to 35	26 to 32	30 to 34	29 to 35
Slightly warm	Slight heat stress	26 to 32	23 to 29	20 to 26		23 to 29
Comfortable	No thermal stress	9 to 26	18 to 23	0 to 20	17 to 30	18 to 23
Slightly cool	Slight cold stress	0 to 9	13 to 18	-13 to 0		13 to 18
Cool	Moderate cold stress	-13 to 0	8 to 13	-26 to -13	<17	8 to 13
Cold	Strong cold stress	-27 to -13	4 to 8	-39 to -26		4 to 8
Very cold	Extreme cold stress	<-27	<4	<-39		<4

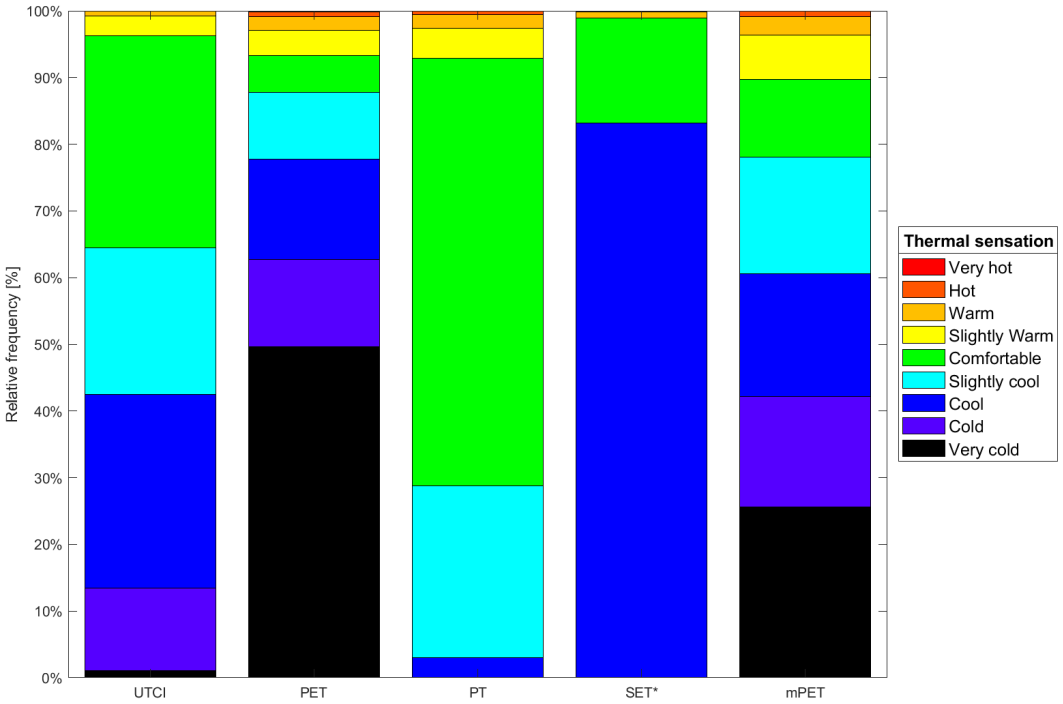

Figure 3.11: The thermal sensation of the five chosen thermal indices applied on all city and rural stations in (1990-2019).

data in warmer categories. SET* was drawn with no values in Very cold, Cold, Slightly cool and Slightly warm category due to its definition. The most values in comfortable perception have PT with more than 60%. The Very hot category has almost no representation (together only 0,013%) and Very cold is the largest category in the PET and mPET indices (47% and 39% respectively).

3.5 Final selection of one thermal index

With the five chosen thermal indices the gender differences and time course are studied to compare the indices in terms of gender dependence and change in time.

The personal data were used for both male and female gender. Table 3.3 specifies the personal data input for male and female given by WorldData [2019] as average height and weight of men and women in Germany (G) and Czech Republic (C). Age has been chosen as default 35 years. Clothing was adjusted to less than formal clothes. Furthermore, activity was set to represent fully standing person walking in the city as it is the most common behaviour. The choice of the values was made based on Figures 1.2 and 1.3.

The fundamental difference for a thermal sensation of a male and female body is not the biological attributes, but the physical quality, i. e. body height and weight. In Figure 3.12, there is a comparison of the male and female thermal sensation for all data. The figure shows the minimum difference between the perception of both genders. Therefore, both are not distinguished for the subsequent studies. Figure 3.13 shows the comparison of the PET, SET*, UTCI, PT and mPET leaving no gender difference for UTCI and PT and a slight dissimilarity for PET, SET* and mPET. The index PET is mostly higher for males and indices

SET* and mPET are in most cases higher for females. The mPET difference corresponds to the findings of Tung et al. [2014].

Table 3.3: The personal data used for both male and female, Germany is denoted by G, Czechia by C, based on WorldData [2019]

Gender	Male	Female
Height [m]	G: 1.80, C: 1.80	G: 1.66, C: 1.68
Weight [kg]	G: 88.8, C: 91.0	G: 71.6, C: 74.5
Age [years]	35	35
Clothing [Clo]	0.9	0.9
Activity [W]	140	140
Position	Standing	Standing

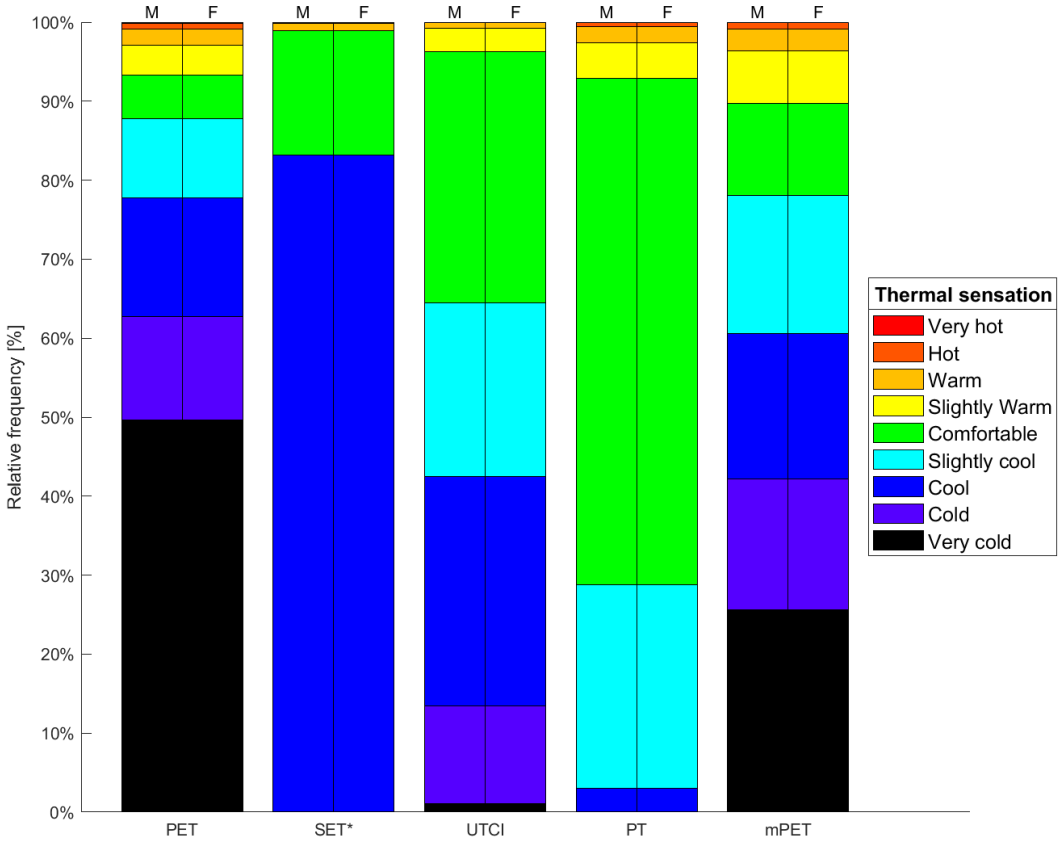

Figure 3.12: Thermal perception comparison of both male and female body according to the five chosen indices PET, SET*, UTCI, PT and mPET. Male data are denoted by M, female by F.

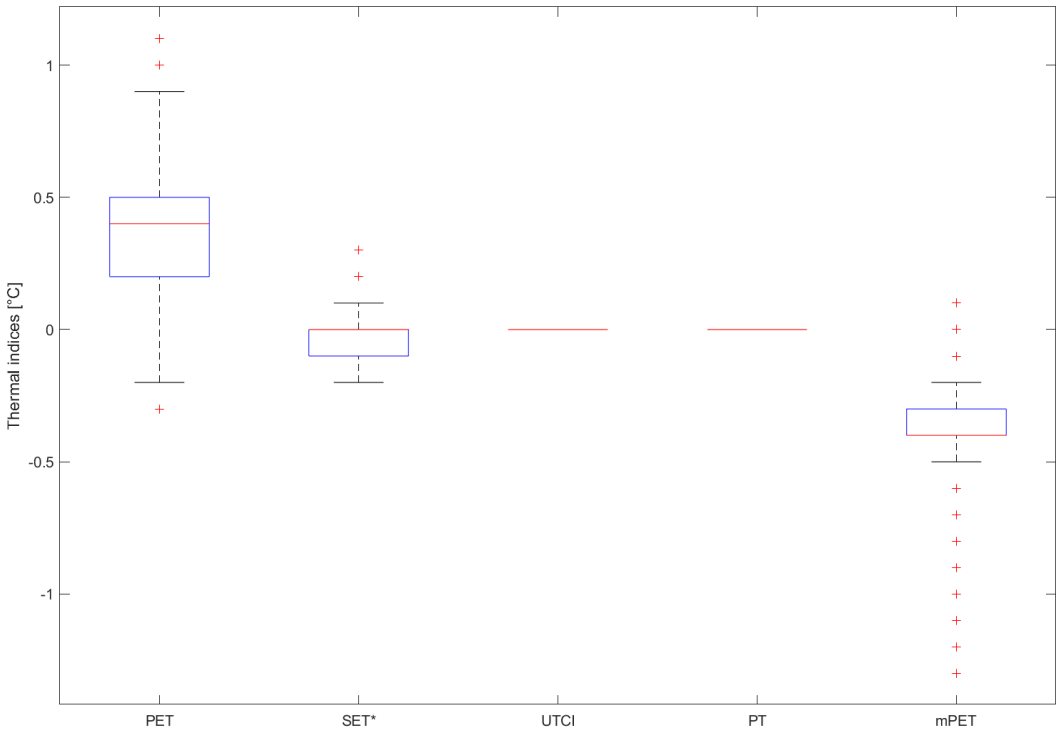

Figure 3.13: The difference between male and female calculated thermal indices PET, SET* UTCI, PT and mPET for all mentioned cities.

A comparison between all five thermal indices has been made according to their change in time. It will show the differences in several periods. For the 30 years, there are plenty of different weather situations as well as climate change. Therefore the 30 years data are divided into decades and compared to obtain an insight into the time variation. In Figure 3.14 and Table 3.4, there is a visible change towards thermal sensation connected with warmth for all five indices. For the colder sensations, the change has been more pronounced between the first decades (1990-1999 and 2000-2010), whereas for the warmer sensations, the change is more prominent between the last two decades (2000-2009 and 2010-2019). The comparison aims at the selection of the appropriate thermal index and not at the study of a time course.

As Charalampopoulos and Santos Nouri [2019] states, indices UTCI, mPET, PET and PT were approved for their behaviour to be appropriate for further studies. Although considering all of the variations, gender difference and time changes, the index mPET has been chosen to be the most appropriate index. PET was not chosen for its similarity with mPET, where mPET has a more advanced and more precise model with better results as Figure 3.11, Chen and Matzarakis [2018] and Chen and Matzarakis [2014] shows. SET* was mainly removed for its more than 83.5% of values being in the Cool category which covers all cold stress grades and therefore only 15.5% are in a comfortable zone, and less than 1.5% belongs to warm stress. SET* was also defined only for indoors and Staiger et al. [2019] made the extension for outdoors.

This chapter has shown that UTCI behaves differently from the other four indices. Moreover, mPET is a successor of UTCI and PET and therefore, it is the most appropriate thermal index for this study.

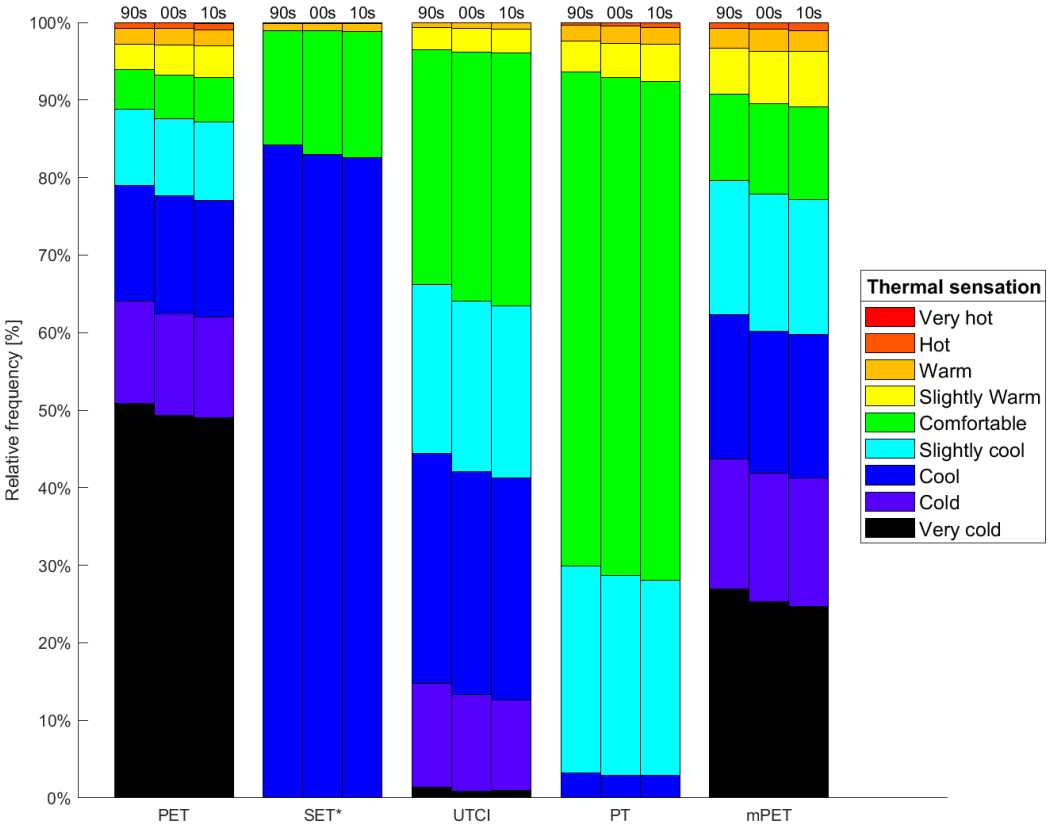

Figure 3.14: Thermal perceptions for the data between years 1990 and 2019 divided into three decades 1990-1999 (90s), 2000-2009 (00s), 2010-2019 (10s), according to the five chosen indices PET, SET*, UTCI, PT and mPET.

Table 3.4: The relative frequency of thermal perceptions for the data between years 1990 and 2019 divided into three decades 1990-1999 (90s), 2000-2009 (00s), 2010-2019 (10s), according to indices PET, SET*, UTCI, PT and mPET. The values are in %. DC marks the according decades and thermal sensations are as follows: very hot (VH), hot (HT), warm (WM), slightly warm (SW), comfortable (CO), slightly cool (SC), cool (CL), cold (CD), very cold (VC).

index	DC	VC	CD	CL	SC	CO	SW	WM	HT	VH
PET	90s	50.83	13.26	14.84	9.85	5.07	3.37	2.01	0.66	0.09
	00s	49.38	13.03	15.25	9.94	5.62	3.87	2.11	0.70	0.10
	10s	49.05	12.91	15.06	10.16	5.75	4.10	2.01	0.80	0.16
SET*	90s	0.00	0.00	84.19	0.00	14.78	0.00	0.86	0.15	0.02
	00s	0.00	0.00	82.96	0.00	16.00	0.00	0.92	0.11	0.01
	10s	0.00	0.00	82.58	0.00	16.30	0.00	0.95	0.16	0.01
UTCI	90s	1.38	13.42	29.64	21.72	30.32	2.81	0.67	0.03	0.00
	00s	0.90	12.43	28.78	21.97	32.08	3.08	0.72	0.05	0.00
	10s	0.95	11.69	28.61	22.22	32.63	2.99	0.83	0.08	0.00
PT	90s	0.00	0.05	3.12	26.76	63.66	3.97	2.03	0.40	0.01
	00s	0.00	0.03	2.93	25.71	64.20	4.43	2.25	0.44	0.01
	10s	0.00	0.04	2.92	25.15	64.33	4.78	2.11	0.66	0.01
mPET	90s	26.97	16.75	18.59	17.28	11.15	5.91	2.55	0.75	0.05
	00s	25.35	16.52	18.30	17.66	11.65	6.84	2.79	0.84	0.05
	10s	24.72	16.55	18.49	17.41	11.88	7.18	2.73	0.94	0.09

The choice corresponds with Matzarakis et al. [2015], where UTCI and PET were chosen to be the most precise indices. Chen and Matzarakis [2014] presents the mPET as a combination of UTCI and PET, making it the most appropriate index for the study.

4. Results

With the chosen thermal index, the data from each city and the surrounding stations are studied. The main aim is to compare the behaviour of mPET and the thermal sensation deduced in the cities and the surrounding stations.

One of the most obvious comparisons is the thermal comfort of the city station and rural stations showing the percentage of occurrence of each thermal sensation for months at each of the three timestamps of the day (7, 14 and 21 CET). The time course of the thermal comfort and its variation are being studied as well using the data from the three timestamps combined.

Regarding Prague, street canyons are chosen to study its effect on thermal comfort using different scenarios, i. e. modifications of the real streets. The canyons make a difference in the perceived temperature changing the wind direction. Changes in tree planting and the albedo of the buildings will show the importance of urban planning by thermal comfort differences for all scenarios.

Heat stress can appear, based on our data, only between March and October. As for the results, only the data from April to September are analysed because during the remaining months, there occurred less than 5% of heat stress situations.

4.1 Comparison between urban and non-urban areas

With the assumption of gender independent thermal sensation, the graphs for the studied cities were drawn and the thermal sensation was compared between the city and the surrounding area. When choosing the meteorological station in the desired city, there was an opportunity to use more than one station in Berlin and Prague as it was discussed in Chapter 3.3. The meteorological stations for Berlin are Dahlem, Schönefeld, Tegel and Tempelhof, for Prague the stations are Karlov and Libuš.

The multiple meteorological stations in Prague and Berlin provide us with information about the differences inside the city. One of the most interesting views in the city is the heat stress comparison. Heat stress is defined as mPET $> 23°C$ (see Table 3.2). Thus, such a comparison is made for both cities.

Another point of view is the time course of the thermal comfort for the selected stations and cities. This is studied using decadal separation of the data into three sets. Using this approach, the inter-annual variability is suppressed in favour of a decadal change of the thermal sensation.

4.1.1 Prague

To study the thermal sensation in Prague, Figure 4.1 has been plotted. It shows warmer thermal sensation in the rural areas for 7 CET in April, June and September by 0.8%, 3.2% and 1.9% respectively. In the other months, the warmest thermal sensation is in Karlov. As regards to the evening 21 CET temperatures, the city stations are warmer in May, June, July and August. Concerning all displayed

months, station Karlov is warmer than Libuš station in the evening. As for the sensations at 14 CET, Libuš station is overall warmer than the Karlov station and rural stations except for April (by 0.6%) and June (by 0.1%). Although, in Karlov, there are more cases with hot and very hot sensations. Prague has a notable difference between the stations in the town among themselves in comparison with the surrounding stations.

According to Geletič et al. [2019], the most significant differences in the morning and afternoon surface temperature are during summer (June, July and August). With a direct connection of the surface temperature and mPET, Figure 4.1 corresponds to the statement. The April sensations have a smaller difference between morning and afternoon mPET in all stations than July or August.

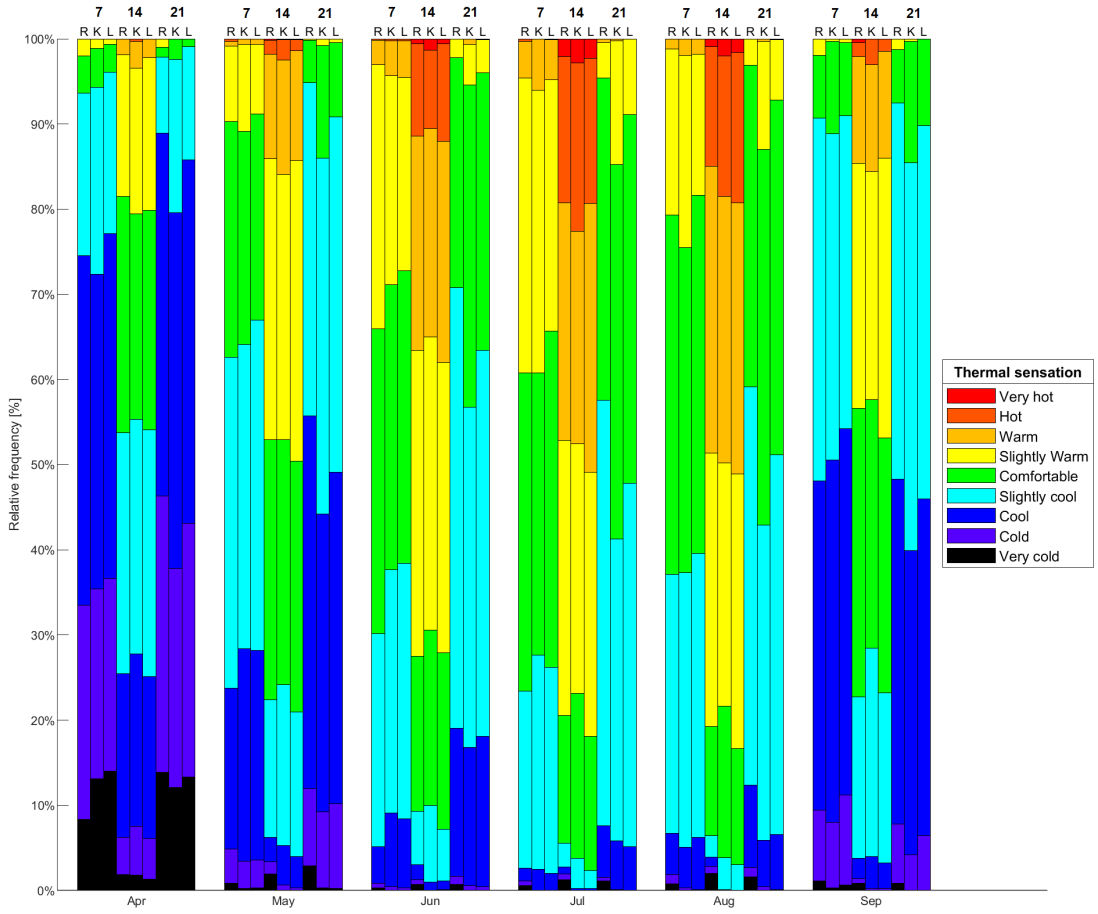

Figure 4.1: Thermal sensation in Prague according to mPET at 7, 14 and 21 hours CET. The percentage of occurrence of different thermal sensations are shown for different months during a year and all three times of day. (R) is the set of stations around the city and the other letters represent the city stations: (K) as Karlov and (L) represents Libuš.

In the graph 4.2, there is a percentage of hours with heat stress during the 30 years. It shows that the highest percentage of warm mornings are in the non-urban areas which are closely followed by Karlov and Libuš. Among the afternoon temperatures, there is surprisingly the most days with heat stress in Libuš compared to rural stations. The least heat stress at 14 CET is in Karlov in the centre of the city. The most significant differences are recorded in the evening

where the percentage of days with heat stress in Karlov is 3.1% and in Libuš 1.6% which is far more than in the rural stations having only 1.0% of evenings with heat stress. The city has more days with heat stress, especially in the evening, and the hot and very hot sensations are more present than in rural areas.

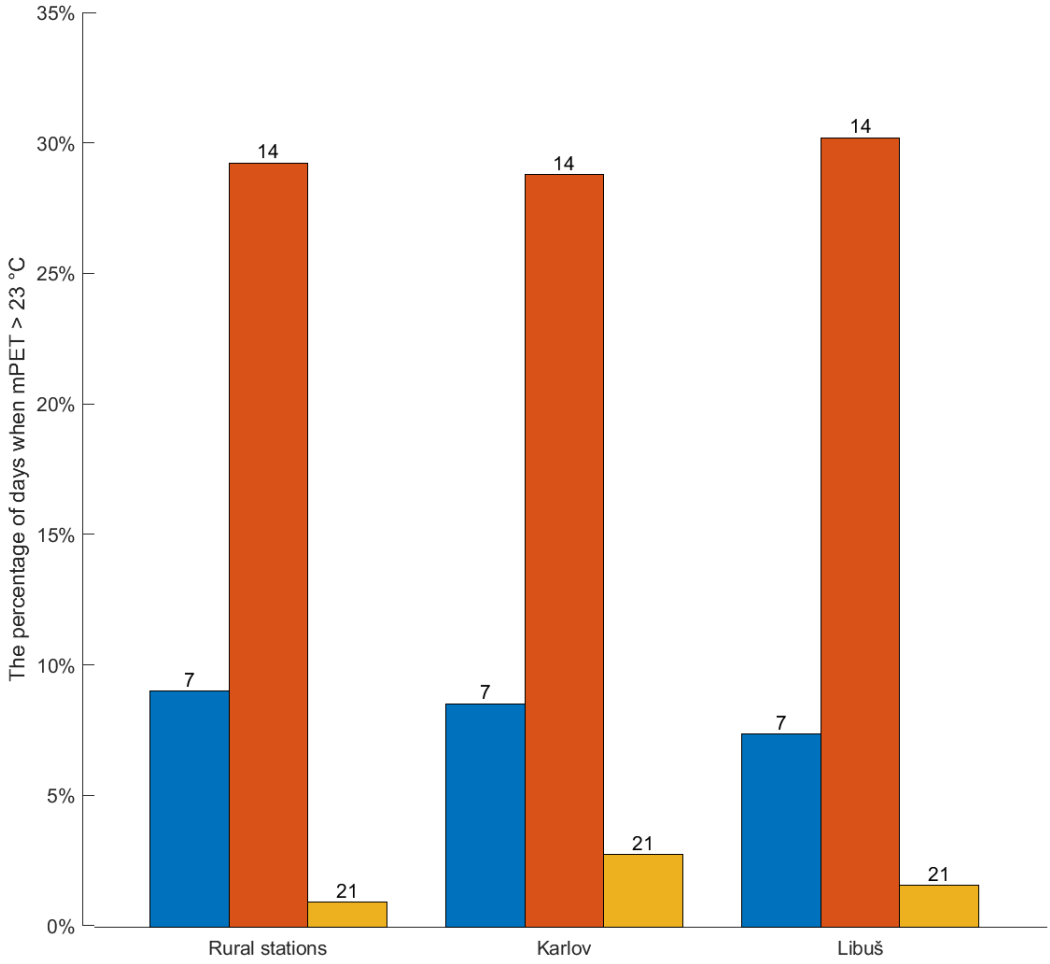

Figure 4.2: The percentage of days where mPET exceeds 23°C in Prague for different city stations and a set of stations around the city at different timestamps during a day for 30 years. Blue values are for 7:00, red values denote 14:00 and orange values refer to 21:00 as hours in a day.

Figure 4.3 shows the temporal development of thermal sensation in the three studied decades. According to the figure, heat stress is increasing in all discussed stations. In Karlov and rural areas, it decreases and increases again. The most significant change is taken between the second and third decade for the city stations which is 1.7% in Libuš, 1.6% in Karlov which means 186 more recorded hours with heat stress from the three timestamps in a day and 0.3% for rural stations.

The cold stress decreases in the city stations, yet in the rural stations, it decreased and then increased again. The comfortable zone shrinks at every station but only by 0.2% at the most. The shrinking of 0.2% occurs in the rural area.

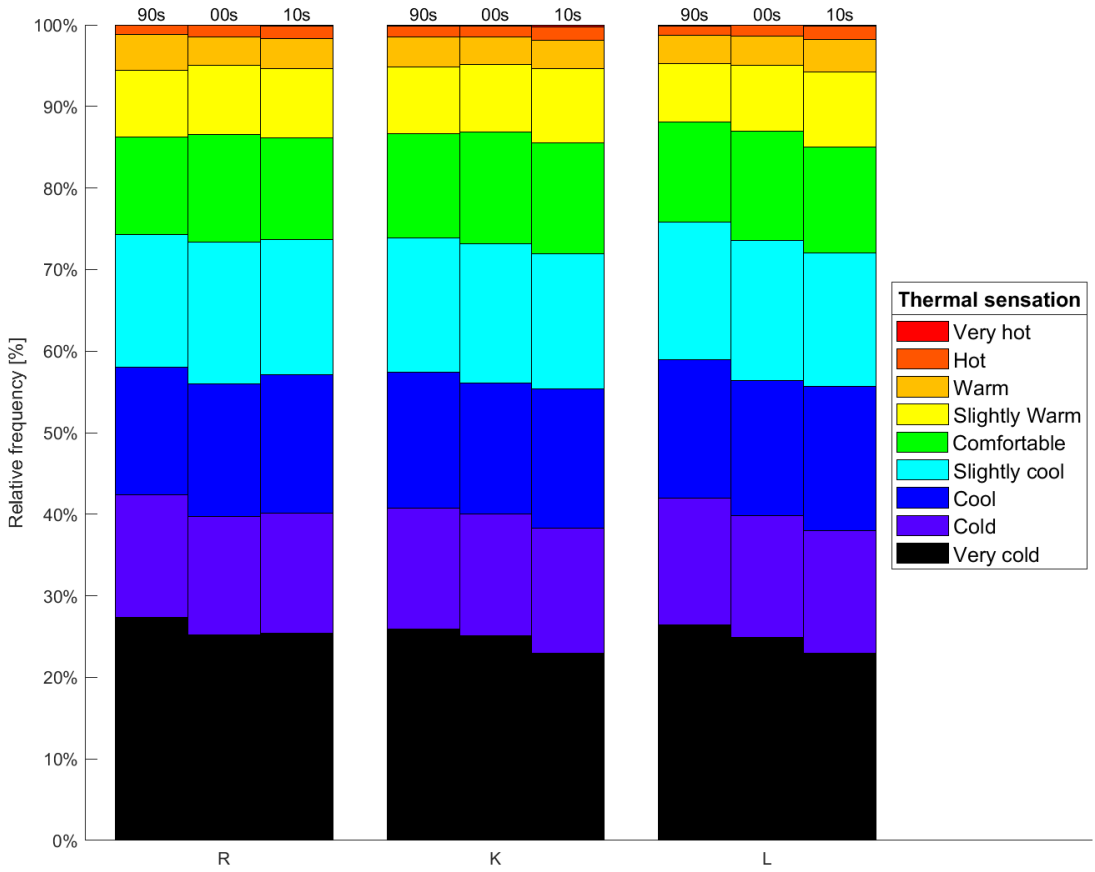

Figure 4.3: Decadal course in Prague's stations and the set of surrounding stations according to the frequency of thermal sensations evaluated using mPET at 7, 14 and 21 hours CET. R stands for rural stations, K is Karlín and L is Libuš and decades are 1990-1999 (90s), 2000-2009 (00s) and 2010-2019 (10s).

4.1.2 Berlin

In Figure 4.4, all city stations in Berlin are displayed on the map of Berlin. Tegel, Tempelhof and Schönefeld are airport stations having specifically different environment than city stations in the centre, in our case Dahlem. Schönefeld is located at the edge of the city and Tempelhof is the closest to the city centre.

Figure 4.4: The meteorological stations in Berlin and their locations are shown by yellow pins. The light grey line is the border of the city. Source: Google Earth Pro [2020].

The figure displaying Berlin data is split into two graphs. The first, Figure 4.5, shows stations Tempelhof, Schönefeld and Tegel with the rural set through the whole 30-year period even though Tegel and Tempelhof did not measure the whole time. The second graphs, Figure 4.6, presents only station Dahlem and rural set in years 2009-2019.

In Figure 4.5, there are thermal sensations in Berlin for months April to September for three parts of the day: 7, 14 and 21 CET. For most of the months, stations Tempelhof and Tegel show the highest mPET for morning and evening hours (7 and 21 CET). The rural stations have the lowest sensation for 7 and 21 CET. As for the middle of the day (14 CET), the warmest sensation is in the rural areas and Tegel. The stations Tempelhof and Schönefeld have the coldest sensation at 14 CET.

Figure 4.6 shows warmer morning sensation in Dahlem during the chosen months except for May and June. The thermal sensation at 21 CET is warmer in rural areas than in Dahlem. At 14 CET rural stations have warmer sensation in all months except April and August, but the most frequently are hot and very hot sensations in Dahlem.

Having displayed Figures 4.5, the rural stations are colder than the airport stations in the morning and evening, primary due to the UHI effect and including heavy traffic causing heat increase. Thus, the airport stations do not measure

such low temperatures.

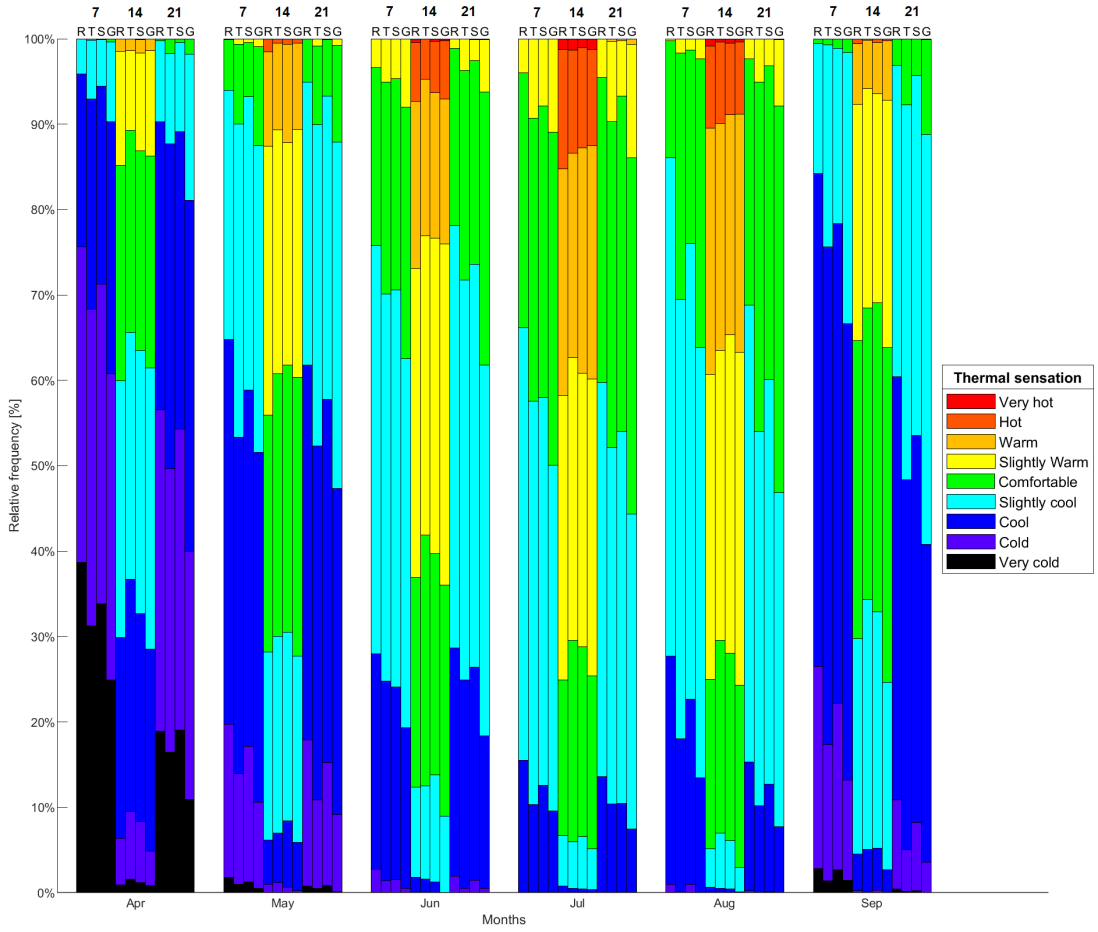

Figure 4.5: Same as 4.1, but for Berlin and the city stations are: (T) as Tempelhof, (S) is Schönefeld and (G) denotes Tegel.

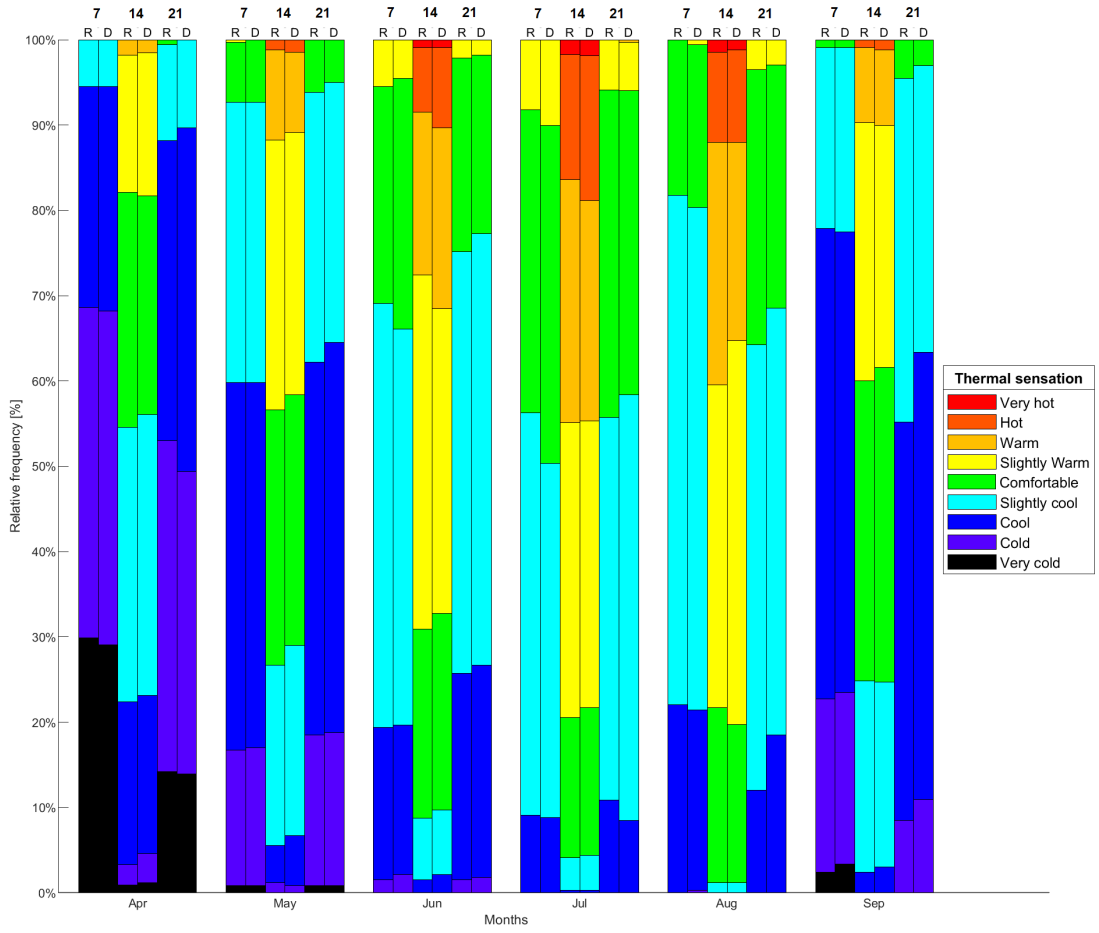

Figure 4.6: Same as 4.1, but for Berlin city station in Dahlem (D) and the considered years are 2009-2020.

In Figure 4.7, there is a percentage of hours when mPET $>$ 23°C for each of the three hours in a day (7, 14 and 21) during the whole 30-year period causing heat stress. It displays the highest number in the morning for Tegel station and the lowest for rural stations which are followed by Tempelhof and Schönefeld. The afternoon heat discomfort appears the most at the surrounding stations and the least it appears in Tempelhof and Schönefeld. As for the evening warm sensations, Tegel station has the most situations with heat stress followed by Tempelhof and Schönefeld, leaving the rural stations the coldest.

Figure 4.7 confirms the quick cooling from daily maximum to evening in Dahlem. Rural stations have this effect lower and the least changes occur in the airport stations. The morning heat stress is not the lowest in Dahlem which can be caused by the heat accumulation in the city during the night. The data from Dahlem are only from the last 11 years. Therefore, the length of the time series affects the comparison.

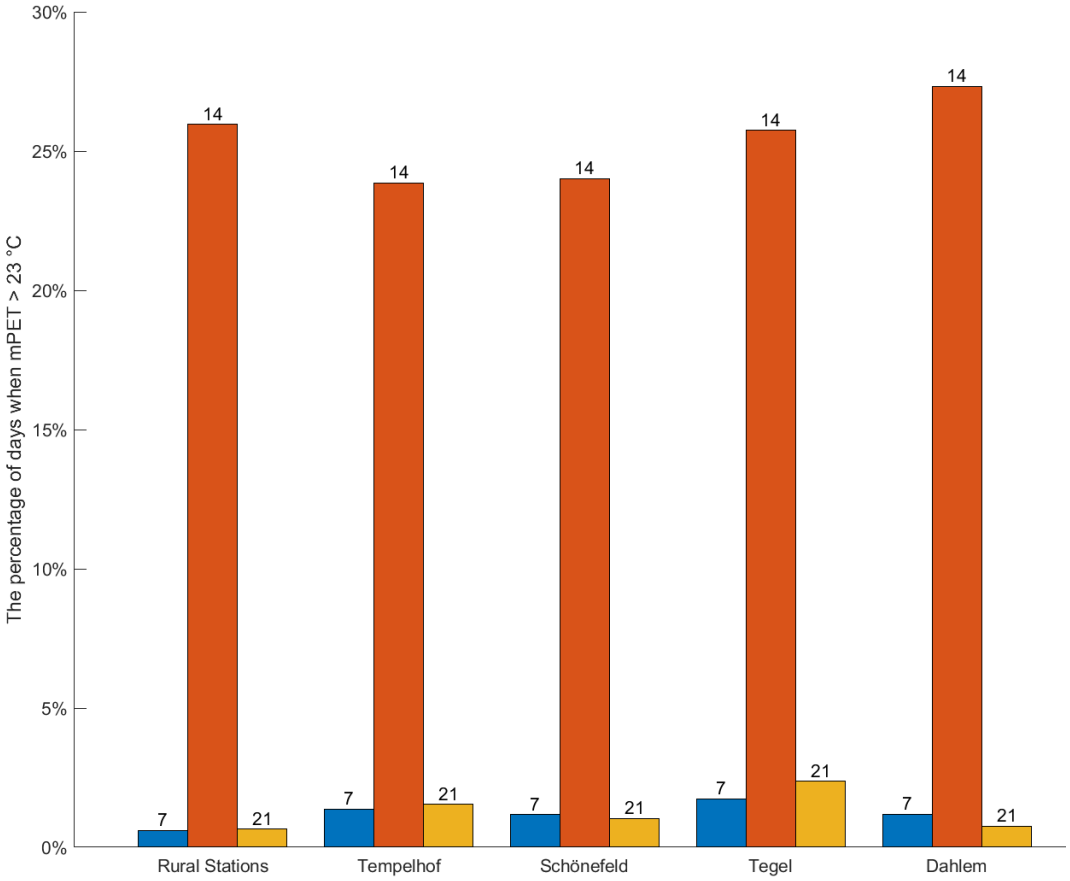

Figure 4.7: Same as 4.2, but for Berlin.

Berlin station Dahlem for the first decade and the station Tempelhof for the third decade have incomplete data leaving Figure 4.8 only two decades for both stations. Other stations provide all decades. It displays the same course for all stations, i.e. towards more heat stress and less cold stress. The mildest decadal differences are in Tegel while the biggest are in Schönefeld and the surrounding stations. The most significant change is taken between the first and second decade for rural stations, Schönefeld and Tegel. The most significant change in the graph, beside Dahlem, is in the rural stations by 2.6% at its maximum.

According to Mahlkow and Donner [2017], there is an ongoing climate change adaptation plan which aims at reducing heat stress in the city. In Figure 4.8, the time course shows a slow and comparable increase in heat stress for all the stations.

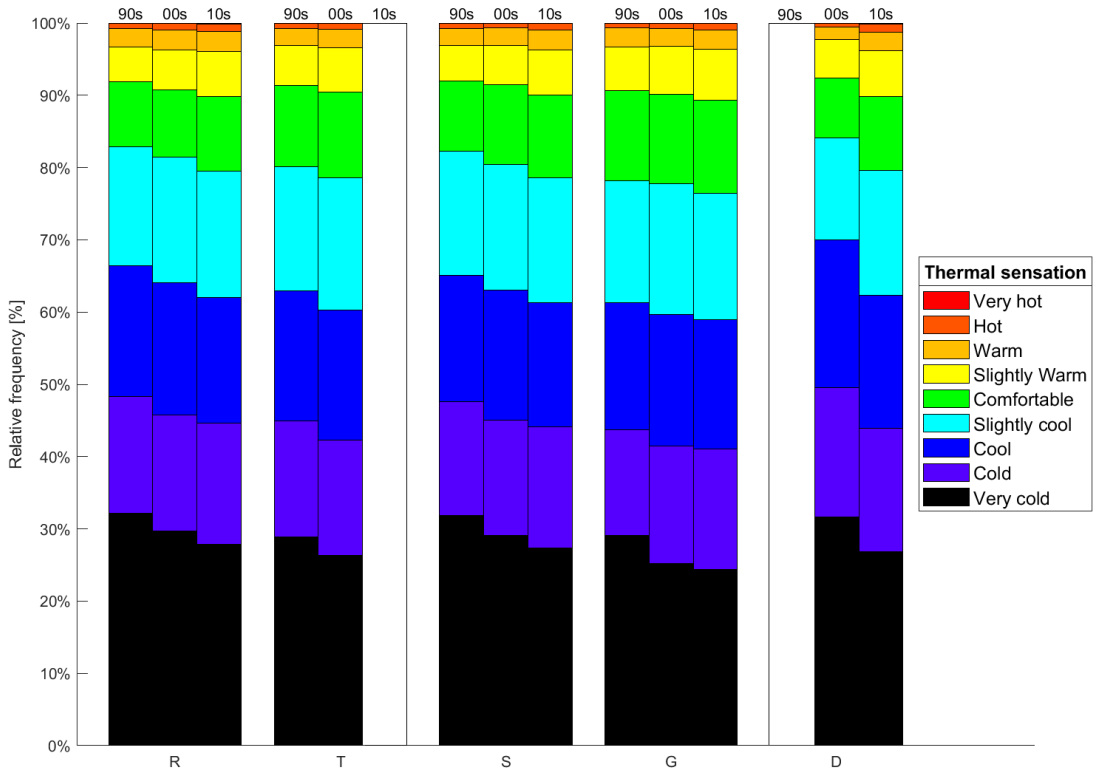

Figure 4.8: Same as Figure 4.3, but for Berlin and the city stations are: (T) as Tempelhof, (S) is Schönefeld, (G) denotes Tegel and (D) represents Dahlem.

4.1.3 Hamburg

The meteorological station in Hamburg is located 10 kilometres northerly from the city centre at the airport. Thus, it may differ from the thermal comfort received right in the centre of Hamburg. The city is located approximately 100 km from the sea but there is no hill to affect the wind for there is no location with an altitude higher than 40 m. The rural station it was compared with is in Soltau, located approximately 80 kilometres southerly form the airport.

Figure 4.9 shows the thermal sensations in Hamburg for months April to September for three parts of the day: 7, 14 and 21 CET. For all mentioned months, the mPET in Hamburg is lower than in the surrounding stations at 14 CET. Similarly, the city does not have more days with heat stress than the surrounding area at 7 CET, but it certainly experiences more days with cold stress. However, the cold and very cold category is more present in rural areas. As for thermal sensation at 21 CET, it is the same as the morning sensation but in most of the months, the cold and very cold categories are more present in Hamburg.

Hamburg is usually colder than the rural areas. Only in extreme events, where the sensation is in the cold or very cold category, the city is warmer, thus not reaching the cold extreme as frequently as the rural areas, as in Figure 4.9 shows. The findings of Hoffmann et al. [2016] shows that the airport experiences only around half of the UHI strength compared to the city centre. Therefore, the city centre should be warmer. At the airport and its neighbourhood are not as many streets as in the centre and the population density is also lower, as Schoetter et al.

[2013] states.

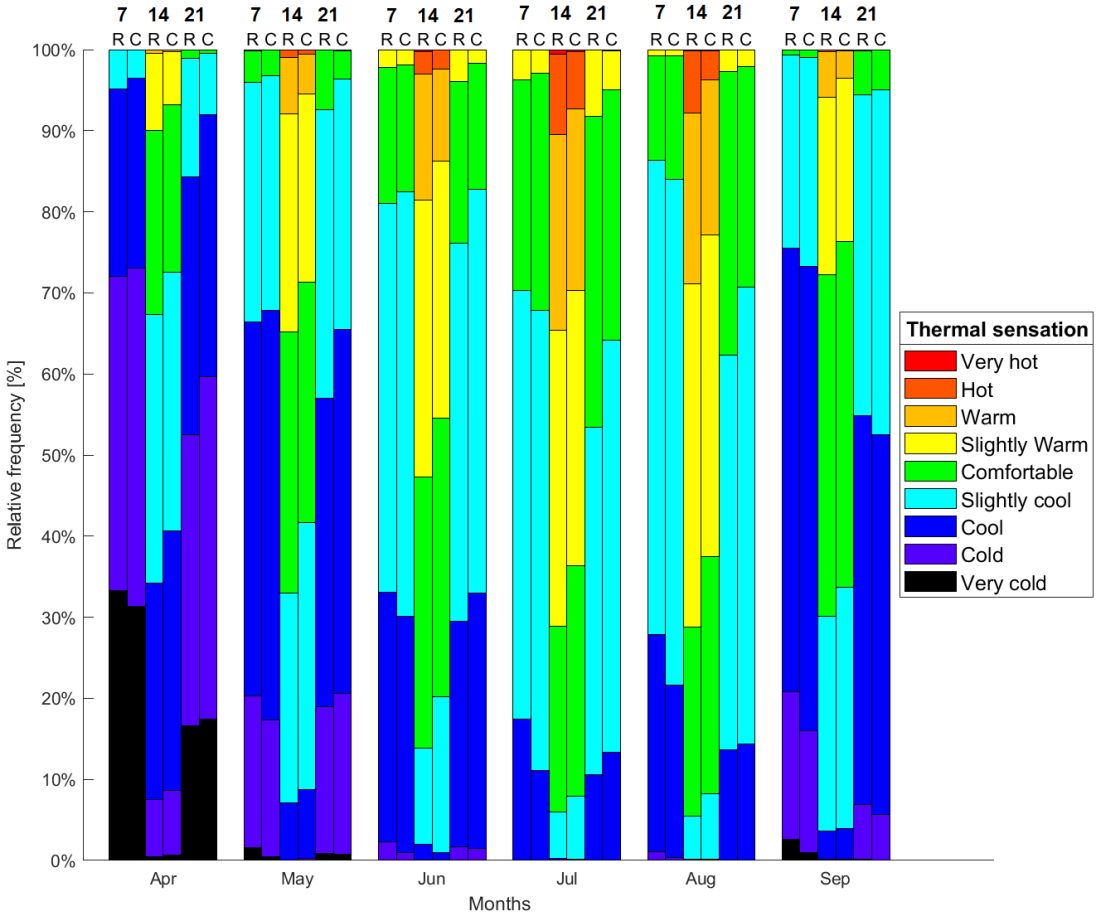

Figure 4.9: Same as 4.1, but for Hamburg and (C) is the city station.

The decadal course of the mPET in Hamburg and its surroundings is shown in Figure 4.10. Each decade the city has slightly more heat stress and less cold stress, having the most considerable difference between the first decades. In the rural area, the course of heat stress is quite stable. It increases and decreases slightly. Cold stress has the same time course.

The city station has the least visible changes in heat stress compared to other city stations. This can be caused by low city expansion to the north and no significant changes in the currently inhabited neighbourhood of the airport.

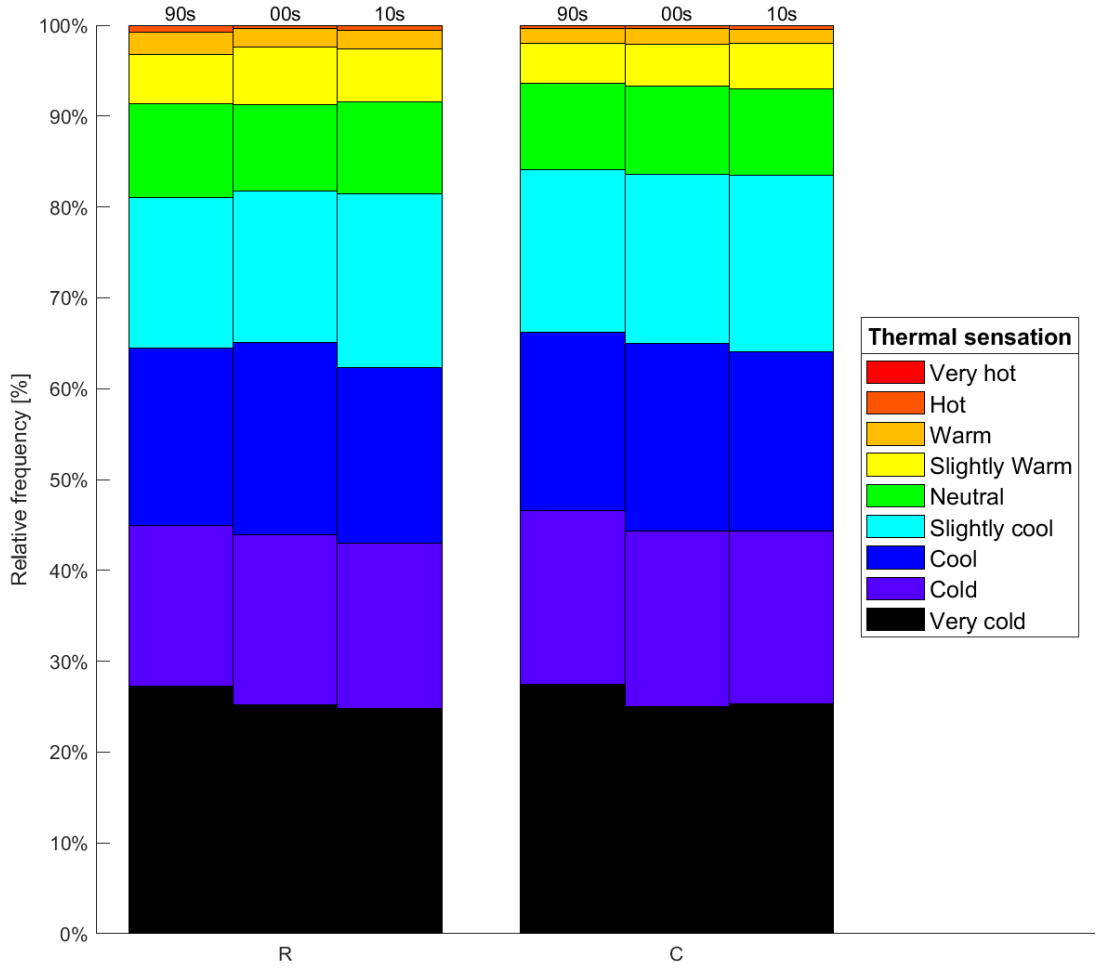

Figure 4.10: Same as Figure 4.3, but for Hamburg and the city station is denoted by (C).

4.1.4 Nürnberg

Nürnberg has a meteorological station similar to Hamburg. It is an airport station located northerly from the city station. The city also has the highest altitude in this study.

Thermal sensations in Nürnberg are displayed in Figure 4.11 similarly as for the other cities. For the morning at 7 CET sensation, the city station is warmer than the rural areas except for heat stress in June, where the rural stations have about 0.2% more mornings in the slightly warm category. In the evening at 21 CET, the city is for all mentioned months warmer at least by 3% in total sensations. At 14 CET, the city station has more of the warm sensations. It implies more heat stress in the city during the afternoon.

Nürnberg is warmer than the rural areas for almost all cases in the morning, afternoon and evening. Expectedly, the most considerable differences are in the evening sensations where the city has up to 9% fewer days with cold stress than in the surroundings.

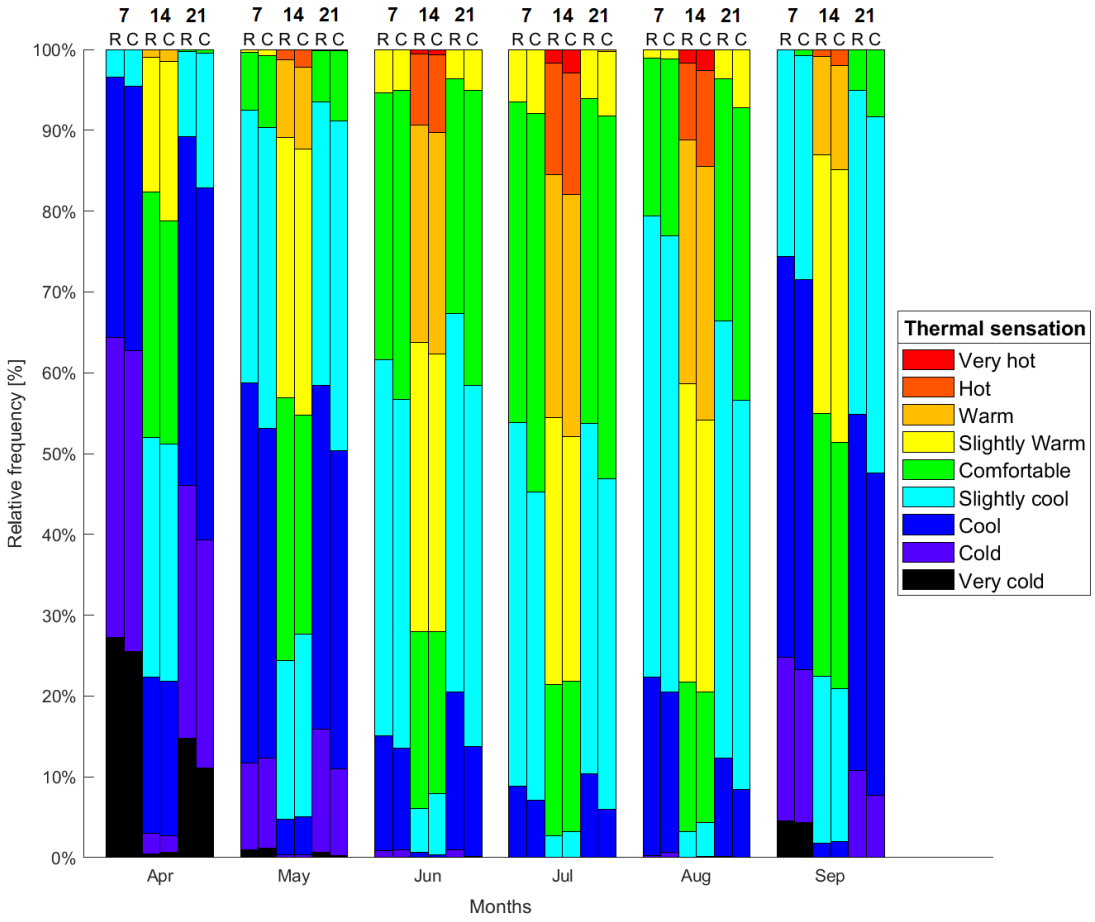

Figure 4.11: Same as 4.1, but for Nürnberg and (C) is the city station.

As for the decadal course in Nürnberg, Figure 4.12 was drawn with missing data between 1990 and 2001. Regarding the city, heat stress increases by 0.8% and cold stress decrease by 0.9% over the 20 years. In the surrounding area, the decrease of cold stress is making changes of 0.2%. The heat stress is less frequent nowadays, being decreases by 0.1% in total over 20 years. It leads to a slight expansion of the comfort zone in rural areas.

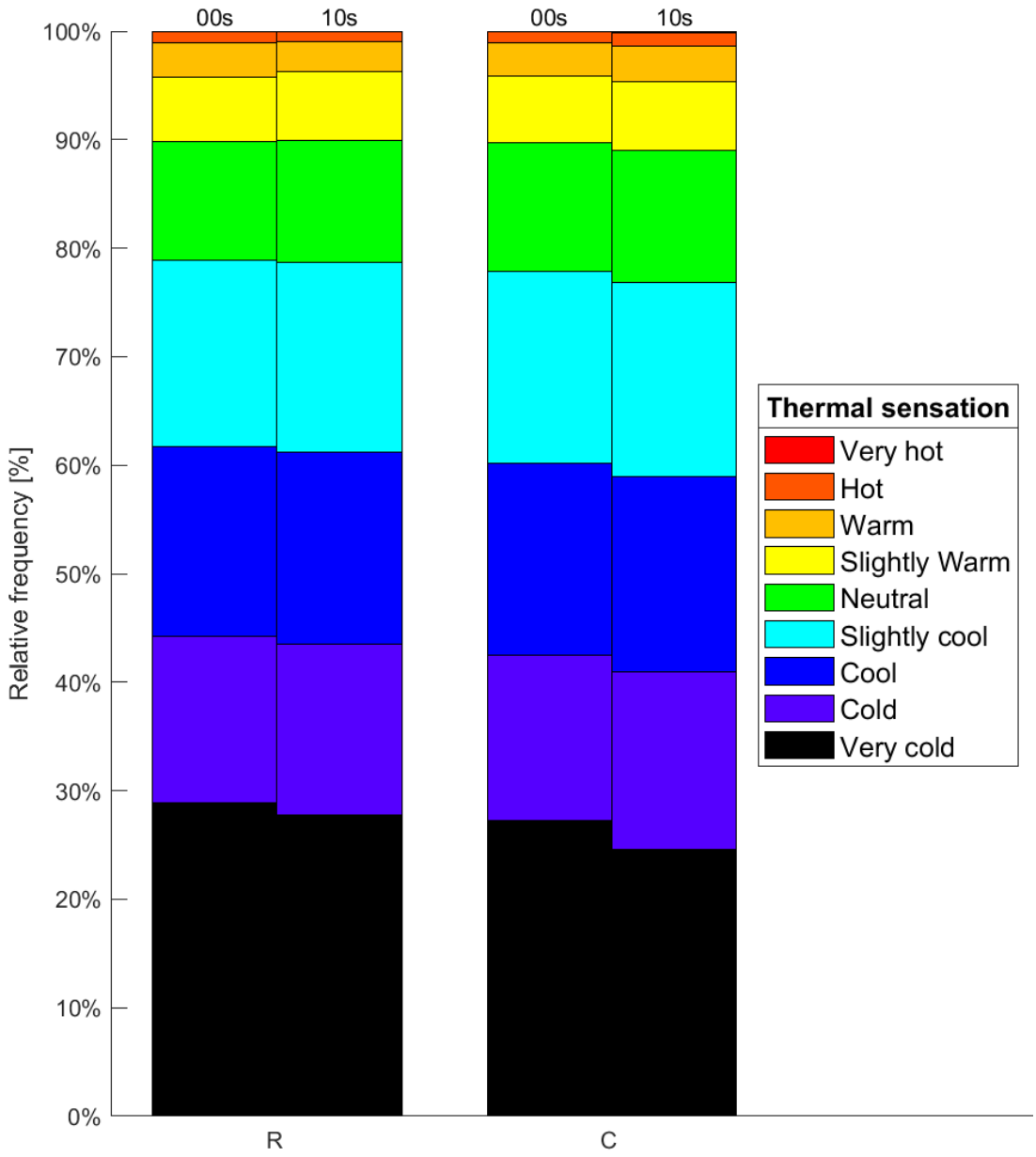

Figure 4.12: Same as Figure 4.3, but for Nürnberg and the city station is denoted by (C).

4.1.5 Köln

Köln has its used meteorological station located at the airport similarly to Hamburg and Nürnberg. The airport is located 15 kilometres south-easterly from the city centre, and it has about 10-metre difference in altitude compared to the centre.

Figure 4.13 describes the thermal sensation in Köln. As regards to the 7, 14 and 21 CET sensations, it shows higher mPET in the rural areas than in the city. The most significant difference in heat stress is in August at 14 CET, where in rural areas is 16% more days with heat stress than in Köln. There is more cold stress in the city, reaching even lower temperatures than the surroundings. The most significant difference in cold stress is also in August, but at 21 CET having

34% more days with cold stress in Köln.

Köln is not experiencing more heat stress than the rural areas for all the cases in the morning, afternoon and evening. The most important hours for UHI are in the evening, where none of the months is warmer in Köln compared to the surroundings. No typical behaviour of UHI was observed in Köln probably due to the location of the meteorological station at the airport far from the city centre.

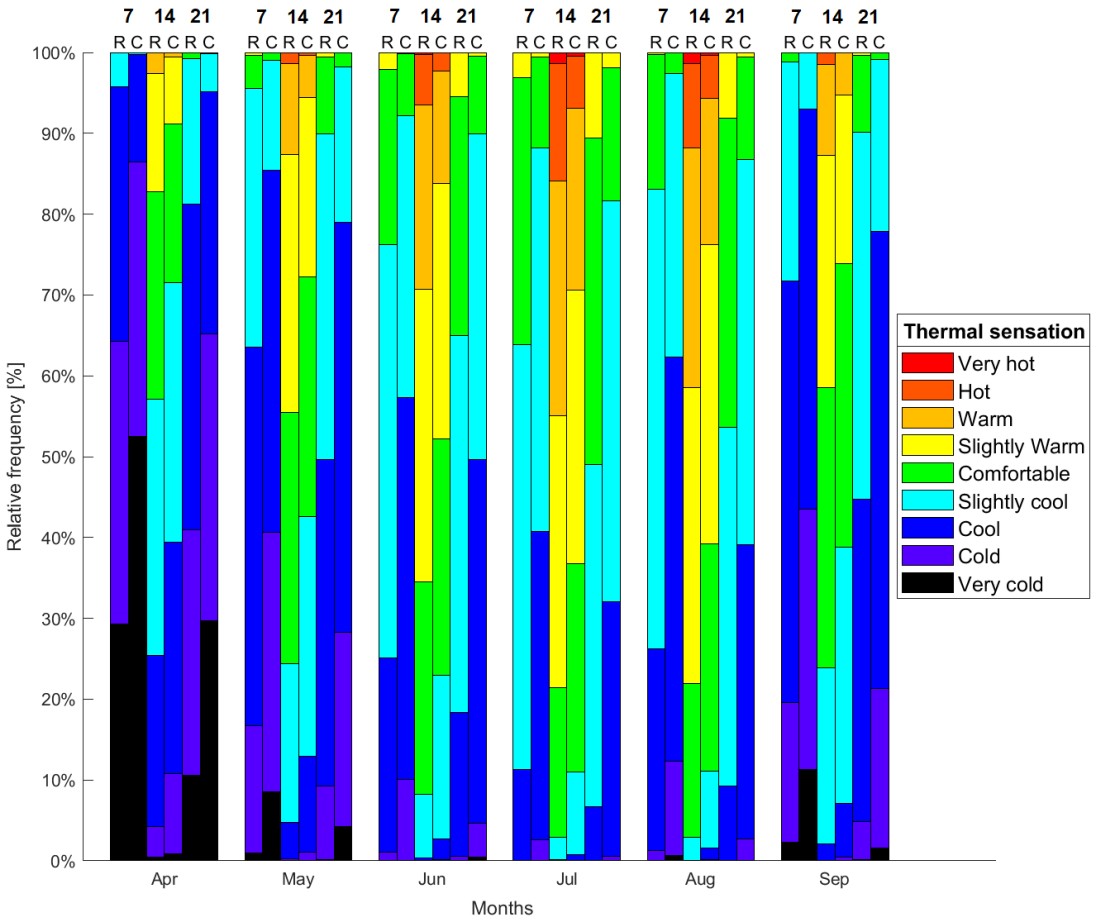

Figure 4.13: Same as 4.1, but for Köln and (C) is the city station.

In Figure 4.14, there is a time course of mPET in Köln. Similarly to other cities, the heat stress increases (by 1.1% in 30 years) and the cold stress decreases (in 2.3% of cases during the whole period) in the city. There are fewer changes in the surrounding area. The heat stress increases by 0.1% during three decades. The cold stress firstly increases by 0.3% and then decreases by 0.3%.

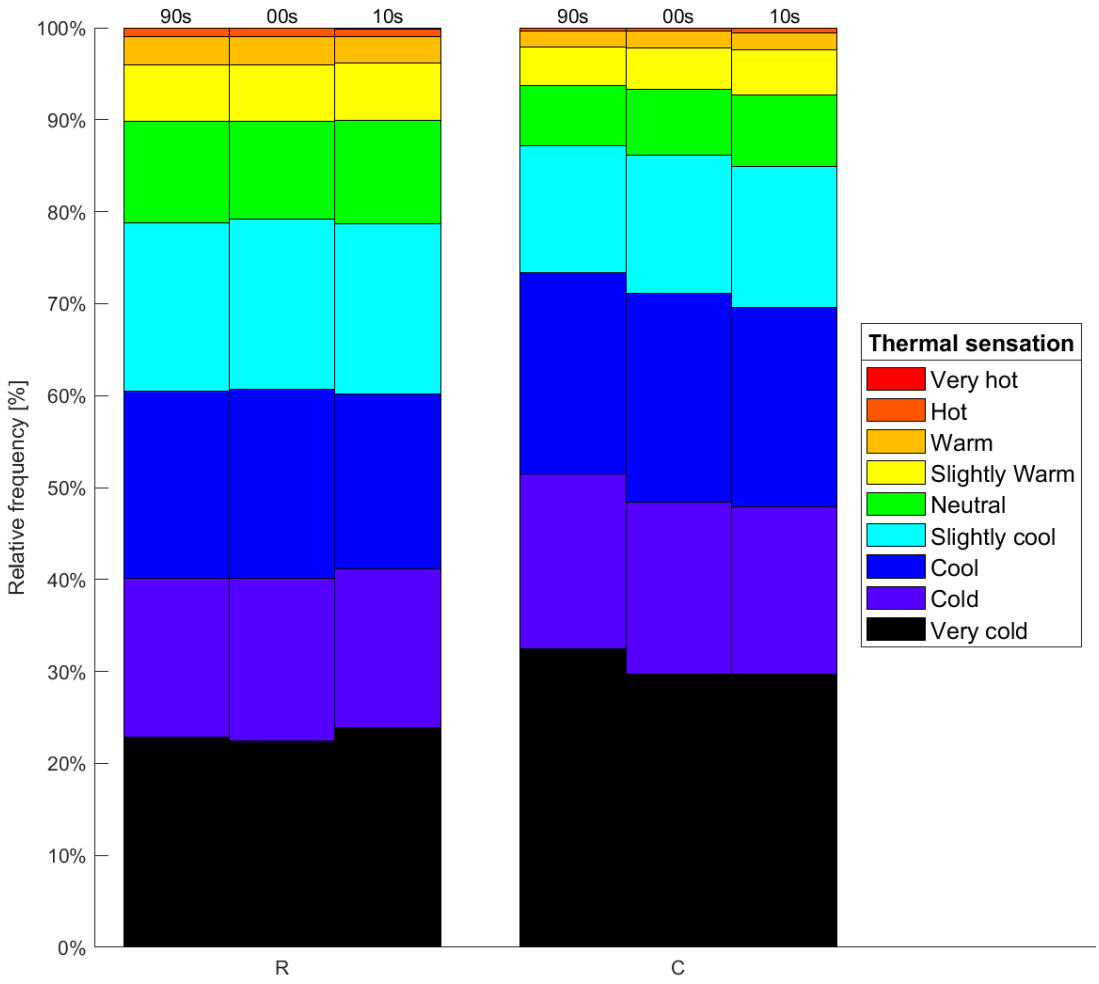

Figure 4.14: Same as Figure 4.3, but for Köln and the city station is denoted by (C).

4.1.6 Frankfurt

Frankfurt am Main is well-known for its international airport where even the city meteorological station has been established. It is located south-westerly from the city centre at a similar altitude and more distant from the river.

In Figure 4.15, there are thermal sensations for Frankfurt. At 7 CET, the city is generally warmer than the rural areas. In the evening, the city also warmer than the surrounding stations, on average in 2.8% of days. As for the 14 CET sensations, the rural stations are again colder than Frankfurt, on average in 1.9% of the cases.

The total amount of days with heat stress in the afternoon is more significant in Frankfurt than in its surroundings. The morning and evening sensations have the same results. Considering only the warmest sensations, the thermal sensation in the city is also warmer.

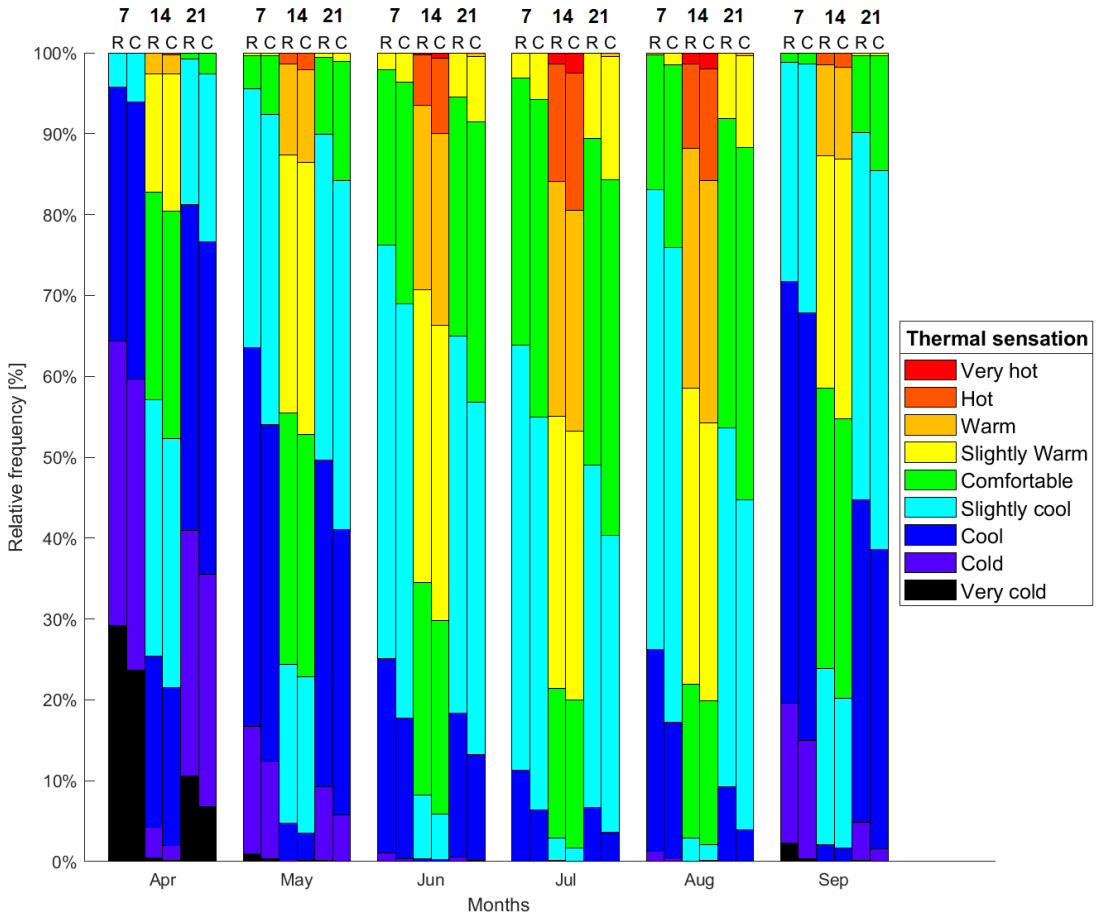

Figure 4.15: Same as 4.1, but for Frankfurt and (C) is the city station.

For Frankfurt, Figure 4.16 presents the time course of mPET and thermal sensation. The city station shows a course comparable with other cities having more heat stress (an increase of 1.7%) and less cold stress (decrease of 3.2%) nowadays compared to 1990. The more significant change is taken between the last decade for heat stress (0.9%) and for cold stress between the first decades (1.8%). The rural stations have almost no change in thermal sensation. Considering there is only one rural station for the surroundings of both Köln and Frankfurt, it has the same behaviour as in Figure 4.14. The rural station around Frankfurt and Köln is a station with the least mPET changes in this study.

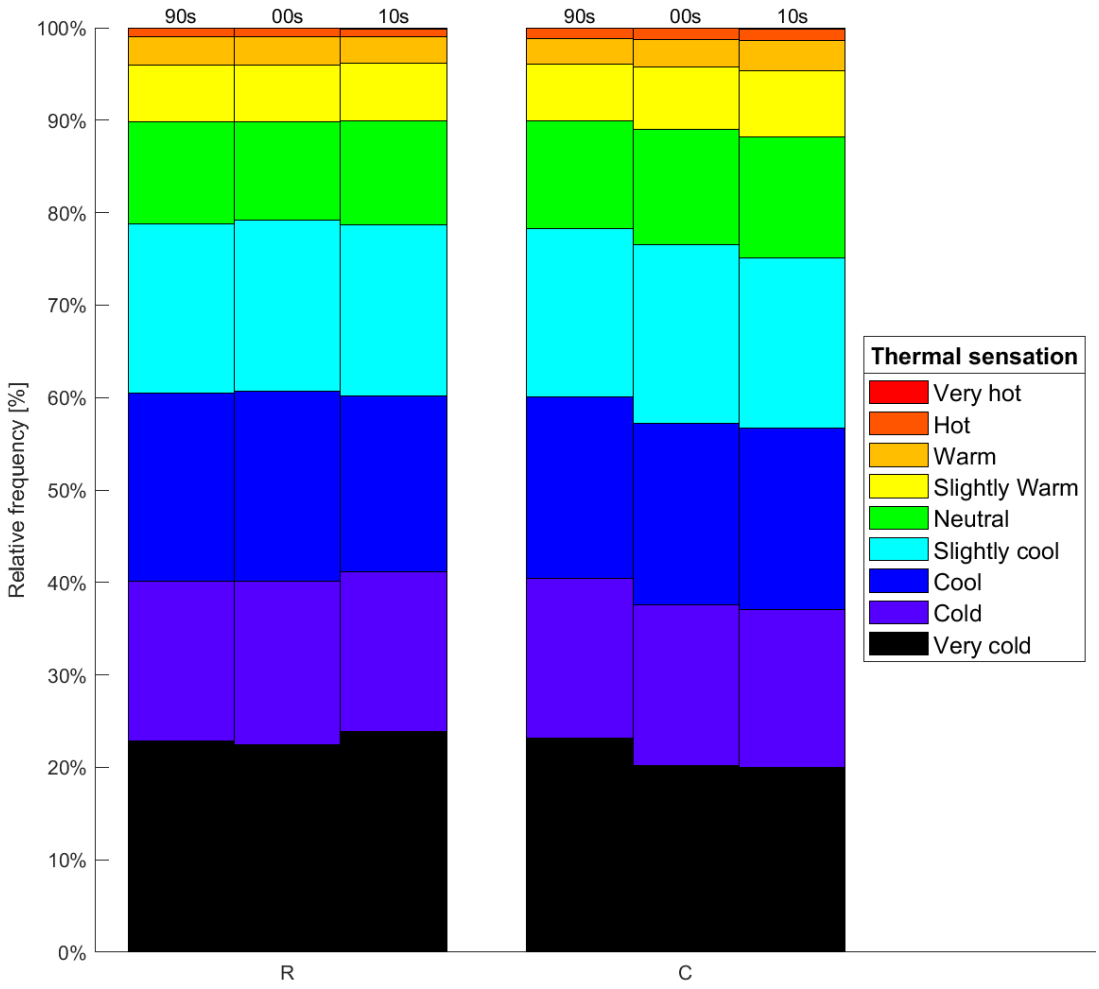

Figure 4.16: Same as Figure 4.3, but for Frankfurt and the city station is denoted by (C).

4.2 The city streets model

Another point of view on thermal comfort can be made by modelling a part of a city using buildings and trees. It provides an insight into the changes of street canyon effect formed by long narrow streets for different scenarios. The street canyon is studied in terms of thermal comfort connected more with radiation than with a flow of wind through the street. Four areas in Prague have been chosen to be modelled and used for the study of thermal comfort by modifying albedo of buildings and changing the number of trees in the streets. As for the modelling environment, program Rayman described in Chapter 3.2.1 was chosen.

The building and green space data have their origin in the OpenStreetMap project, where numerous buildings and other objects are stored and saved on the world map. After extracting the desired maps of the streets, the files are converted by program OSM2World to form files with objects added by additional building information found automatically on the internet. Next step is the translation of the object file into an obstacle file native for RayMan program. For this step has been developed a simple script to perform any object file containing only buildings and trees.

When the model was complete, a calculation of the thermal indices was performed together with meteorological data from Karlov station for it offers the best, most relevant and consistent data while being close to all of the studied streets. Thus, the inputs into the model are:

1. Geographical: modelled buildings and trees, longitude, latitude and altitude
2. Time: date, time and offset from UTC
3. Meteorological: air temperature, wind velocity, relative humidity and cloud cover
4. Personal: height, weight, age and sex
5. Other: clothing, activity and position

The chosen streets are Dělnická, Rohanské nábřeží, Legerova and Vinohradská for their length, width, location near the centre and in Rohanské nábřeží, new buildings have been constructed. Therefore, it is possible to compare the old and present configurations in the means of thermal comfort. Their locations are shown in Figure 4.17. The point in a street for calculation of mPET was chosen to be in the middle of the streets.

Figure 4.17: The map of Prague. The red lines are the studied parts of the streets in the RayMan model

In comparison, there are four (for Rohanské nábřeží five) configurations that were modelled and calculated. The real state displays the actual configuration. Added trees configuration has more trees in the street both coniferous and deciduous with a uniform height of 10 m. For details see Figures 4.18, 4.21, 4.24, 4.27. The high albedo of buildings differs from the real state only in the albedo of all buildings and lastly Added trees and High albedo buildings scenario combines the previous two. The tree planting was suggested in Musco [2016] for

Table 4.1: The configurations studied in street model comparison

Description	Mark	Building Albedo	Tree Albedo
Real state	R	0.30	0.15
Added trees	T	0.30	0.15
High albedo buildings	A	0.70	0.15
Added trees and High albedo buildings	+	0.70	0.15

any street canyons with a heavy traffic volume to provide more thermal comfort due to shadow casting and greenery expansion. The trees were added similar to trees in the neighbourhood along both sides of the streets. See Table 4.1 for the comparison of the scenarios. The fifth situation has the same attributes as the real situation, but some buildings in the model are removed. It represents the street Rohanské nábřeží in 2003 before new buildings were constructed and the circulation may change.

For each street, two analysis are presented. Firstly, the relative percentage of the thermal sensation categories was studied to see the general differences between the scenarios for 7, 14 and 21 CET. Moreover, one warm summer day with zero cloud cover in Prague was chosen to study hourly course of mPET during the day.

4.2.1 Dělnická

As the first street, Dělnická was modelled by the process described above and the resulting model is shown in Figure 4.18. Two configurations are showing the real state of the street and when trees were added to see the real difference. Dělnická is a west-easterly oriented street more than 20 metres wide having two lines for cars and two lines for trams. The street is surrounded by buildings and parking spots as well. Thus, it is mostly in asphalt and concrete environment having high thermal sensation during a warm day.

As Figure 4.19 shows, the real state has up to 3% of July the very hot sensation. The tree planting does not decrease the thermal discomfort as much as using higher albedo materials for the buildings around the street. Unfortunately, it has a positive effect only for the highest thermal sensations leaving the total number of days with heat stress higher than in the real state but the strength of the heat stress is mitigated.

The most significant difference between the scenarios is 6% which is in the morning in April. The rest of the differences are lower than 4%. The evening sensation is the coldest for scenarios using high albedo materials, whereas the tree planting scenario and real state are warmer than them. In the morning, it is mostly the other way around.

Considering Figure 4.20, the improvement of the thermal sensation during a sunny day is not very significant. A slightly more comfortable thermal environment is using the combination of added trees and high albedo materials which offers lower mPET from 10 CET to the end of the day. Nevertheless, in the morn-

ing, the combined scenario brings 1.4°C more mPET then the other versions of Dělnická street. Interesting is also the increase of evening mPET for the added trees scenario compared to the real state. The warmest scenario during the day is the added trees being on average warmer by 0.2°C.

For Dělnická street, the scenario with a combination of added trees and high albedo materials is the optimal solution to reduce the situations with the highest heat stress and provide shadow for sidewalks.

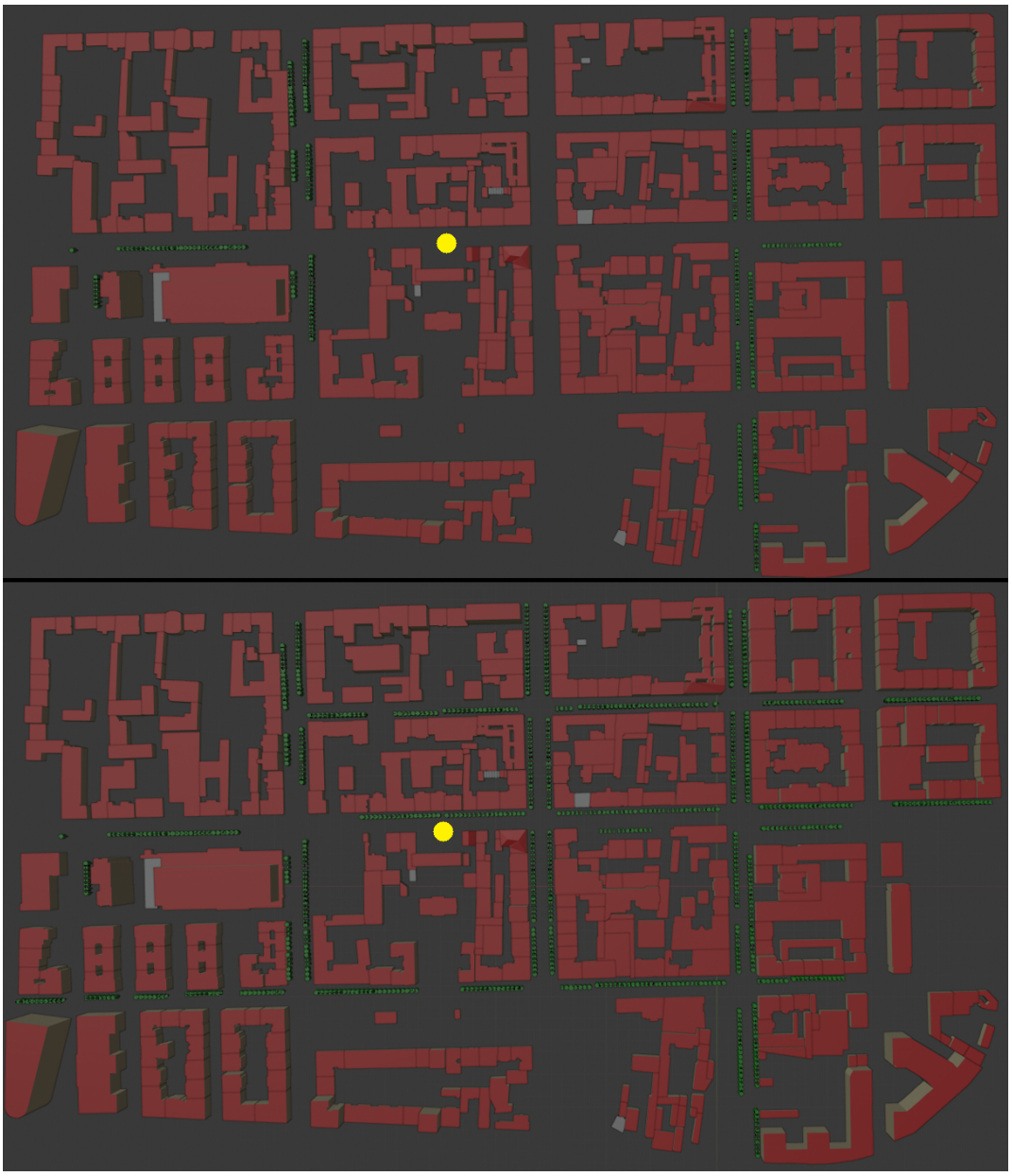

Figure 4.18: The model of Dělnická street and its surroundings concerning only buildings (red) and trees (green). The top picture displays the real situation and the bottom was modified by adding trees. The yellow dot represents the point of the calculation and grey epitomises the ground.

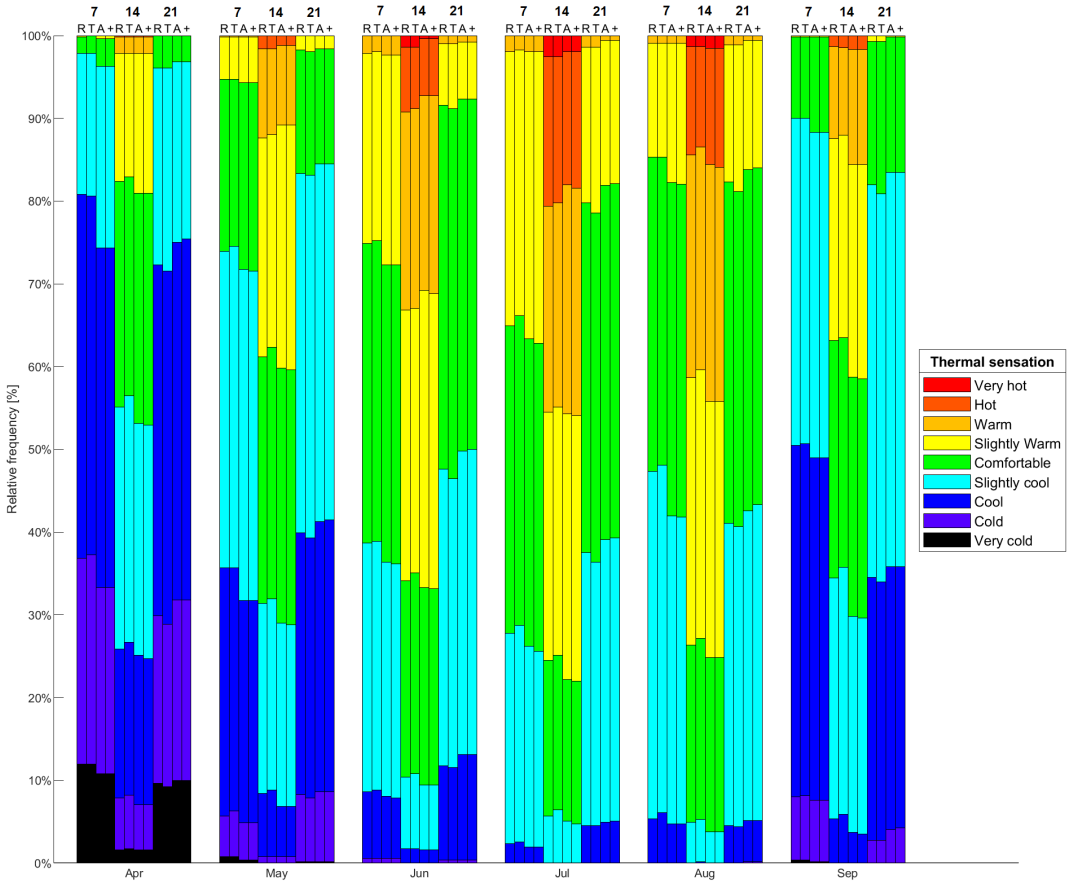

Figure 4.19: Thermal sensation in Prague at modelled street Dělnická at 7, 14 and 21 CET. The percentage of occurrence of different thermal sensations are shown for chosen months and hours for years 1990-2019. (R) stands for a real situation, (T) for a scenario with added trees, (A) for high albedo materials used in buildings and (+) for added trees and high albedo materials together.

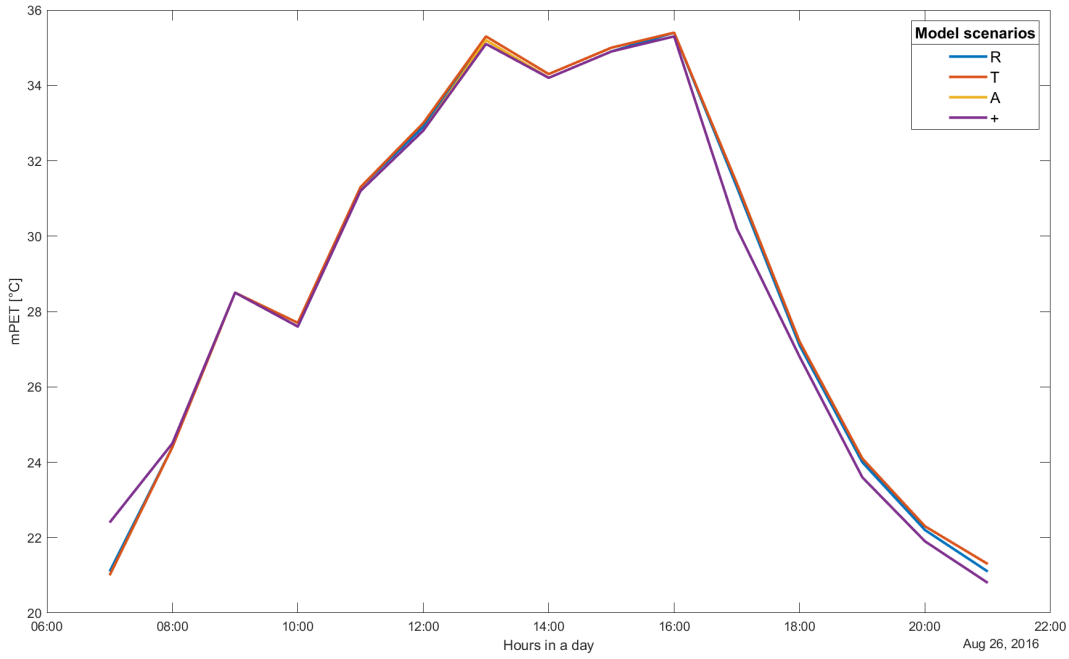

Figure 4.20: Hourly mPET in Prague Dělnická during a sunny day for August 26, 2016. (R) stands for a real situation, (T) for a scenario with added trees, (A) for high albedo materials used in buildings and (+) for added trees and high albedo materials together.

4.2.2 Rohanské nábřeží

Prague's street Rohanské nábřeží is oriented from south-west to north-east. It is wider than 30 m with four lanes for cars, two lanes for bicycles and joined by one-line street with parking spots. The traffic density is high since it is one of the main streets in Prague. The street has also been modelled, as shown in Figure 4.21. There are three different configurations for the street. From top to bottom it is the real state, a state with added trees and situation in 2003.

Figure 4.22 presents, among other things, the difference between an old state (2003) and nowadays state. Overall, the current state has lower heat stress in terms of total days with heat stress and even the very hot sensation. It means that the new buildings helped the street canyon to increase the thermal comfort in Rohanské nábřeží. Although, in the evening, the UHI effect has increased after the construction of the buildings.

The modified scenarios bring even more thermal comfort, having the added trees scenario being the best for the daily maxima and the combined scenario for the rest of the day. Rohanské nábřeží has the most significant difference between the two scenarios among all studied streets. It is 17.2% and 17.7% in the morning in June and July respectively. The added trees scenario has the greatest differences compared to the other scenarios where the changes are lower than 5%.

Considering all the months, the added trees scenario is the coldest in the mornings and afternoons. In contrast, in the evening, the high albedo and old state scenarios are at least in 0.9% of days colder than others.

Studying Figure 4.23, the added trees scenario helps to reduce daily maxima

significantly during a clear sky day, up to by 2.6°C mPET. However, from 17 CET, it is the warmest scenario, having evening mPET by 0.6°C warmer. The combined, high albedo and even old state scenarios have slightly lower mPET than the real state, mostly in the evening.

In case of Rohanské nábřeží, the scenarios with added trees and the combined scenario are the optimal future configurations. The best way would be starting with the tree planting and all new building constructions from high albedo materials would result in the combination of the two optimal scenarios.

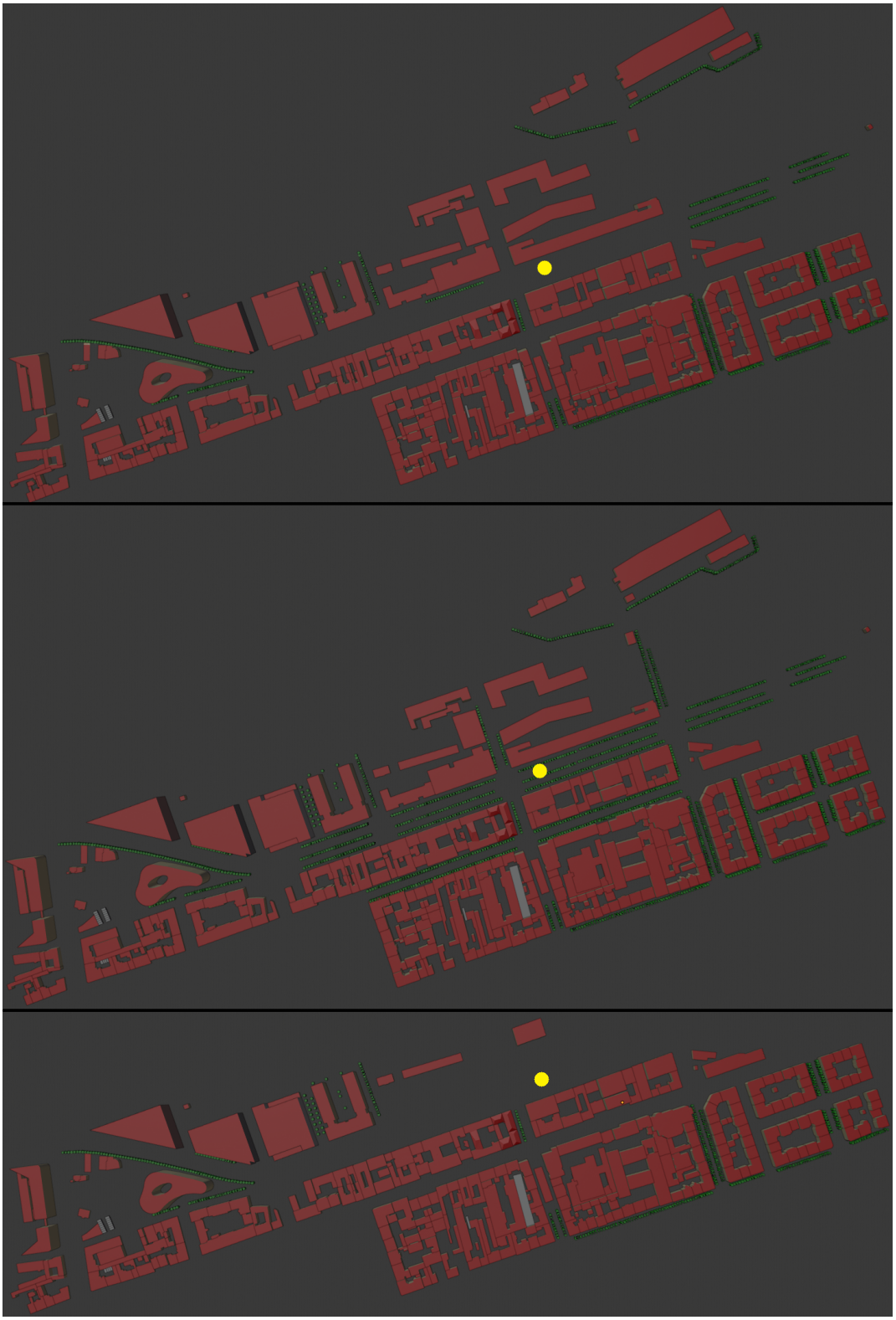

Figure 4.21: The model of Rohanské nábřeží street concerning only buildings (red) and trees (green). The top picture displays the real situation, the central picture was modified by adding trees and the bottom picture shows the situation before 2003. The yellow dot represents the point of the calculation and grey constitutes the ground.

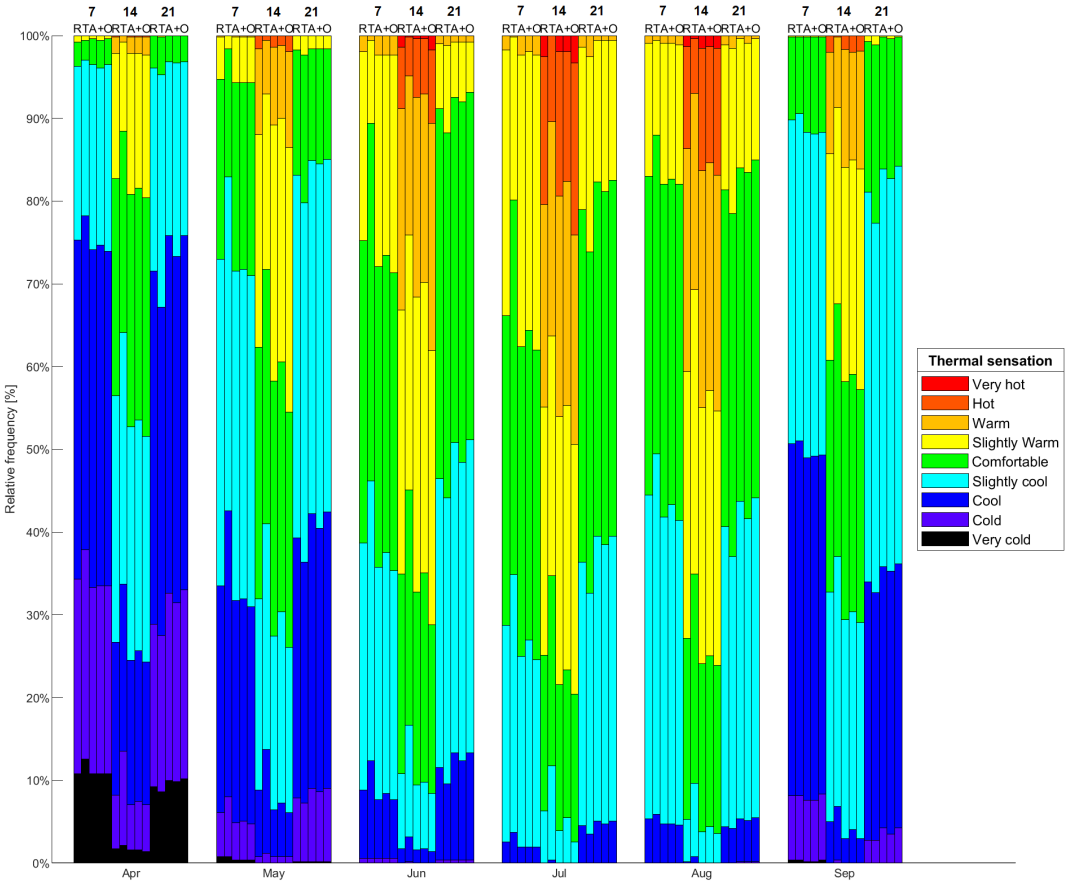

Figure 4.22: Same as Figure 4.19, but for Rohanské nábřeží and (O) denotes situations before new buildings were constructed.

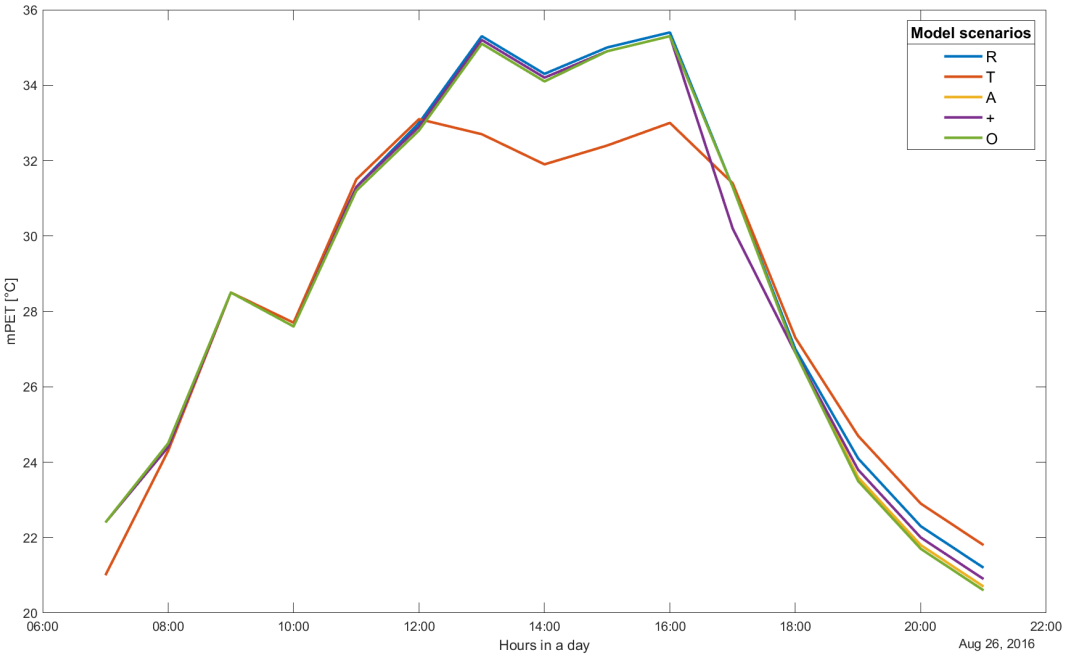

Figure 4.23: Same as Figure 4.20, but for Rohanské nábřeží and (O) denotes situations before new buildings were constructed.

4.2.3 Legerova

Another chosen street is Legerova which is the closest to the Karlov meteorological station. It is 25 metres wide and surrounded by 21 m high buildings. It has four lines for cars and is oriented in a north-south direction. It has very high traffic density and it is a narrow street leading through the centre of Prague. Its models are shown in Figure 4.24 with the location of the point of calculation. On the left-hand side, there is the real state and the right picture represents the model with added trees.

Figure 4.25 shows only minor cooling effect of tree planting during the warmest months but the effect increases in colder seasons. Overall, Legerova street is showing the smallest differences between the scenarios, having a maximum change of 5.3% in the afternoon in September. Except for September afternoon, the changes are not greater than 1.5%.

The scenarios with added trees seem to be colder than those without any extra tree planting for Legerova street. Trees seem to have more effect on the thermal comfort there than the albedo of buildings but it is only a minor change in thermal sensation. Those scenarios are also warmer in the evening compared to the real state but on average, the difference is lower than 0.2%.

Shown in Figure 4.26, none of the modified scenarios improves the thermal sensation during the clear sky day in the street. The most significant differences in mPET are in the evening but only 0.1°C, which is the minimum measurable difference. Therefore, all the scenarios seem to be equal under clear sky conditions.

The best scenario, in order to minimise the heat stress in the street and mainly the highest discomfort, for Legerova street is the added trees scenario.

Musco [2016] has shown an optimal solution of UHI mitigation for Legerova street using a scenario with planting small trees along the sidewalks. It does not affect ventilation conditions negatively and supports more comfortable thermal sensation. It supports the results of the present study, though the used trees are higher than Musco [2016] describes.

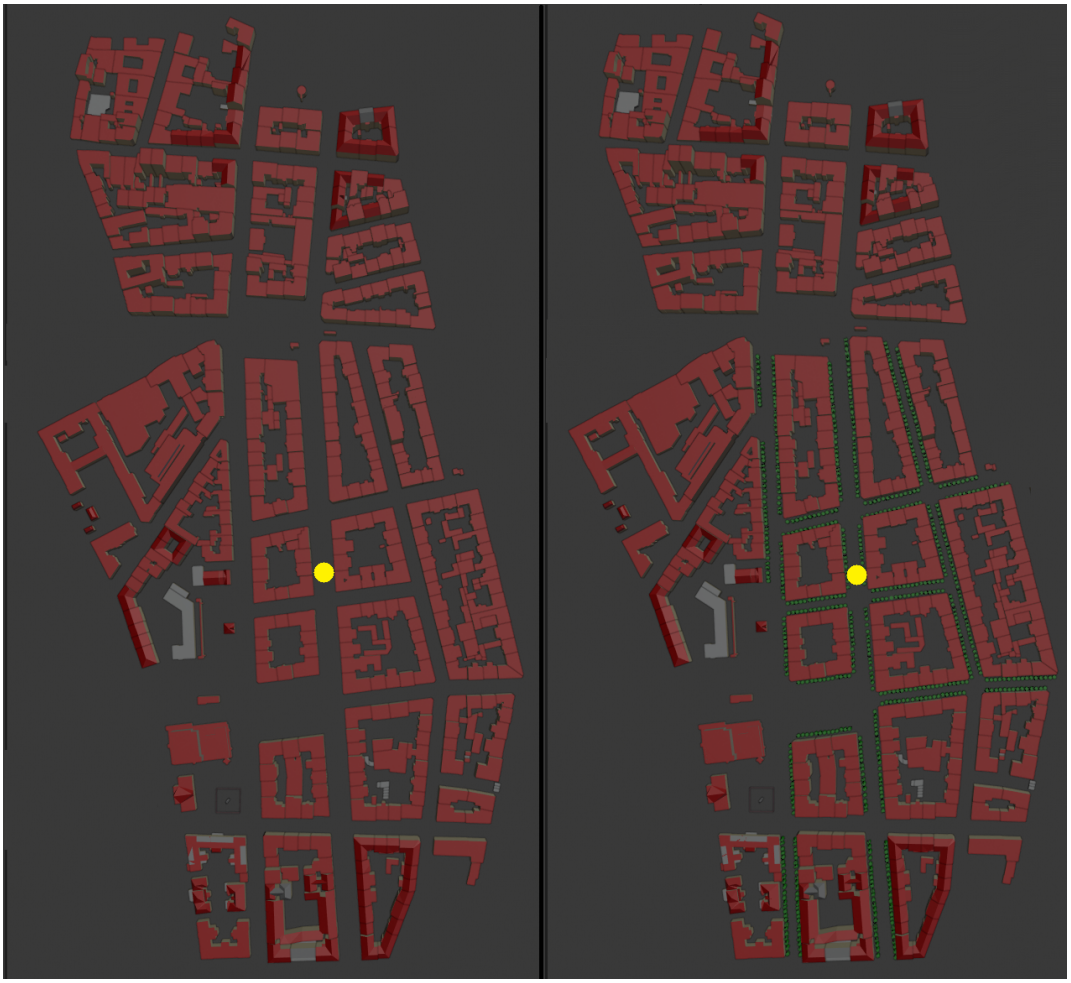

Figure 4.24: The model of Legerova street concerning only buildings (red) and trees (green). The left picture displays the real situation and the right was modified by adding trees. The yellow dot represents the point of the calculation and grey is the ground.

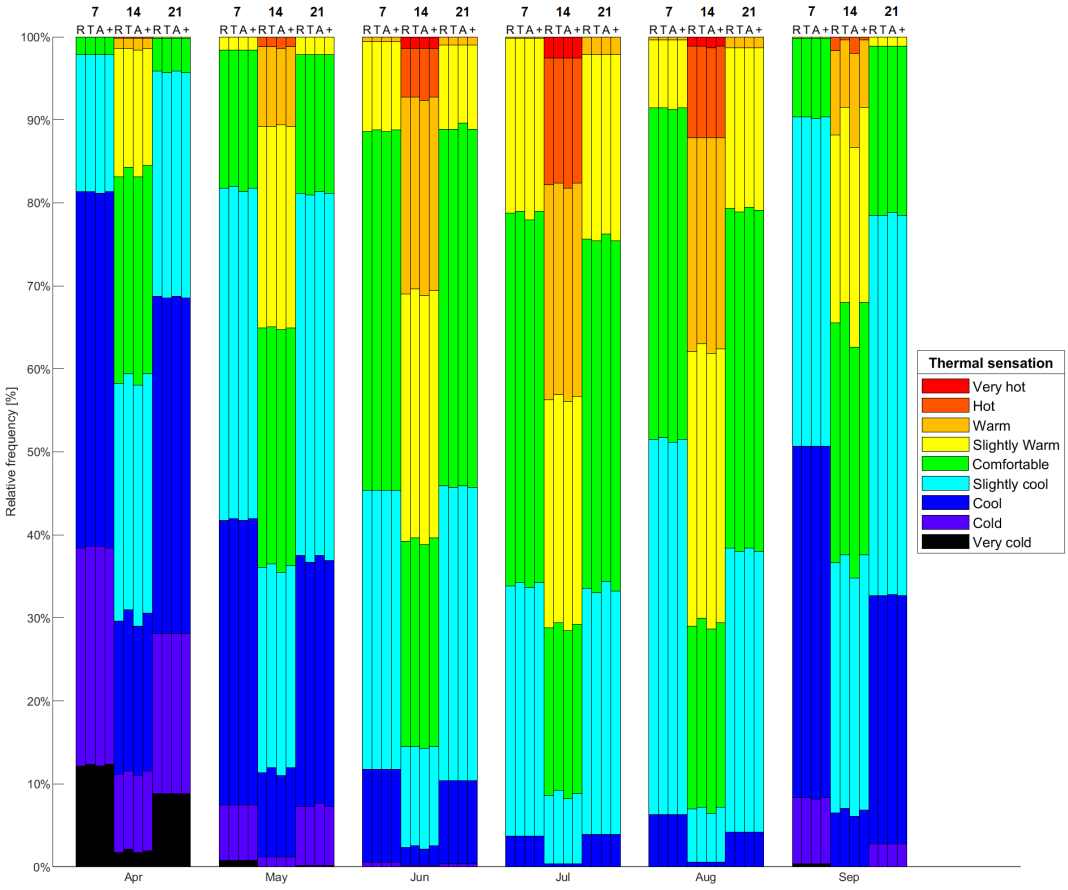

Figure 4.25: Same as Figure 4.19, but for Legerova.

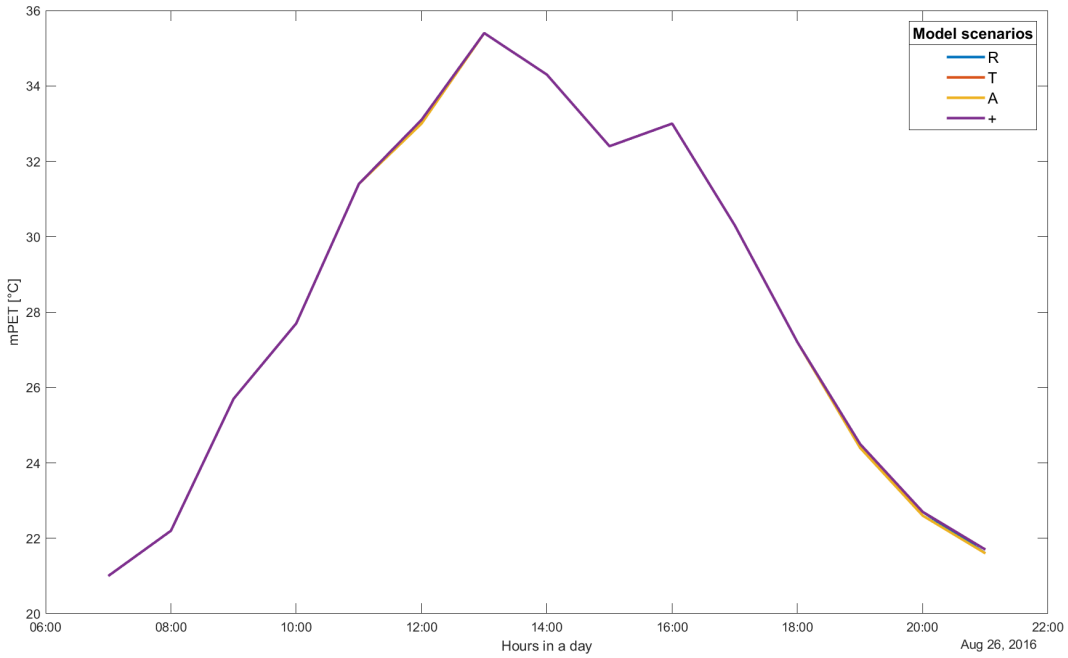

Figure 4.26: Same as Figure 4.20, but for Legerova.

4.2.4 Vinohradská

Vinohradská is a more than 20 metres wide street with two lines for both cars and trams and two lines for parking. It is west-easterly oriented with high traffic density complicated by the low number of lines. For the model, a part of the Vinohradská street located near the Prague Main Railway Station was chosen. Its models are presented in Figure 4.27, where the top picture is the current real state of the street and the bottom picture shows modification by adding trees.

In Figure 4.28, the thermal sensations are quite similar to each other having the most significant colder sensation for added trees scenario during the afternoon. Other modifications seem to have a lesser effect on the thermal comfort in Vinohradská street. Considering all scenarios without the added trees, the most significant difference would be only 1.6%. Added trees scenario gives the most considerable change of 6.2% in the afternoon in August.

In total, the most significant differences are in the afternoon and the smallest ones take place in the evening. There are also cases with no difference at all in terms of the second decimal space. It would mean that the differences between the mPET are small and in some cases were the values close to the border of two thermal sensations.

More interesting for this street canyon is the behaviour of thermal sensation during the clear sky day (Figure 4.29). The morning and evening temperatures are the same, while the differences are during the heat stress hours between 11 and 16 CET. Added trees scenario provides the least heat stress lowering mPET by 2.6°C compared to the real state. It is followed by real state and high albedo leaving the combined scenario the most uncomfortable scenario.

The added trees scenario has the most positive effect on thermal comfort in Vinohradská street, ensuring the reduction of daily maxima and providing shadows in the streets which correspond with Musco [2016].

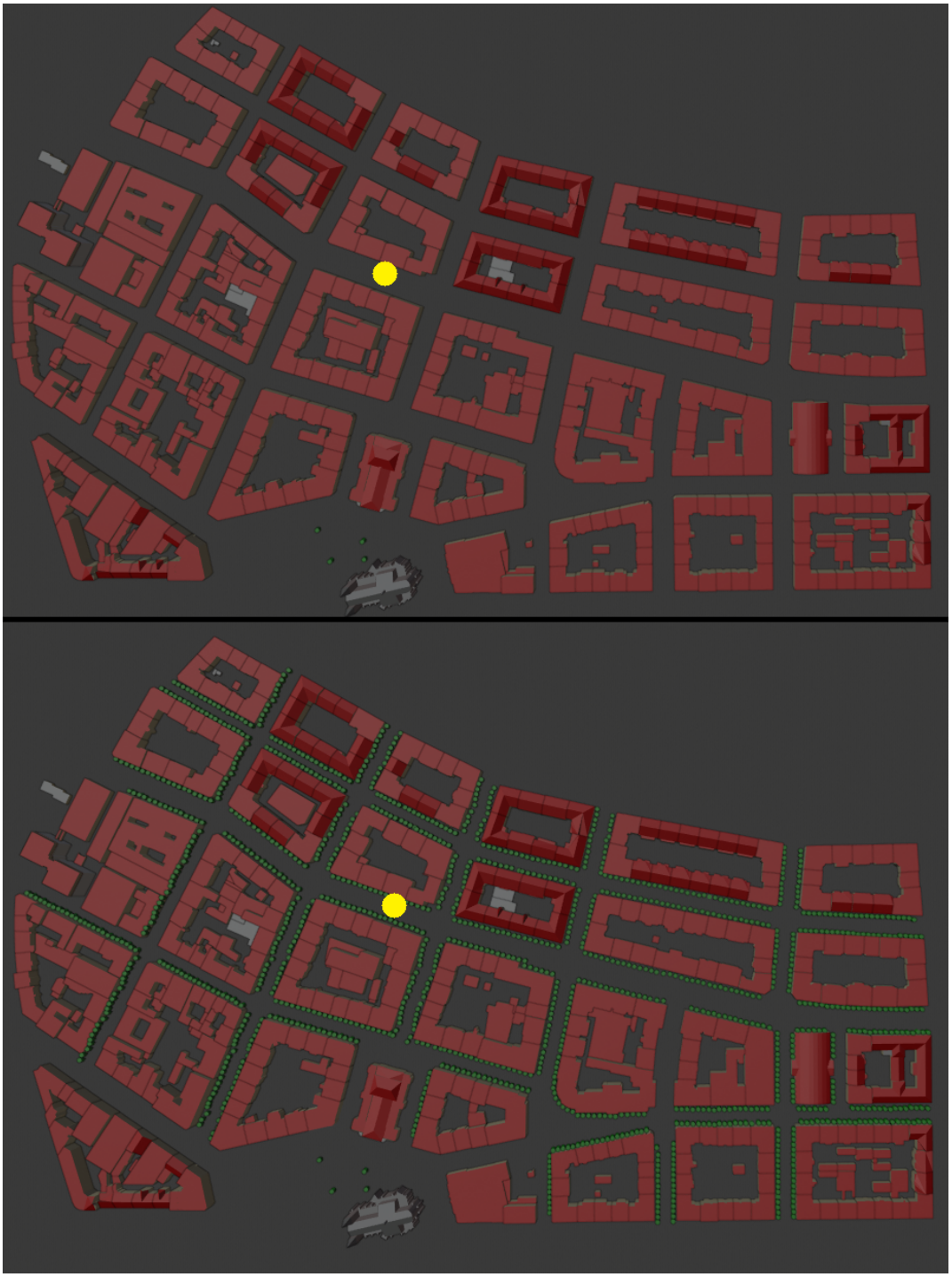

Figure 4.27: The model of Vinohradská street concerning only buildings (red) and trees (green). The top picture displays the real situation and the bottom was modified by adding trees. The yellow dot represents the point of the calculation and grey is the ground.

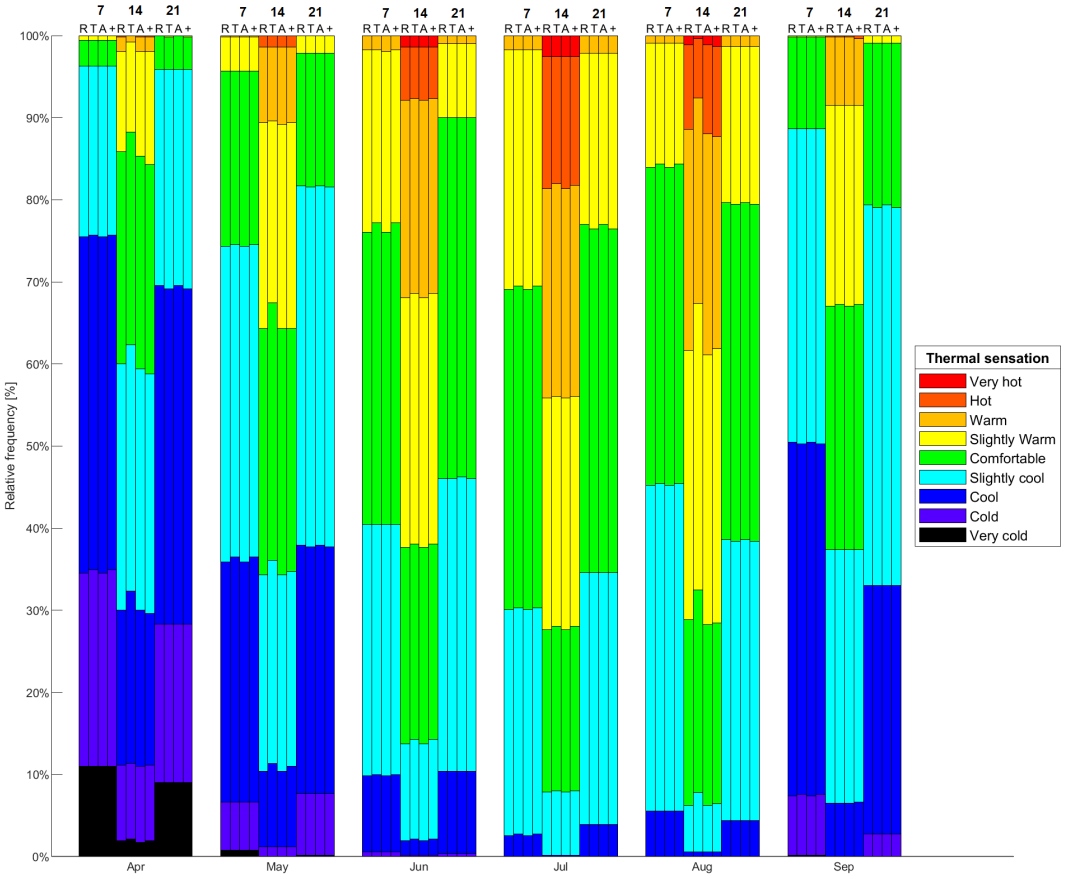

Figure 4.28: Same as Figure 4.19, but for Vinohradská.

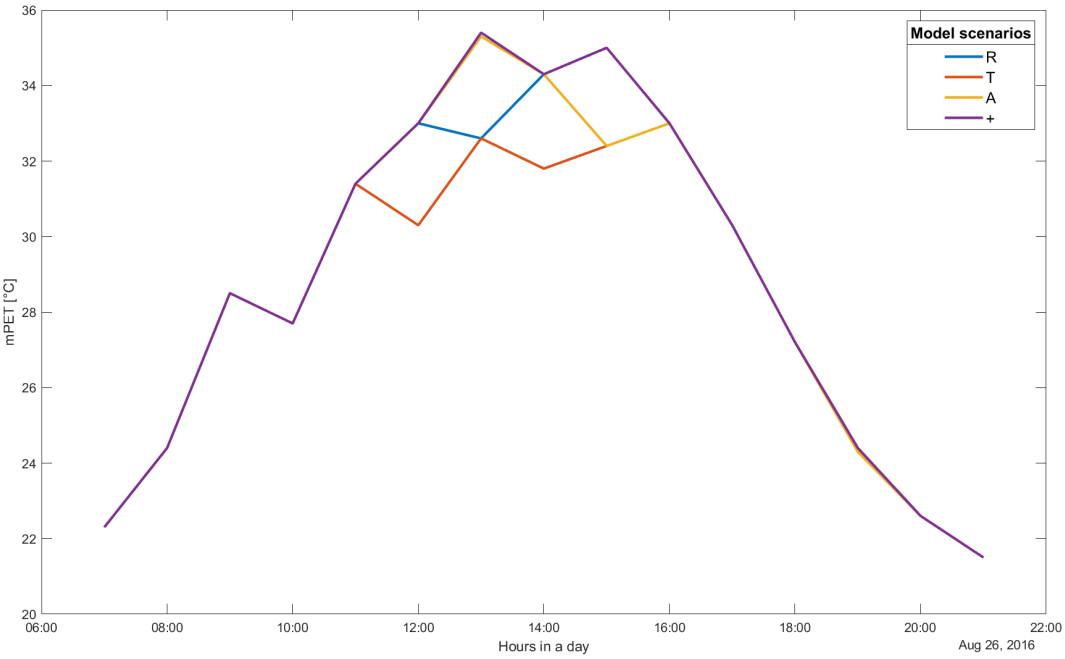

Figure 4.29: Same as Figure 4.20, but for Vinohradská.

5. Interpretation of the thermal indices

The analysis of outdoor thermal comfort has been done according to mPET thermal index. It is the youngest index based on both UTCI and PET and combines their multi-node approach with a stable MEMI model. The definition of mPET was constructed for European citizens, and therefore no corrections are needed for this study. There are also other indices suitable for this study, such as PET, PT, UTCI and SET*. If one of them was chosen, the results might differ as is shown in Figure 3.11.

Regarding thermal sensation in Prague (Chapter 4.1.1), the warmer sensations in the evening in the city is a clear example of UHI in a city with a population higher than one million citizens and the city centre being a dense build-up area. In Figures 4.1 and 4.2, there are visible step-by-step differences between the stations. Karlov is in the centre of Prague having the most intensive UHI being pronounced in the evening. Libuš is located in the uptown having weaker UHI when comparing the evening sensations. Moreover, rural areas have the lowest thermal sensations just before the night when considering only data from 7, 14 and 21 CET. During the night, the differences will be lowering and city stations may have even colder sensation than the rural areas (not shown).

For the results in Prague, the warm sensation in Libuš is interesting when compared to station Karlov. It can be seen in Figure 4.1, where Libuš station has warmer sensation than Karlov in the afternoon except April and May. It also has more days with hot and very hot category combined in June and August than Karlov. It can be caused by housing estate in the proximity of the station Libuš and the geometry of the falling sun rays. Near Libuš, there are meadows which can also affect the temperature in different months due to albedo changes during a year.

Significant differences between the urban and rural thermal sensations are recorded in Berlin (Chapter 4.1.2), as is displayed in Figures 4.5 and 4.7. The UHI effect is taking place in stations Tempelhof, Schönefeld and Tegel enhancing thermal sensation in the evening. The heat stress causes more harmful environment for the citizens of Berlin in terms of long-term health compared to the surroundings of the city. Stoops [2014] connects the thermal discomfort and cardiovascular health and also suggests psychological and sociological impacts. The discomfort is strengthened at the airports (Tempelhof, Tegel and Schönefeld) during clear sky days due to usage of low albedo materials such as concrete and asphalt causing an increase in surface temperature and heat accumulation.

In Berlin Dahlem, the afternoon sensation is slightly warmer than in rural stations and the evening sensation is slightly colder compared to the surroundings, as Figure 4.6 shows. As can be seen in Figure 4.4, Dahlem is located between the centre and uptown of Berlin. There are parks as well as the university campus and botanical garden. The environment differs from the centre of Berlin, and thus it is showing a different urban phenomenon. The temperature amplitude cannot explain the high amplitude of mPET because it is smaller in Dahlem than in rural areas. However, using temperature, humidity and wind speed, the high amplitude

of mPET could be caused by a low amount of water in the city. The water in the city is lead by a sewer system outside lowering the temperature inertia effect, which is suggested in Ascione et al. [2017]. Due to streets consisting of different materials and lack of fertile soil, cities can hold water only in the form of lakes, ponds or in the green spaces like parks. This effect depends on the exact location of the meteorological station suggesting no body of water nearby. However, there is plentiful greenery in Dahlem. Thus it is not likely to be the case because of the greenery near the station. It can be caused by various reasons. However, this matter is beyond the scope of this study.

Comparing Prague and Berlin, the capital of Germany has a more noticeable difference of evening mPET than Prague, considering stations Tegel and Karlov and their difference from the respective rural areas which might be caused by more inhabitants. Berlin has 3,421,800 and Prague has 1,259,100 citizens, according to Population.City [2015]. The difference of evening mPET is not likely made by a percentage of public green spaces because Berlin has 59% and Prague has 57%, as City Mayors [2017] and Štěpánek [2018] state. The cities are also in the same climatological categories, according to Beck et al. [2018]. It gives them similar climatological conditions. The largest geographical difference is that there are mountains between Prague and any sea, whereas Berlin is closer to the sea and it has a more opened landscape towards the sea. Therefore, Berlin has more maritime climate than Prague, which is connected with a more humid climate. However, it has a minor effect. The difference in thermal sensations in Prague and Berlin is more likely caused by their population and greenery.

A significant UHI has been observed in Nürnberg and Frankfurt. In both cities is the thermal sensation overall warmer than the other areas and the biggest differences are measured in the evening sensation. There is also a trend of having more heat stress in the city nowadays compared to 90s and almost no changes in heat stress in rural areas. It might be caused by high population in Frankfurt (1 034 200 citizens) and a low percentage of greenery in Nürnberg (48%), which is the lowest among all studied cities.

In Hamburg and Köln were detected no UHI behaviours and the thermal sensation was mainly colder than in the rural stations. The results for both cities would be different if there were used meteorological stations in the centre of the cities. The choice of the city meteorological stations is as important as the choice of the rural stations. The more city stations are available, the more precise the study. The location of the city station is also important. UHI is more pronounced in the city centre than in the uptown, as can be seen in Prague in Figure 4.1, where Karlov represents the city centre and Libuš is in uptown.

In Hamburg, there are the smallest decadal changes regarding thermal sensation, which can be a consequence of a different climate connected with the location in lowlands not far from the sea. Higher wind speed together with the direction from the sea brings mostly colder and more humid air from the North sea, which can mitigate the increase of mPET.

Studying the time course of thermal sensation, both Prague and Berlin have more hours with heat stress in the last decade than in the 90s, as Figures 4.3 and 4.8 show. It seems that the warming trend in Berlin is correlated with the warming trend in rural areas because both courses have similar decadal changes. Both warmings correspond with the current warming in Europe, which is described

in IPCC 2019 [2019]. Nevertheless, the warming tendency in Prague is stronger than in the surroundings, which can be explained by strengthening of the UHI. The statement is supported by the fact that the time course is mainly affected by afternoon and evening sensation while the morning thermal sensation does not change so much.

An interesting finding is the time course in the rural stations around Hamburg, Nürnberg, Köln and Frankfurt shown in Figures 4.10, 4.12, 4.14 and 4.16 respectively. In terms of heat stress, the rural stations show a decrease of heat stress by 0.1%. In the surroundings of the other cities, there is also no case of a faster increase in heat stress compared to the respective city stations. It can be a result of a fluctuation of the mPET value. However, it disagrees with the findings of Scott et al. [2018], who analysis thermal comfort in 54 cities in the US in the years 2000-2015. Scott et al. [2018] states that heat stress increases in rural areas more rapidly than in the urban environment.

The increase in the thermal stress mentioned above is also known to many city authorities not only in Europe but worldwide as well. Therefore, the relevant policymakers published plans aiming at the increase of thermal comfort in the cities, mainly by a decrease of temperature, especially during heatwaves. Such plans have been accepted also for Prague (Strategie adaptace hl. m. Prahy na klimatickou změnu [2019]), Berlin (Gaebler [2015] and Mahlkow and Donner [2017]), Hamburg (Klocke [2011]), Nürnberg (Hackner [2007]), Köln (Grothues et al. [2013]) and Frankfurt City of Frankfurt am Main [2017]. Model Rayman provides a basic insight into the thermal comfort in the city by modelling on a scale of a building up to the whole city. Due to easy application and modification of the objects in the model, it offers a powerful tool to study the city thermal comfort dependency on various modification scaling from changes of the greenery up to the modifications of buildings with its albedo and emission coefficients considered.

Therefore, four scenarios have been studied for four streets Dělnická, Rohanské nábřeží, Legerova and Vinohradská in Prague. The scenarios were: real state, added trees, a high albedo of buildings and a combination of added trees and high albedo buildings scenario.

Scenario with added trees mitigates the heat stress in Rohanské nábřeží, Legerova and Vinohradská street. The high albedo of buildings brought less heat stress only to Dělnická street and the combined scenario is ideal for Dělnická and Rohanské nábřeží street.

The cooling effect of high albedo buildings scenario in Dělnická can be explained by the constellation of the buildings and the direction of the street and the position of the point of calculation. The sun rays falling on the building are reflected away, lowering the radiation absorbed by the environment. On the other hand, in Legerova and Vinohradská, the high albedo scenario has the same thermal sensation as the real state. It can be caused by the position, orientation and shape of the buildings, which can result in different reflection of the sun rays. The sun rays can reflect from the buildings and be absorbed by the surface. Thus, the surface is heated by the additional sunray and thermal sensation is warmer than in the real state.

Added trees scenario successfully lowers the mPET in three out of the four streets. It is due to a shadow that trees cast on the ground during the day and

their ability to cool faster in the evening than the building materials, e.g. asphalt and concrete. Dělnická street was not affected so much by the tree planing probably for it already has some greenery. Moreover, the buildings are not forming a narrow canyon for there are some parking spots.

Surprisingly, the combined scenario brought colder sensations only in two of the studied streets. There are more complex connections between tree planting and using high albedo materials. In some cases, the cooling effect of both prevails (Figure 4.20, but in some, it results in warmer sensation (Figure 4.29).

Comparing the thermal sensation in all four streets, the relationship between the orientation of a street and the direction of prevailing wind might also be important to determine thermal comfort. However, it is not seen in the data because all meteorological inputs are from station Karlov. To study those differences, measurements of air temperature, humidity, wind speed, cloud cover and wind direction should be done in all studied streets and a more complex model than Rayman should be used.

Conclusion

One of the main aims of this thesis was to study different thermal comfort indices in urban climate conditions which are connected with the effect of UHI. This was achieved by the review of the three types of the indices: Experimental, Commercial and Analytical. For each of the types, a few representative indices were mentioned. For all mentioned analytical indices, thermal sensation scale was presented as the connection between the value of the indices and real perceived temperature. Their general usage was then explained in different fields of interest. In urban planning, thermal indices are used to study thermal comfort, mainly according to tree planting and using high albedo materials. Other applications are in tourism to simplify the climatological information about a specified location, which can be done via climate–tourism–information–scheme (CTIS). Last but not least important matter is the usage in the research of mortality connected with thermal discomfort, mainly during a heatwave.

Comparing various indices by their complexity, variability and overall suitability for the meteorological data, mPET was chosen to represent the thermal perception of human body in this study. It is the newest thermal index combining the virtues of PET and UTCI, which are the most used thermal indices. Model Rayman was also introduced as a tool which can calculate various thermal indices for given general coordinates as well as simulate thermal conditions in streets. The manual on the input data of buildings and trees for the simulation was also introduced. The mentioned data consist of measurements of meteorological variables, i.e. air temperature, wind speed, relative humidity, cloud cover, mean sea level pressure, dew-point temperature, wind direction and precipitation, from stations in Prague, Berlin, Hamburg, Nürnberg, Köln, Frankfurt and their surrounding rural area stations in the years 1990-2019. For the calculation of mPET, only the first four mentioned meteorological variables are needed. In the study, data from hours 7, 14 and 21 CET were mostly used to represent the climatological results.

After the study of the thermal indices, another aim was to study the long-term behaviour and frequency of thermal discomfort in mentioned cities. The comparison was made by monthly frequencies of thermal sensations in hours 7, 14 and 21 CET from April to September for each city station and a set of stations around the cities, in rural areas. The rural set is a weighted mean of measured variables where weight is the reciprocal of the distance between the station and the city station. For Prague and Berlin, the total number of hours with heat stress for all city stations and the rural set were observed to support the research. It was found that in Prague, Berlin, Nürnberg and Frankfurt, the frequencies of thermal discomfort in terms of heat stress are higher in the cities than in surrounding areas. The amount of hours with heat stress also depends on the distance from the city centre, where it is usually the highest, and on the character of the build-up within the station confines. Heat stress is increased in the cities mainly in the evening and slightly in the afternoon, whereas the mornings are the same or warmer in the rural areas around the cities.

As for the long-term behaviour, the data were divided into three decades (1990-9, 2000-9 and 2010-9) and total change for hours 7, 14 and 21 CET com-

bined was studied. The frequency of days with heat stress increases and the number of days with cold stress decreases in Berlin, Prague, Hamburg, Nürnberg, Köln and Frankfurt. In Hamburg are the smallest changes in thermal sensation, which can be a consequence of a different climate connected with the location in lowlands closer to the sea than any other studied city.

Besides, thermal comfort in Prague was analysed according to the chosen thermal indices in dependency on the character of a street canyon and city greenery. The outdoor thermal comfort in a city is in many places affected by a street canyon effect. Meteorological variables, as well as the buildings and green areas defining the street, form the thermal environment. The orientation of the street in a relationship with a prevailing wind direction might also be important to determine thermal comfort.

Four scenarios, real state, added trees, a high albedo of buildings and combined scenario, were simulated in Rayman model to represent the urban planning. Using tree planting and using high albedo materials for construction of buildings are considered in this study. The monthly analysis of hours 7, 14 and 21 CET from April to September was done using frequencies of thermal sensation based on mPET. Furthermore, one day with no cloudiness was chosen to study hourly differences between those scenarios. It was found that for Dělnická and Rohanská nábřeží street, the combination of tree planting and using high albedo materials would mitigate the heat stress perceived. In the other streets, Legerova and Vinohradská, tree planting is more effective than constructing buildings using high albedo materials. Those recommendations mainly lower the heat stress in the streets.

Bibliography

B. Abdi, A. Hami, and D. Zarehaghi. Impact of small-scale tree planting patterns on outdoor cooling and thermal comfort. *Sustainable Cities and Society*, 56: 102085, 2020.

Ambient Weather. Heat index definition, 2017. URL `https://www.ambientweather.com/heind.html`. Last accessed on 2020-03-21.

F. Aram, E. Solgi, E. H. García, A. Mosavi, and A. R. Várkonyi-Kóczy. The Cooling Effect of Large-Scale Urban Parks on Surrounding Area Thermal Comfort. *Energies*, 12(3904):1–21, 2019.

F. Ascione, O. Böttcher, R. Kaltenbrunner, and G. P. Vanoli. Methodology of the cost-optimality for improving the indoor thermal environment during the warm season. Presentation of the method and application to a new multi-storey building in Berlin. *Applied Energy*, 185:1529–1541, 2017.

A. Auliciems and S. Szokolay. *Thermal comfort*. Second Edition. PLEA : Passive and Low Energy Architecture International, Brisbane, 2007. ISBN 0 86776 729 4.

H. Beck, N. Zimmermann, T. McVicar, and et al. Present and future Köppen-Geiger climate classification maps at 1-km resolution. *Scientific data*, 5:180214, 2018.

C. Brandenburg, A. Matzarakis, and A. Arnberger. Weather and cycling – a first approach to the effects of weather conditions on cycling. *Meteorological Applications*, 14:61–67, 2007.

P. Bröde, G. Jendritzky, D. Fiala, and G. Havenith. The universal thermal climate index utci in operational use. *Proceedings of Conference: Adapting to Change: New Thinking on Comfort*, 1:1–6, 2010.

I. Charalampopoulos and A. Santos Nouri. Investigating the behaviour of human thermal indices under divergent atmospheric conditions: A sensitivity analysis approach. *Atmosphere*, 10(580):1–25, 09 2019.

Y. C. Chen and A. Matzarakis. Modification of physiologically equivalent temperature. *Journal of Heat Island Institute International*, 9(2):26–32, 2014.

Y. C. Chen and A. Matzarakis. Modified physiologically equivalent temperature—basics and applications for western European climate. *Theoretical and Applied Climatology*, 132:1275–1289, 2018.

City Mayors. Germany's greenest cities, 2017. URL `http://www.citymayors.com/environment/german-green-cities.html`. Last accessed on 2020-05-15.

City of Frankfurt am Main. Masterplan 100% Climate Protection, 2017. URL `https://frankfurt.de/themen/klima-und-energie/energie/publikationen/masterplan`. Last accessed on 2020-07-21.

C. De Freitas, D. Scott, and G. McBoyle. A second generation climate index for tourism (cit): Specification and verification. *International journal of biometeorology*, 52:399–407, 05 2008.

H. H. Ennes. Analysis of Tissue and Arterial Blood Temperatures in the Resting Human Forearm. *Journal of Applied Physiology*, 85(1):5–34, 1998.

S. Falasca, V. Ciancio, F. Salata, Golasi I., F. Rosso, and G. Curci. High albedo materials to counteract heat waves in cities: An assessment of meteorology, buildings energy needs and pedestrian thermal comfort. *Building and Environment*, 163(106242):1–14, 2019.

P. O. Fanger. *Thermal comfort*. McGraw-Hill, New York, 1972.

L. Feng, M. Zhao, Y. Zhou, L. Zhu, and H. Tian. The seasonal and annual impacts of landscape patterns on the urban thermal comfort using Landsat. *Ecological Indicators*, 110(105798):1–12, 2020.

K. M. A. Gabriel and W. R. Endlicher. Urban and rural mortality rates during heat waves in Berlin and Brandenburg, Germany. *Environmental Pollution*, 159:2044–2050, 2011.

C. Gaebler. Berlin‘s Climate Action and Adaptation Planning, 2015. URL `http://www.circlesofclimate.org/wp-content/uploads/2015/12/GaeblerChristian-Berlin-Adaptation_NO_REGRETS_Workshop-2015.pdf`. Last accessed on 2020-07-21.

E. Gatto, R. Buccolieri, E. Aarrevaara, F. Ippolito, R. Emmanuel, L. Perronace, and J. L. Santiago. Impact of Urban Vegetation on Outdoor Thermal Comfort: Comparison between a Mediterranean City (Lecce, Italy) and a Northern European City (Lahti, Finland). *Forests*, 11(2):1–22, 2020.

J. Geletič, M. Lehnert, S. Savić, and D. Milošević. Inter-/intra-zonal seasonal variability of the surface urban heat island based on local climate zones in three central European cities. *Building and Environment*, 156:21–32, 2019.

T. M. Giannaros, K. Lagouvardos, V. Kotroni, and A. Matzarakis. Operational forecasting of human-biometeorological conditions. *International Journal of Biometeorology*, 62:1339–1343, 2018.

H. D. Goodfellow and E. Tähti. *Industrial ventilation design guidebook*. First Edition. Calif.: Academic, San Diego, 2001. ISBN 978-0-12-289676-7.

Google Earth Pro. Berlin, Germany, 2020. URL `https://www.google.com/earth`. version 7.3.3.7699 (64-bit).

E. Grothues, B. Köllner, D. Ptak, C. Dalelane, T. Deutschländer, H. Ertel, M. Hafer, G. Halbig, T. Kesseler-Lauterkorn, C. Koch, M. Koßmann, G. Malitz, O. Roll, A. Schmitt, E. Weigl, T. Winterrath, C. Hartwig, Y. Wieczorrek, F. Rüsing, and I. Schwerdorf. Klimawandelgerechte Metropole Köln, 2013. URL `https://www.lanuv.nrw.de/fileadmin/lanuvpubl/3_fachberichte/30050.pdf`. Last accessed on 2020-07-21.

R. Hackner. Forschungsprojekt "Urbane Strategien zum Klimawandel", 2007. URL https://www.nuernberg.de/internet/klimaanpassung. Last accessed on 2020-07-21.

P. Hoffmann, R. Schoetter, and K. H. Schlünzen. Statistical-dynamical downscaling of the urban heat island in Hamburg, Germany. *Meteorologische Zeitschrift*, 27:89–109, 2016.

P. Höppe. The physiological equivalent temperature – a universal index for the biometeorological assessment of the thermal environment. *International Journal of Biometeorology*, 43:71–75, 1999.

IPCC 2019. Climate Change and Land: an IPCC special report on climate change, desertification, land degradation, sustainable land management, food security, and greenhouse gas fluxes in terrestrial ecosystems, 2019. Shukla, P.R. and Skea, J. and Calvo Buendia, E. and Masson-Delmotte, V. and Pörtner, H.-O. and Roberts, D. C. and Zhai, P. and Slade, R. and Connors, S. and van Diemen, R. and Ferrat, M. and Haughey, E. and Luz, S. and Neogi, S. and Pathak, M. and Petzold, J. and Portugal Pereira, J. and Vyas, P. and Huntley, E. and Kissick, K. and Belkacemi, M. and Malley, J. and (eds.). In press.

G. Jendritzky and R. de Dear. Adaptation and thermal environment. *Biometeorology for adaptation to climate variability and change*, pages 9–32, 01 2009.

G. Jendritzky, H. Staiger, K. Bucher, A. Graetz, and G. Laschewski. The perceived temperature: The method of the deutscher wetterdienst for the assessment of cold stress and heat load for the human body. *Deutscher Wetterdienst, Germany*, 2000.

G. Jendritzky, R. De Dear, and G. Havenith. UTCI—why another thermal index? *International Journal of Biometeorology*, 56(3):421–428, 2012.

E. Klocke. The Hamburg Climate Action Plan, 2011. URL https://www.hamburg.de/contentblob/4028914/6bdf8a2548ec96c97aa0b0976b05c5d9/data/booklet-englisch).pdf. Last accessed on 2020-07-21.

A. Kon. Method and apparatus for calculating thermal sensitivity. Technical report, Fujisawa Factory YAMATAKE-HONEYWELL CO., LTD., 12-2,Kawana 1-chome Fujisawa-shi, Kanagawa(JP), 1992. URL https://patentimages.storage.googleapis.com/75/18/2f/0d50cc53f539a1/EP0477796A2.pdf. Last accessed on 2020-05-11.

P. Kumar. Winter Is Coming - A sneak peek into the upcoming app for Occupant Thermal Comfort, 2019. URL https://www.simulationhub.com/blog/winter-is-coming-a-sneak-peek-into-the-upcoming-app-for-occupant-thermal-comfort. Last accessed on 2020-05-11.

X. Li, L. Shen, and R. Califano. The comparative study of thermal comfort and sleep quality for innovative designed mattress in hot weather. *Science and Technology for the Built Environment*, 0:1–15, 2020.

T. P. Lin and A. Matzarakis. Tourism climate and thermal comfort in sun moon lake, taiwan. *International journal of biometeorology*, 52:281–90, 04 2008. doi: 10.1007/s00484-007-0122-7.

T. P. Lin, A. Matzarakis, and R. L. Hwang. Shading effect on long-term outdoor thermal comfort. *Building and Environment*, 45:213–221, 2010.

B. Liu, Z. Lian, and R. D. Brown. Effect of Landscape Microclimates on Thermal Comfort and Physiological Wellbeing. *Sustainability*, 11(19):1–13, 2019.

N. Mahlkow and J. Donner. From planning to implementation? The role of climate change adaptation plans to tackle heat stress: A case study of Berlin, Germany. *Journal of Planning Education and Research*, 37:385–396, 2017.

A. Matzarakis. Weather-and climate-related information for tourism. *Tourism and Hospitality Planning and Development*, 3:99–115, 08 2006.

A. Matzarakis. Assessment method for climate and tourism based on daily data. *Developments in Tourism Climatology*, 1:1–7, 01 2007a.

A. Matzarakis. Entwicklung einer bewertungsmethodik zur integration von wetter-und klimabedingungen im tourismus. *Berichte des Meteorologischen Institutes der Universität Freiburg*, 16:73–80, 07 2007b.

A. Matzarakis. Estimation of Thermal Indices in Urban Structures - Simulations by micro scale models. *Proceedings of the Third International Conference on Countermeasures to Urban Heat Island*, 13-15:13–25, 2014.

A. Matzarakis and O. Matuschek. Sky View Factor as a parameter in applied climatology - Rapid estimation by the SkyHelios Model. *Meteorologische Zeitschrift*, 20:39–45, 2011.

A. Matzarakis, F. Rutz, and H. Mayer. Modelling Radiation fluxes in simple and complex environments – Application of the RayMan model. *International Journal of Biometeorology*, 51:323–334, 2007.

A. Matzarakis, E. Rudel, M. Zygmuntowski, and E. Koch. Bioclimatic maps for tourism purposes. *Physics and Chemistry of the Earth*, 25:57–62, 2010a.

A. Matzarakis, F. Rutz, and H. Mayer. Modelling radiation fluxes in simple and complex environments: basics of the rayman model. *International Journal of Biometeorology*, 54:131–139, 2010b.

A. Matzarakis, F. Rutz, and H. Mayer. Modelling Radiation fluxes in simple and complex environments – Basics of the RayMan model. *International Journal of Biometeorology*, 54:131–139, 2010c.

A. Matzarakis, S. Muthers, and E. Koch. Human biometeorological evaluation of heat-related mortality in Vienna. *Theoretical and Applied Climatology*, 105: 1–10, 2011.

A. Matzarakis, J. Rammelberg, and J. Junk. Assessment of thermal bioclimate and tourism climate potential for central Europe—the example of Luxembourg. *Theoretical and Applied Climatology*, 114:193–202, 2013.

A. Matzarakis, S. Muthers, and F. Rutz. Application and comparison of UTCI and PET in temperate climate conditions. *Finisterra*, 49(98):21–31, 2015.

H. Mayer and P. Höppe. Thermal Comfort of Man in Different urban Environments. *Theoretical and Applied Climatology*, 38:43–49, 1987.

F. Musco. Counteracting Urban Heat Island Effects in a Global Climate Change Scenario. *Springer International Publishing*, 2016.

G. Mutani and V. Todeschi. The Effects of Green Roofs on Outdoor Thermal Comfort, Urban Heat Island Mitigation and Energy Savings. *Atmosphere*, 11 (2):1–33, 2020.

P. T. Nastos and A. Matzarakis. The effect of air temperature and human thermal indices on mortality in Athens, Greece. *Theoretical and Applied Climatology*, 108:591–599, 2012.

National Weather Service. Heat Index, 2016. URL `https://www.weather.gov/media/epz/wxcalc/heatIndex.pdf`. Last accessed on 2020-03-30.

National Weather Service. Heat Index, 2018. URL `https://www.weather.gov/safety/heat-index`. Last accessed on 2020-03-30.

N. Netam, S. Sanyal, and S. Bhowmick. Assessing the impact of passive cooling on thermal comfort in LIG house using CDF. *Journal of Thermal Engineering*, 5(5):414–421, 2019.

S. Oliveira and H. Andrade. An initial assessment of the bioclimatic comfort in an outdoor public space in Lisbon. *International journal of biometeorology*, 52: 69–84, 11 2007.

K. Ouali, K. E. Harrouni, M. L. Abidi, and Y. Diab. Analysis of Open Urban Design as a tool for pedestrian thermal comfort enhancement in Moroccan climate. *Journal of Building Engineering*, 28(101042):1–19, 2020.

K. Parsons. *Human thermal environments: The effects of hot, moderate, and cold environments on human health, comfort and performance*. Second Edition. Taylor and Francis, London, 2014. doi: 10.1201/b16750.

PhysLink. What is the Humidex formula used to find subjective temperature as a function of both measured temperature and relative humidity?, 1995. URL `https://www.physlink.com/education/askexperts/ae287.cfm`. Last accessed on 2020-03-25.

PlanetCalc. Apparent temperature, 2012. URL `https://planetcalc.com/2089`. Last accessed on 2020-03-30.

PlanetCalc. Humindex, 2016. URL `https://planetcalc.com/5673`. Last accessed on 2020-03-30.

Population.City. Population in cities, 2015. URL `https://population.city`.

O. Potchter, P. Cohen, T. P. Lin, and A. Matzarakis. Outdoor human thermal perception in various climates: A comprehensive review of approaches, methods and quantification. *Science of the Total Environment*, 631-632:390–406, 2018.

L. R. Rodríguez, J. S. Ramos, F. J. S. De La Flor, and S. Á. Domínguez. Analyzing the urban heat island: Comprehensive methodology for data gathering and optimal design of mobile transects. *Sustainable Cities and Society*, 55:1–18, 2020.

M. Rosenfelder, C. Koppe, J. Pfafferott, and A. Matzarakis. Effects of ventilation behaviour on indoor heat load based on test reference years. *International Journal of Biometeorology*, 60:277–287, 2016.

R. Ruuhela, K. Jylhä, T. Lanki, P. Tiittanen, and A. Matzarakis. Biometeorological Assessment of Mortality Related to Extreme Temperatures in Helsinki Region, finland, 1972–2014. *International Journal of Environmental Research and Public Health*, 14(8):1–19, 2017.

R. Schoetter, D. Grawe, P. Hoffmann, P. Kirschner, A. Grätz, and K. H. Schlünzen. Impact of local adaptation measures and regional climate change on perceived temperature. *Meteorologische Zeitschrift*, 22:117–130, 2013.

A. A. Scott, D. W. Waugh, and B. F. Zaitchik. Reduced urban heat island intensity under warmer conditions. *Environmental Research Letters*, 13(6): 064003, 2018.

H. Staiger, G. Laschewski, and A. Matzarakis. Selection of Appropriate Thermal Indices for Applications in Human Biometeorological Studies. *Atmosphere*, 10 (1):1–15, 2019.

R. G. Steadman. Indices of Windchill of Clothed Person. *Weatherwise*, 12(2): 57–61, 1959.

J. L. Stoops. A possible connection between thermal comfort and health. *California Digital Library*, 1:1–11, 2014.

Strategie adaptace hl. m. Prahy na klimatickou změnu. Capital City of Prague Climate Change Adaptation Strategy, 2019. URL `http://adaptacepraha.cz/wp-content/uploads/2020/05/Climate_Change_Adaptation_Strategy_Prague.pdf`. Last accessed on 2020-07-21.

H. Taha, D. Sailor, and H. Akbari. High-Albedo Materials for Reducing Building Cooling Energy Use. *Lawrence Berkeley National Laboratory*, 1992.

E. C. THOM. The Discomfort Index. *Weatherwise*, 12(2):57–61, 1959.

R. D. Thompson and A. Perry. *Applied Climatology*. First Edition. Routledge, New York, 1997. ISBN 0-415-14100-1.

A. Štěpánek. Zelená praha. Ze světových metropolí má největší podíl přírodních ploch, 2018. URL `https://www.euro.cz/praha/zelena-praha-ze-svetovych-metropoli-ma-nejvetsi-podil-prirodnich-ploch-1403258`. Last accessed on 2020-05-15.

C. H. Tung, C. P. Chen, K. T. Tsai, N. Kántor, R. L. Hwang, A. Matzarakis, and T. P. Lin. Outdoor thermal comfort characteristics in the hot and humid region from a gender perspective. *International Journal of Biometeorology*, 58: 1927–1939, 2014.

University of Oregon. The thermal comfort issues of a Lawrence Hall Circulation Space, 2020. URL `https://pages.uoregon.edu/hof/f02elephant/ecsanalysis.html`. Last accessed on 2020-05-11.

A. Urban and J. Kyselý. Comparison of UTCI with Other Thermal Indices in the Assessment of Heat and Cold Effects on Cardiovascular Mortality in the Czech Republic. *International Journal of Environmental Research and Public Health*, 11:952–967, 2014.

vCalc. Australian Apparent Temperature (AT), 2019. URL `https://www.vcalc.com/wiki/rklarsen/Australian+Apparent+Temperature+%28AT%29`. Last accessed on 2020-04-15.

S. Wonorahardjo, I. M. Sutjahja, Y. Mardiyati, H. Andoni, D. Thomas, R. A. Achsani, and S. Steven. Characterising thermal behaviour of buildings and its effect on urban heat island in tropical areas. *International Journal of Energy and Environmental Engineering*, 11:129–142, 2020.

WorldData. Average sizes of men and women, 2019. URL `https://www.worlddata.info/average-bodyheight.php`. Last accessed on 2020-03-25.

S. Q. Yang and A. Matzarakis. Implementation of human thermal comfort information in Köppen-Geiger climate classification—the example of China. *International Journal of Biometeorology*, 60:1801–1805, 2016.

G. Ye, C. Yang, Y. Chen, and Y. Li. A new approach for measuring predicted mean vote (PMV) and standard effective temperature (SET*). *Building and Environment*, 38(1):33–44, 2003.

M. Yokota, L. G. Berglund, and X. Xu. Thermoregulatory modeling use and application in the military workforce. *Applied Ergonomics*, 45:663–670, 2014.

T. Yousif and H. Tahir. Application of thom's thermal discomfort index. *Journal of forest products and industries*, 2(5):36–38, 09 2013.

K. Zaninović and A. Matzarakis. The bioclimatological leaflet as a means conveying climatological information to tourists and the tourism industry. *International Journal of Biometeorology*, 53:369–374, 2009.

K. Zaninović and A. Matzarakis. Impact of heat waves on mortality in croatia. *International Journal of Biometeorology*, 58:1135–1145, 2014.

S. Zare, N. Hasheminejad, H. E. Shirvan, R. Hemmatjo, K. Sarebanzadeh, and S. Ahmadi. Comparing Universal Thermal Climate Index (UTCI) with selected thermal indices/environmental parameters during 12 months of the year. *Weather and Climate Extremes*, 19:49–57, 2018.

List of Figures

List of Tables

List of Abbreviations

ASHRAE American Society of Heating, Refrigerating and Air-Conditioning Engineers

AT Apparent Temperature

CC Cloud Cover

CTIS Climate–tourism–information–scheme

FPC Fiala's multi-node human physiology and thermal comfort model

HI Heat Index

Hum Humidex

mPET Modified physiological equivalent temperature

PET Physiological equivalent temperature

PMV Predicted Mean Vote

PPD Predicted Percentage of Dissatisfied

PT Perceived Temperature

$\mathbf{p_{WV}}$ Water vapour pressure

RH Relative humidity

SET* Standard effective temperature

T Air temperature or Dry bulb temperature

$\mathbf{T_{MRT}}$ Mean radiant temperature

UHI Urban Heat Island

UTCI Universal Thermal Climate Index

v Wind speed

WCI Wind-Chill Index